



Ross River Landscape Hazards

Geoscience Mapping for Climate
Change Adaptation Planning



Northern Climate ExChange
YUKON RESEARCH CENTRE • Yukon College



Aboriginal Affairs and
Northern Development Canada

Affaires autochtones et
Développement du Nord Canada

This publication may be obtained from:

Northern Climate ExChange
Yukon Research Centre, Yukon College
500 College Drive
P.O. Box 2799
Whitehorse, Yukon
Y1A 5K4
867.668.8895
1.800.661.0504
yukoncollege.yk.ca/research

Recommended citation: Benkert, B.E., Fortier, D., Lipovsky, P., Lewkowicz, A., de Grandpré, I., Grandmont, K., Turner, D., Laxton, S., Moote, K., and Roy, L.-P., 2015. Ross River Landscape Hazards: Geoscience Mapping for Climate Change Adaptation Planning. Northern Climate ExChange, Yukon Research Centre, Yukon College. 116 p. and 2 maps.

Front cover photograph: Aerial view of the community of Ross River looking southeast.

Photo credit: Yukon Geological Survey

Disclaimer: The report including any associated maps, tables and figures (the “Information”) convey general observations only. The Information is based on an interpretation and extrapolation of discrete data points and is not necessarily indicative of actual conditions at any location. The Information cannot be used or relied upon for design or construction at any location without first conducting site-specific geotechnical investigations by a qualified geotechnical engineer to determine the actual conditions at a specific location (“Site-Specific Investigations”). The Information should only be used or relied upon as a guide to compare locations under consideration for such Site-Specific Investigations. Use of or reliance upon the Information for any other purpose is solely at the user’s own risk. Yukon College and the individual authors and contributors to the Information accept no liability for any loss or damage arising from the use of the Information.

LEAD AUTHORS

Bronwyn Benkert	Northern Climate ExChange, Yukon Research Centre, Yukon College
Daniel Fortier	Université de Montréal
Panya Lipovsky	Yukon Geological Survey, Government of Yukon
Antoni Lewkowicz	University of Ottawa

CONTRIBUTING AUTHORS

Isabelle de Grandpré	Université de Montréal
Katerine Grandmont	Université de Montréal
Derek Turner	Yukon Geological Survey, Government of Yukon
Sarah Laxton	Yukon Geological Survey, Government of Yukon
Kelly Moote	Northern Climate Exchange, Yukon Research Centre, Yukon College
Louis-Philippe Roy	Northern Climate ExChange, Yukon Research Centre, Yukon College

TECHNICAL ADVISORS

Jeff Bond	Yukon Geological Survey, Government of Yukon
Lacia Kinnear	Northern Climate ExChange, Yukon Research Centre, Yukon College

TECHNICAL EDITING AND PRODUCTION

Leyla Weston, private consultant, Whitehorse, Yukon

ACKNOWLEDGEMENTS

The project team would like to thank all the participants in this project for their enthusiasm and commitment. We would like to express our appreciation to the Yukon Geological Survey, Yukon Research Centre, Université de Montréal, University of Ottawa, Université Laval, Government of Yukon, and all those noted above for their support.

We would especially like to thank the community of Ross River and the Ross River Dena Council for supporting this project and welcoming us on their lands and within the Traditional Territory of Kaska Dena. We appreciate the support and cooperation of community residents, which have led to fruitful conversations that enhanced the research presented here. Thank you also to Kitty Sperling, Yukon College's Ross River Campus community coordinator.

Thank you to the many field assistants involved in the project, including several of our contributing authors, as well as Alexandre Bevington, Michel Sliger and Alex Brooker. Bob Sagar compiled the instrumental climate data that appears in this report, and Philip Bonnaventure prepared the air temperature and permafrost probability models. Cover design by Lalena Designs.

Funding for this project was provided by Aboriginal Affairs and Northern Development, Government of Canada, and in-kind contributions were made by project partners. Project management was conducted by the Northern Climate ExChange, part of the Yukon Research Centre at Yukon College.

TABLE OF CONTENTS

INTRODUCTION	1
Climate Change Adaptation Planning.....	1
What are Hazards Maps?.....	1
Hazards Maps and Decision Making.....	1
HOW HAZARDS MAPS ARE CREATED	2
Community Consultation.....	2
Disturbance History.....	2
Surficial Geology Characterization.....	3
Permafrost Distribution and Characteristics.....	3
Hydrological Characterization.....	4
Projections of Future Environmental Conditions.....	4
Hazard Ranking.....	4
<i>Limitations and uncertainty</i>	4
THE ROSS RIVER REGION	5
Physiography.....	6
Vegetation.....	7
Contemporary Climate.....	8
Past Climate Trends.....	9
Hydrology.....	10
<i>Surface water</i>	10
<i>Groundwater</i>	12
Environmental Disturbance History.....	13
Bedrock Geology.....	15
Landscape Evolution During the Pleistocene and Holocene Epochs.....	17
Surficial Materials.....	18
<i>Organic materials</i>	19
<i>Volcanic materials</i>	19
<i>Colluvial materials</i>	19
<i>Fluvial materials</i>	20
<i>Glaciofluvial materials</i>	20
<i>Morainal materials</i>	22
<i>Glaciolacustrine materials</i>	22
Stratigraphy.....	23
Permafrost.....	24
<i>Organic cover</i>	24
<i>Forest cover</i>	24
<i>Surface material texture</i>	25
<i>Contemporary permafrost distribution</i>	25
POTENTIAL HAZARD RISKS FOR THE ROSS RIVER REGION	27
Landslide Processes.....	27
Permafrost Processes.....	29
<i>Permafrost development</i>	29
<i>Geotechnical properties</i>	29

<i>Permafrost as a hazard risk</i>	32
Seismicity.....	35
ASSESSING CURRENT HAZARDS FOR THE ROSS RIVER REGION	35
Case Study Sites.....	35
Central Ross River.....	36
Rifle Range.....	40
Kulan Street.....	43
Old Ross.....	45
PROJECTING HAZARD RISKS IN A CHANGING CLIMATE	48
Projected climate change for the Ross River region.....	48
<i>Global climate models</i>	48
<i>Climate change scenarios</i>	48
Landscape Sensitivity to Climate Change.....	50
<i>Sensitivity of local surface material types</i>	51
<i>Projected changes in permafrost distribution</i>	51
INTEGRATING RISK IN A LANDSCAPE HAZARDS MAP FOR THE ROSS RIVER REGION	56
GENERATING ACTION FROM SCIENCE	58
REFERENCES	60
APPENDIX A - APPROACH AND METHODS	67
APPENDIX B - BOREHOLE LOGS	78
APPENDIX C - GRAIN SIZE ANALYSIS	82
APPENDIX D - CLIMATE PROJECTIONS	88
APPENDIX E - HAZARD RANKINGS	95
APPENDIX F - SAFE HOME CONSTRUCTION ON PERMAFROST	101

INTRODUCTION

Climate change is a significant challenge for northern communities, where the impacts of a warming climate are already having considerable effects (Huntington and Weller, 2005). Many people living in small, isolated communities in northern Yukon are concerned about climate-related risks in their regions. Because adverse impacts are a reality, it is important to implement measures to reduce or moderate the negative effects of climate change – in other words, to implement climate change adaptation strategies.

CLIMATE CHANGE ADAPTATION PLANNING

Community-based adaptation planning aims to incorporate the potential impacts of climate change into decision-making for community development. For example, the design of a new building that is resilient to permafrost thaw, or the selection of future development zones away from areas that may be prone to flooding during the spring melt, are both decisions rooted in adaptation planning. Ultimately, adaptation planning anticipates future scenarios, reduces risk, increases resilience, and may even seek to reap the benefits of certain aspects of climate change.

In order to better prepare our communities to incorporate adaptation planning in the decision-making process, we must first identify the risks of, or vulnerabilities to, climate change, and then mitigate or reduce these risks so that we may adapt in a safe, sustainable manner.

Hazards maps help identify potential future risks associated with natural phenomena such as permafrost thaw, landslides and flooding. In order to adequately measure the potential risks associated with climate change, it is critical to gather scientific baseline data. These data, in conjunction with complementary research and future climate projections, strive to reduce vulnerability by increasing our knowledge base; this in turn will increase a community's adaptive capacity to climate change.

WHAT ARE HAZARDS MAPS?

A hazards map is a map that delineates or highlights areas on the land that are affected by, or are vulnerable to, a particular hazard. For example, in northern latitudes such as Yukon, thawing permafrost can be a significant climate change-related hazard. Flooding is another common hazard faced by Yukon communities, which may or may not be directly related to thawing permafrost. Hazards maps illustrate the risk associated with these and other hazards (ranked by risk severity), and are represented graphically in stoplight colours.

Hazards maps integrate complex environmental data into an easy-to-interpret, user-friendly tool for decision-making. The maps are created on a community-by-community basis and combine information about current and future landscape and climate conditions in order to rank the risk related to environmental change. As a result, they are tailored to each community's unique environment.

HAZARDS MAPS AND DECISION MAKING

Hazard mapping, in conjunction with risk assessment, forms the basis of the risk management decision-making process by providing a community with baseline information that is necessary to understanding what risks may exist. One of the main objectives of the risk management process is to determine "what risks potentially interfere with the community's ability to meet the goals and objectives defining the community's vision for the future" (Noson, 2002). In this case, hazards

maps help address a community's goal of incorporating climate change adaptation planning into its approaches to decision making and community development.

The series of landscape hazards maps produced by Northern Climate ExChange (NCE) and its partners are prepared as guides; that is, they act as one of the first steps in community planning and development. They identify areas where there is low risk of hazards exposure, as well as areas requiring more advanced and detailed scientific and engineering studies, should development be desired. Because hazards maps depict risk using stoplight colours, they are accessible and easy to interpret; in addition to community planning, hazards maps are useful educational tools illustrating local environmental conditions. They may also be used by scientists studying hazard phenomena (Noson, 2002), or could be revisited several years in the future to assess landscape change over time.

While hazards maps are tailored to local conditions and provide more detail than most other existing map products, it is important to note that they do not capture fine-scale variability within a site. For example, a slope underlain by permafrost may be more susceptible to thaw slumps in some areas compared to others because of small-scale variations in ice content of the surface material or morphology of the slope. However, the entire slope may be classified as moderate risk to encompass the highest possible degree of vulnerability. Because of this, it is important to recognize the limitations of hazards maps – they provide an initial guide to local conditions, but detailed site studies (e.g., geotechnical or engineering studies) will still be required.

HOW HAZARDS MAPS ARE CREATED

There are many different approaches to creating hazards maps. Different mapping projects from different jurisdictions around Canada's North, and globally, will incorporate different hazards elements and types of data. For this project, we developed an approach that incorporates local community concerns and infrastructure, disturbance history, permafrost distribution and characteristics, surficial geology conditions, hydrology, and projections of future climate. Approaches for each stage are briefly described below. Detailed descriptions of each approach, including equipment used, lab analyses conducted, and data processing specifics are included in Appendix A.

COMMUNITY CONSULTATION

Support from local community governments and First Nations is sought for each hazards mapping project when project funding proposals are developed. Upon project commencement, community consultations, meetings and interviews are held with members of the public and local decision-makers to identify areas of concern and sites for potential future development. These areas of interest then become case-study sites as part of the hazards project. Where local capacity exists, a community project liaison is hired to serve as a link between the research team and the community.

DISTURBANCE HISTORY

The research team gathers information about natural and human-caused disturbances that may affect current landscape conditions. For example, forest fires change vegetation cover and affect active layer thickness, while regulating and re-routing waterways or clearing land for development can affect local hydrology and permafrost conditions (De Grandpré et al., 2012). Old disturbances help explain why current landscape dynamics operate as they do, while newer disturbances offer insight into potential future landscape evolution.

SURFICIAL GEOLOGY CHARACTERIZATION

Surficial geology is the study of the unconsolidated material (i.e., the surficial material that overlies bedrock) on the Earth's surface, including all sediments and soils. Surficial geology mapping involves a combination of aerial photograph interpretation and fieldwork. Surficial geology maps provide information on the physical properties and characteristics of the surface sediments, the morphology (shape) of the landforms produced, and the genesis or origin of the landforms. In the process of mapping the surficial geology, the distribution of permafrost is also captured, making these maps an essential part of the hazards assessment process. The surficial geology maps become the basis for the final hazards maps produced through each project.

PERMAFROST DISTRIBUTION AND CHARACTERISTICS

Permafrost is defined as ground (including rock, unconsolidated sediments and organic material) that remains at or below 0°C for a minimum of two consecutive years (Brown et al., 1997). For this project, the research team studied both the distribution and characteristics of permafrost as part of the hazards map development.

Permafrost distribution is studied via the application of two geophysical surveys: 1) ground penetrating radar (GPR), and 2) electrical resistivity tomography (ERT). Ground penetrating radar uses electromagnetic radiation to send a tiny pulse of energy into the ground, and then measures the speed and strength of that pulse's reflection back to the instrument. It produces an image that delineates boundaries created by changes in surface material or soil characteristics (for example, the presence of frozen ground or stratigraphic layers). Electrical resistivity tomography is another type of non-invasive geophysical survey that measures the changes in the ability of the ground to conduct electricity along a transect. ERT profiling has been used extensively to investigate mountain permafrost in Europe (e.g., Kneisel et al., 2000, 2008; Hauck et al., 2004; Hilbich et al., 2008, 2009) and is growing in importance in North America as a technique for permafrost investigations in mountains and elsewhere (e.g., Lewkowicz et al., 2011). An electrical resistivity survey produces a two-dimensional image of the subsurface which can be used to identify frozen (high resistivity) versus unfrozen (low resistivity) surface materials or soils, and can therefore be used to map permafrost distribution along a transect. A critical part of the interpretation is the threshold resistivity value that represents the boundary between frozen and thawed surface materials or soils. This value is typically between 300 and 800 ohm m in the southern Yukon (Lewkowicz et al., 2011), but it depends on the local ground temperatures and stratigraphy. The value used for most of the ERT profiles in this report is 800 ohm m which generally coincided with a gradient in resistivity indicative of phase change. A uniform shading scale has been used for all the resistivity profiles presented so that visual comparisons can be made among the figures.

Permafrost characteristics are studied by extracting cores of permafrost from the ground and conducting a series of laboratory analyses on subsections of these cores. These analyses provide information about grain size, porosity, ice volume, and settlement potential, among other properties. These characteristics affect how different surface materials or soils will behave if permafrost thaws, and are also useful in verifying interpretations of the geophysical techniques described above.

HYDROLOGICAL CHARACTERIZATION

The study of the movement and distribution of water is critical in understanding responses to climate change. Having baseline knowledge of the hydrologic regime in an area is essential in defining potential future hazards that are related to climate change. To incorporate hydrological conditions and risk into hazards maps, data about river discharge, lake level and the groundwater table are gathered from monitoring stations. Flood histories are also compiled from existing records and anecdotal evidence. Historical patterns are analyzed, and current conditions are assessed on the context of projected future changes in climate.

PROJECTIONS OF FUTURE ENVIRONMENTAL CONDITIONS

An important component of the hazards mapping projects involves projections of future environmental conditions. They represent an important aspect of adaptation planning, which by definition requires a future focus; thus incorporating future-oriented data is a key element of the development of hazards maps.

The future environmental conditions modelled through this project are done through permafrost probability projections and climate projections. Models of permafrost probability are developed using data from a series of meteorological and permafrost monitoring stations established by research partners throughout the territory. These models build on existing knowledge of permafrost distribution to depict future changes in permafrost under different scenarios of annual air temperature increase as a result of climate change.

Climate projections for each community are developed by using a variety of Global Climate Models (GCMs) in combination with discrete scenarios, in order to make a range of projections for numerous climate variables (e.g., temperature and precipitation) on a local scale. Hazards projects typically incorporate a range of scenarios (reflecting escalating degrees of climate change) at several points in the future (e.g., 2020, 2050 and 2080).

HAZARD RANKING

Hazard mapping applies a variety of scientific data in order to arrive at a hazard risk ranking. The combination of surficial material type (glacial deposits and soils), landform shape and slope, permafrost nature and distribution, hydrological conditions, and present and future climate regime are used to rank hazard risk. For easy interpretation, a stop-light colour coding system is applied to each risk ranking.

The hazards ranking is tailored to suit the conditions in each of the communities mapped. For example, in communities where permafrost presence or absence largely determines risk, three risk categories are sufficient. In environments with more complex landscape conditions (e.g., where permafrost conditions are more nuanced), a fourth risk category is introduced. Tailoring risk ranking to community conditions makes hazards maps relevant and reflective of the local landscape. The hazards risk ranking matrix used in this project is discussed in more detail in the section *“Integrating Risk in a Landscape Hazards Map for the Ross River Region”*, p. 57 of this report.

LIMITATIONS AND UNCERTAINTY

It is very important to note that this report is prepared as a guide for planning. It should not be used as the basis for final site selection for development, and it does not replace geotechnical and/or engineering assessments completed on a site level. Rather, it should be treated as a tool for use in identifying areas of interest with regards to future large scale land use planning, which

will then undergo subsequent site-specific investigations (which may include geotechnical or engineering assessments).

It is also important to note that the classification scheme applied here does contain a level of uncertainty. Because of the scale at which the study area was mapped, and the duration of the field program for this project, researchers were unable to visit all the areas denoted by polygons in the map area. Therefore, results have been extrapolated to polygons beyond case study sites and areas visited by researchers. While we make our most informed assessment of hazards ranking for all polygons, this approach does introduce some uncertainty when making a determination of classification.

Finally, it is important to note that in some cases, a polygon may contain areas of both higher and lower risk. In such cases, we have taken a precautionary approach and applied a category of higher risk where we were not confident in lower categories. This is another reason why the hazards map should serve only as an initial guide for planning purposes, and should not replace site-specific investigations – the landscape within each polygon will vary naturally.

THE ROSS RIVER REGION

Ross River (61.98°N, 132.45°W) is located at the confluence of the Ross and Pelly rivers, on the Canol Road seven kilometres northeast of the Robert Campbell Highway (Figure 1). The community is located 360 km from Whitehorse via the Canol Road, and 410 km from Whitehorse via Carmacks.

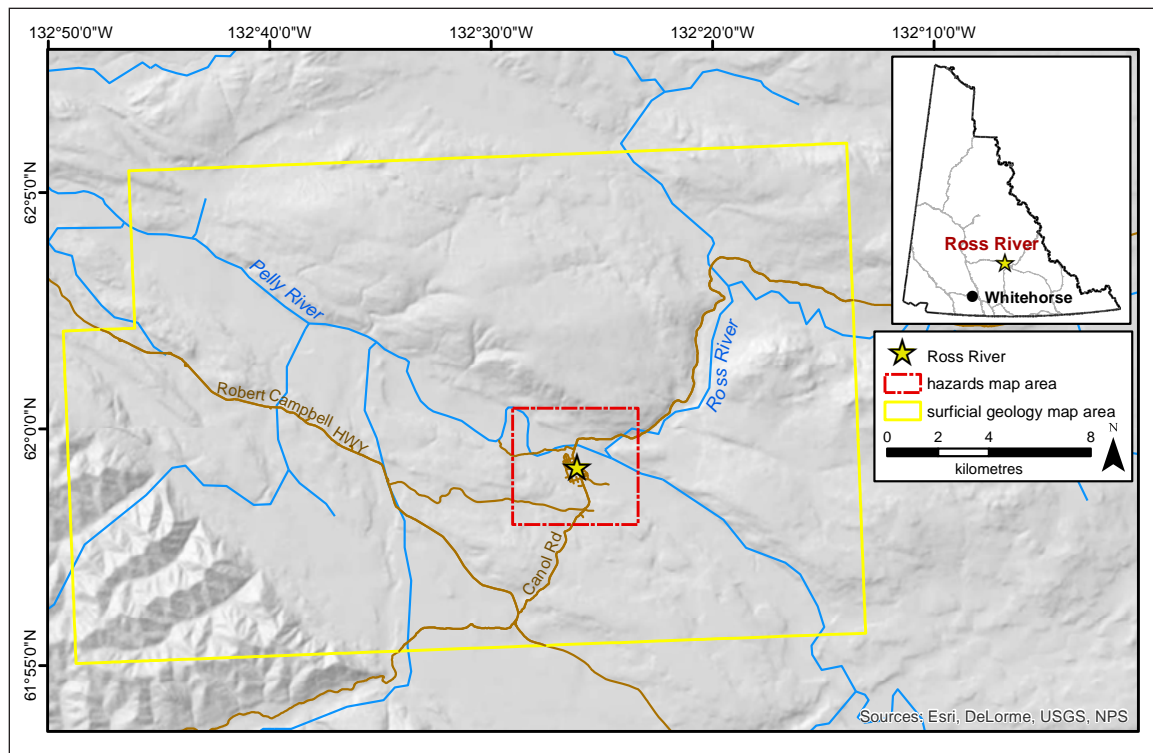


Figure 1. Location of the study area, illustrating the footprints for the surficial geology and hazard maps.

Originally, First Nations people used the area near Ross River as a seasonal camp and gathering place. In 1901, the first permanent settlement was established when Tom Smith started a small fur trading post on the north bank of the Pelly River and called it Smiths Landing. That winter,

approximately 15 First Nation families spent the winter near the trading post and created the beginnings of the permanent community of Ross River. Around this time, prospecting and mining were increasing in the area, and in 1903, a second trading post was established.

The area of Ross River had not experienced any significant changes until the Second World War. In the early 1940s the need for a secure source of oil led the American army to build the Canadian Oil (Canol) pipeline and associated Canol Road. The pipeline ran from Norman Wells in the Northwest Territories to Whitehorse, and the Canol Road opened the Ross River area to overland traffic. Consequently, the commercial centre of the community shifted to the south bank of the Pelly River. Continued change came after the end of the war when government offices were established in Ross River. By the late 1940s and early 1950s the area suffered from the collapse of fur prices and most of the region's fur trading posts were permanently closed. By 1952, Ross River was designated as a band village and had the only remaining trading post in the region (Selwyn Resources Ltd., 2009). At the urging of the Federal Government, the historical settlement on the north side of the Pelly River was abandoned in the mid-1960s. The new town was constructed on the south bank, where it still remains (Zanasi and Taggart, 2006). Today, the community of Ross River provides a gateway to the North and South Canol roads and offers the only service station on the Canol Road. A summer ferry service provides access to the North Canol Road.

The Ross River Dena Council is included in the broader Kaska nation. The Ross River Dena Council has 483 registered members and is a member of the Kaska Tribal Council. The language originally spoken by the people of this First Nation was mainly Kaska, although a number of the First Nation's citizens are Slavey speakers (Ross River Dena Council, 2014). In 2013, 352 people lived in Ross River and approximately 85% of the residents were of Kaska descent (Government of Yukon, 2014).

In 2006, there were 130 occupied private dwellings in Ross River (YBS, 2010), and in 2011, the median value of a single detached house in the community was \$113,878 (Government of Yukon, 2014). In addition to administration buildings, Ross River has an arena, community centre, swimming pool, daycare, nursing facility and emergency health services, and a school that also houses a community library and the Dene Cho Kê'endj campus of Yukon College.

Ross River acts as the administrative hub for the Ross River Dena Council, and along with the territorial and federal departments located here, is the main employer of the community (Government of Yukon, 2014). Accommodation, food services, recreation services and the arts sector also provide employment in Ross River. Many residents of Ross River continue the long-established custom of subsistence living through hunting and fishing, which provides a significant portion of food resources for residents.

PHYSIOGRAPHY

Ross River is located within the Yukon Plateau-North Ecoregion and encompasses the Stewart Plateau, the MacMillan Highland and the Ross Lowland (Smith et al., 2004), and is within the Tintina Trench physiographic region (Mathews, 1986). The Tintina Trench is a prominent linear valley which follows the trace of the Tintina fault (next section) and extends in a northwesterly direction for almost 1000 km from the Northern Rocky Mountain Trench in British Columbia to central Alaska. Within the map area, the 5 to 10 km-wide trench separates the Ross Lowlands to the northeast from the Pelly Mountains and St. Cyr Range to the southwest (Mathews, 1986). The Tintina Trench is abruptly bounded by scarps where it abuts Ross Lowland, MacMillan Highland, and the Pelly Mountains. These scarps range in relief from 100 to 1200 m (Jackson, 1994). The Tintina Trench becomes a deep, narrow, linear valley between the Pelly Mountains and the Simpson Range.

The Stewart Plateau is a series of tablelands separated by a network of broad, deeply cut valleys. The MacMillan Highland consists of small mountain ranges called the Anvil, South Fork, Wilkinson and Russell. The Ross Lowland is slightly lower in elevation and has rolling, rounded hills separated by broad valleys and includes the wide, drift-filled valleys of the Ross, upper Pelly and MacMillan rivers. The rugged Pelly Mountains are a steeply rising range with a local relief of up to 1700 m above sea level (a.s.l.) in the study area. The Pelly River hugs the north side of the Tintina Trench and has an elevation of approximately 700 m a.s.l. near Ross River; the Pelly River drains northwest into the Yukon River. The Ross Lowlands in the region consist of rolling, rounded hills (less than 1500 m a.s.l.) and wide, low-elevation valleys. This area contains the headwaters of the Pelly and Ross rivers, as well as the community of Ross River (Jackson, 1994).

In the vicinity of Ross River, the Yukon Plateau-North Ecoregion is bounded on the southwest by the Pelly Mountains and on the southeast by the Simpson Range, both of which are marked by classic alpine arête and horn peaks (Jackson, 1994). In the Pelly Mountains, elevations range from major valley floors at 700 m to summits exceeding 2100 m (Jackson, 1994). The Tintina Trench, a major northeast-trending valley controlled by the Tintina and its related faults, separates the Pelly Mountains from the MacMillan Highland, Ross Lowland and Simpson Range (Jackson, 1994). The Yukon Plateau-North Ecoregion includes a 450-km length of the Tintina Trench.

Jackson (1994) reports that throughout this ecoregion:

“Evidence of past glaciation is ubiquitous. Summits above 1800 meters typically feature arête ridges, cirques and horn peaks. Lower plateaus and the sides of larger valleys are marked by whaleback ridges and crag-and-tails, which indicate past ice flow directions. Valley bottoms contain complexes of glaciofluvial deposits or thick fills of glaciolacustrine sediments. Flights of gravelly benches are common on mountain sides and are nearly continuous from valley floor to mountain summit. The gravelly benches are the beds of former ice-walled channels.” (Page 6)

VEGETATION

Vegetation is determined by elevation, topography and microclimate. The vegetation of this ecoregion ranges from boreal to alpine. Northern boreal forest exists at elevations up to 1500 m. Areas of higher elevation in this ecoregion are characterized by shrub and lichen tundra. In the subalpine environment, the dominant vegetation types include shrub birch, pine, white spruce, subalpine fir, and a lichen understory. Extensive shrublands exist at mid-elevations and on valley bottoms subject to cold air drainage. In the boreal zone, open black spruce with a moist moss or drier lichen understory is the dominant forest type. Black spruce dominates under poorly drained conditions and commonly indicates the presence of underlying permafrost (Jackson, 1994).

Mixed canopy forests are common due to frequent forest fires (Smith et al., 2004). The fires are caused by a high incidence of thunderstorms and lightning strikes along the Tintina Trench. Lodgepole pine frequently invades burned areas, occasionally forming extensive forests. Also common on disturbed sites are trembling aspen and balsam poplar. Paper birch is scattered throughout the ecoregion, usually occurring on cooler sites.

Low ericaceous shrubs, prostrate willows and lichens dominate the alpine. Talus slopes, common at high elevations, support communities of crustose lichens. Moister sites support more moss and graminoids than lichen.

Grasslands consisting of sagewort, juniper, kinnikinnick, forbs and aspen are common along the banks of large rivers and are often contiguous with unglaciated high-elevation areas that would

have supported similar vegetation during the last glacial period. These grassland plant communities are considered relicts of the glacial period.

The wetlands that exist on the margins of small lakes, marshes and shallow open water are dominated by willows, sedges and aquatic plants. Black spruce bogs, containing sedge tussocks and sphagnum moss and underlain by permafrost, occur in lowland areas throughout the ecoregion.

CONTEMPORARY CLIMATE

Ross River is located in the Central Yukon Basin (Wahl et al., 1987). The St. Elias Mountains and the region’s distance from the Gulf of Alaska influences its climate, making it climatically different from those areas in southern Yukon. Temperatures are highly variable – summers can be extremely warm, while winters can have long, very cold periods. The record-low temperature for continental North America was recorded in this climate zone at Snag, Yukon (-62.8°C on February 3, 1947). Precipitation in Ross River is typically lower than other stations in this region, due to a local rain shadow provided by the St. Cyr Range in the Pelly Mountains. Storm centres commonly skirt this region, especially in winter (Wahl et al., 1987).

Based on 30-year (1981-2010) climate normal data collected from the Faro Airport meteorological monitoring station (the closest station with a long-term monitoring record; 62°12’ N, 133°22’ W), average January and July temperatures are -20.1°C and 15.0°C, respectively, while average annual precipitation is 319.7 mm; approximately one-third of the precipitation falls as snow during the winter season (Environment Canada, 2014a). Month-by-month climate normal temperature and precipitation data are summarized in Figure 2.

Mean annual air temperatures (MAAT) vary with elevation across the region. Measurements made at Faro, which is comparable to the Ross River region, show an average change in MAAT up to treeline of -2.3°C per 1000 m (Lewkowicz and Bonnaventure, 2011), which is a much slower rate of cooling than the global average of -6.5°C per 1000 m. This is due to the cold air pooling in the valley bottoms in winter which offsets the more normal warmer conditions in the valley bottoms in summer.

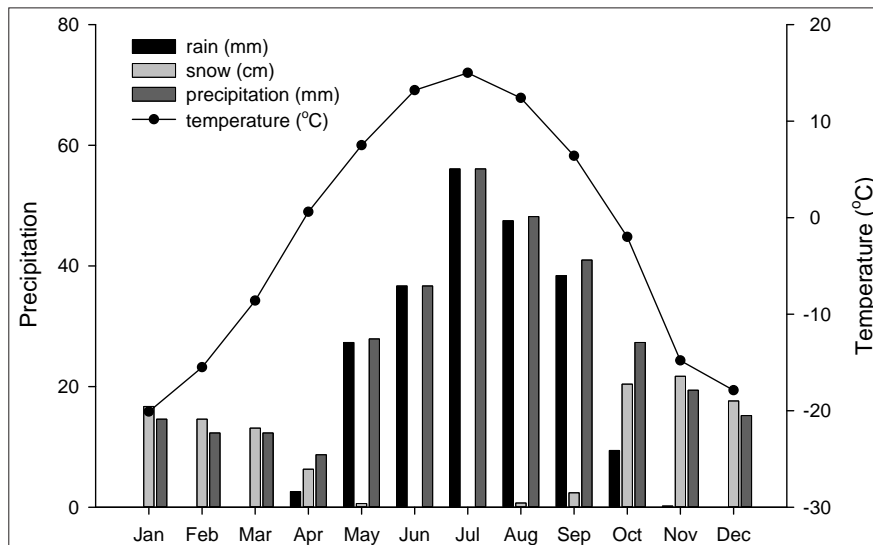


Figure 2. Climate normal (1981-2010) temperature and precipitation data for the Faro Airport meteorological monitoring station (Environment Canada, 2014a). To calculate total precipitation in millimetres, snowfall was converted to snow water equivalent (SWE) and summed with rainfall.

PAST CLIMATE TRENDS

Environment Canada produces regional summaries of climate and precipitation data that provide a generalization of climate trends by integrating instrumental data from several stations (Environment Canada, 2014b). For this region, Environment Canada amalgamates data from northern British Columbia and Yukon stations, which has allowed them to develop a record of regional climate trends that spans the past 65 years. Data indicate that between ~1950 and 1975, the regional climate was generally cooler and drier than normal (based on 1961-1990 climate conditions), while between ~1975 and 2013, the climate was generally warmer and wetter than normal (Figure 3).

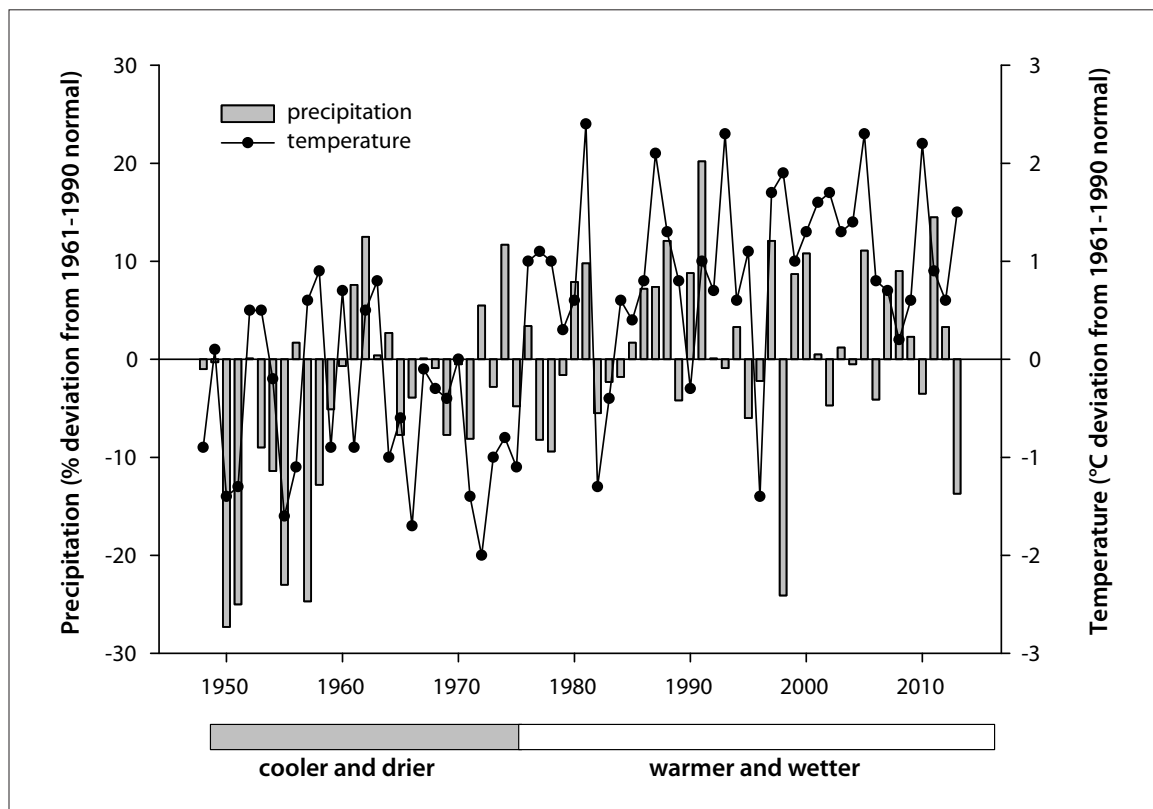


Figure 3. Regional climate trends for northern British Columbia and Yukon, developed using data amalgamated by Environment Canada (2014b). Data has been normalized to indicate deviation from 1961-1990 climate normal conditions. Negative values indicate precipitation amounts and temperatures below normal for the 1961-1990 period, while positive values indicate exceedance of normal conditions.

To examine past climate trends, the historical data record from the Faro Airport meteorological monitoring station was examined. Temperature data is available for the period 1979-2013 (Figure 4). The data were amalgamated by season for simplicity, and linear regressions were superimposed on seasonal data records. While the trends they represent are not statistically significant, the regression lines do provide a basis for identifying potential trends in temperature over the period of record.

The greatest range in seasonal temperature variability occurred in the winter, with a 14.8°C difference in the highest and lowest recorded temperatures over the period of record. In contrast, summer temperature variability was lowest (3.7°C). Temperature ranges in spring and fall are comparable (6.4°C and 8.1°C, respectively). Regression lines suggest winter temperatures are

increasing slightly over the period of record, which is consistent with modelling that predicts climate change-induced temperature increases will be greatest in winter (Warren and Lemmen, 2014). Interestingly, summer temperatures also appear to be increasing slightly over the period of record, while shoulder-season temperatures (spring and fall) remain relatively stable or show a slight decline.

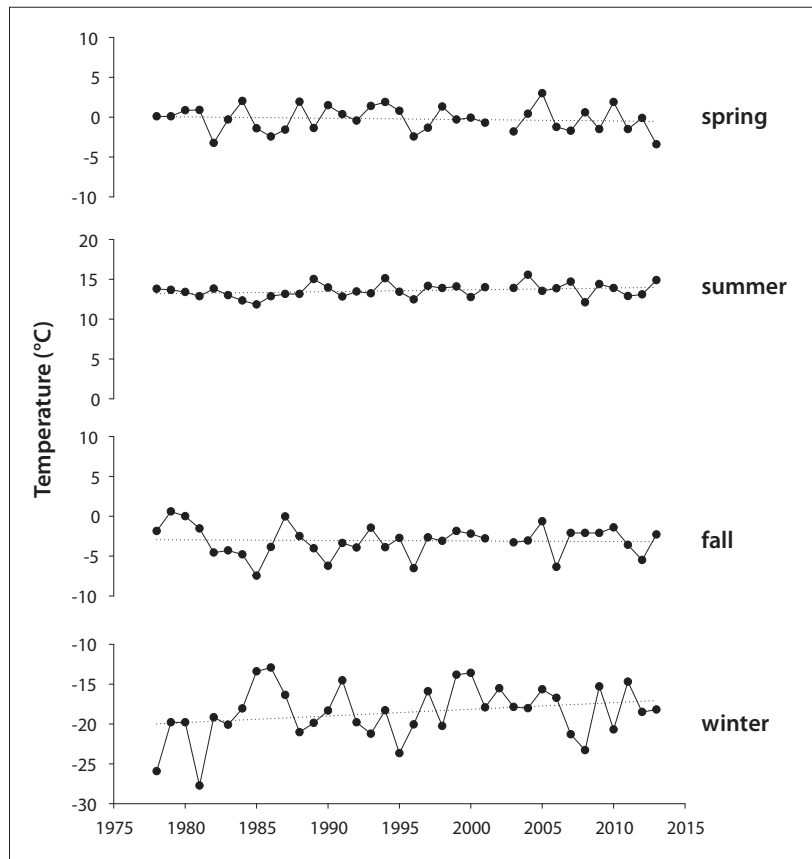


Figure 4. Past temperature records measured at the Faro Airport meteorological monitoring station (Environment Canada, 2014a). Seasonal average and mean annual temperatures are illustrated (spring = Mar-May; summer = Jun-Aug; fall = Sep-Nov; winter = Dec-Feb). Dotted lines denote linear regressions for each data series.

HYDROLOGY

SURFACE WATER

The subwatershed of the Ross River region forms part of the Yukon River watershed, which covers 260 000 km² or 54% of Yukon Territory (Smith et al., 2004). The area is situated in the Interior Hydrologic Region of the Territory, where drainage from the southern foothills of the Selwyn Mountains flows west to the Yukon River. The first and second-order streams descending from the foothills are generally steep and relatively short, producing rapid, flashy streamflow responses during the spring melt and some of the highest peak flows in Yukon. Mean annual runoff in the region is moderately high compared with other regions of the Territory, at 236-385 mm (average 309 mm; Smith et al., 2004). Peak river flows in the Interior Hydrologic Region generally occur in May and June in response to snowmelt inputs during the spring freshet, while secondary discharge

peaks in response to late summer and autumn rainfall are also possible. Lowest flows are typically exhibited in this region in March and April, when groundwater contributions to streamflow, the only inputs to river discharge at this time, are minimal (Janowicz, 2008).

The community of Ross River is situated at the junction of the Ross and Pelly rivers, at 693 m a.s.l. on an alluvial terrace of the Pelly River (see Figure 1). Here, the 100-year flood elevation of the Pelly River is estimated at 694.0 m a.s.l. (Gartner Lee Limited, 2003), making the community susceptible to flooding. Notably, localized flooding occurred twice in Ross River in summer 2013, when high water due to heavy snowpacks and a break in an upstream ice jam breached the dike that protects the community (CBC, 2013).

From its headwaters in the Mackenzie Mountains, the Pelly River flows generally west 530 km to its confluence with the Yukon River at Fort Selkirk, 25 km downstream of Pelly Crossing. By the time it reaches the community of Pelly Crossing, the Pelly River has drained an area of approximately 49 000 km². In contrast, the Ross River, between its headwaters (also in the Mackenzie Mountains, north of the headwaters of the Pelly River) and its confluence with the Pelly River at the town of Ross River, drains an area of approximately 7300 km² (Water Survey of Canada, 2015).

The Water Survey of Canada (WSC) has maintained several gauging stations in the region over the past several decades, some of which provide real-time hydrometric data. (See Table 1 for a summary of station information.) The WSC reports daily average, monthly average, and peak yearly discharge for each station (Water Survey of Canada, 2015). A hydrograph of monthly average discharge for the Pelly River at Vangorda Creek (the station closest to Ross River with the most complete recent record; Figure 5) demonstrates the typical seasonal pattern of a river in Yukon’s Interior Hydrologic Region, with rapid increases in discharge in April, May and June, followed by a recession through summer and autumn. Average monthly discharge is low through the winter months, when groundwater is the only input to the river, and the lowest flows occur in March, prior to the spring freshet. Figure 5 also illustrates monthly average discharge for 1980 and 1992, the two years on record with the lowest and highest June peak discharge, respectively.

Table 1. Summary of Water Survey of Canada’s stations in the Ross River region (Water Survey of Canada, 2015). Stations are listed roughly in the order that they appear, from headwaters to mouth.

Station name	Station ID	Latitude	Longitude	Gross drainage area (km ²)	Parameter	Period of record*
Ross River at Ross River	09BA001	61.989	-132.408	7250	flow, level	1960-2013
Pelly River below Fortin Creek	09BA002	62.031	-130.603	5020	flow	1986-1994
Pelly River at Pelly Crossing	09BC001	62.830	-136.581	49000	flow, level	1960-2013
Pelly River at Ross River	09BC002	61.987	-132.448	18400	flow, level	1954-2013
Rose Creek below Faro Creek	09BC003	62.342	-133.408	208	flow	1966-1969
Pelly River below Vangorda Creek	09BC004	62.222	-133.378	22100	flow, level	1972-2013

* Periods of record do not always contain complete datasets.

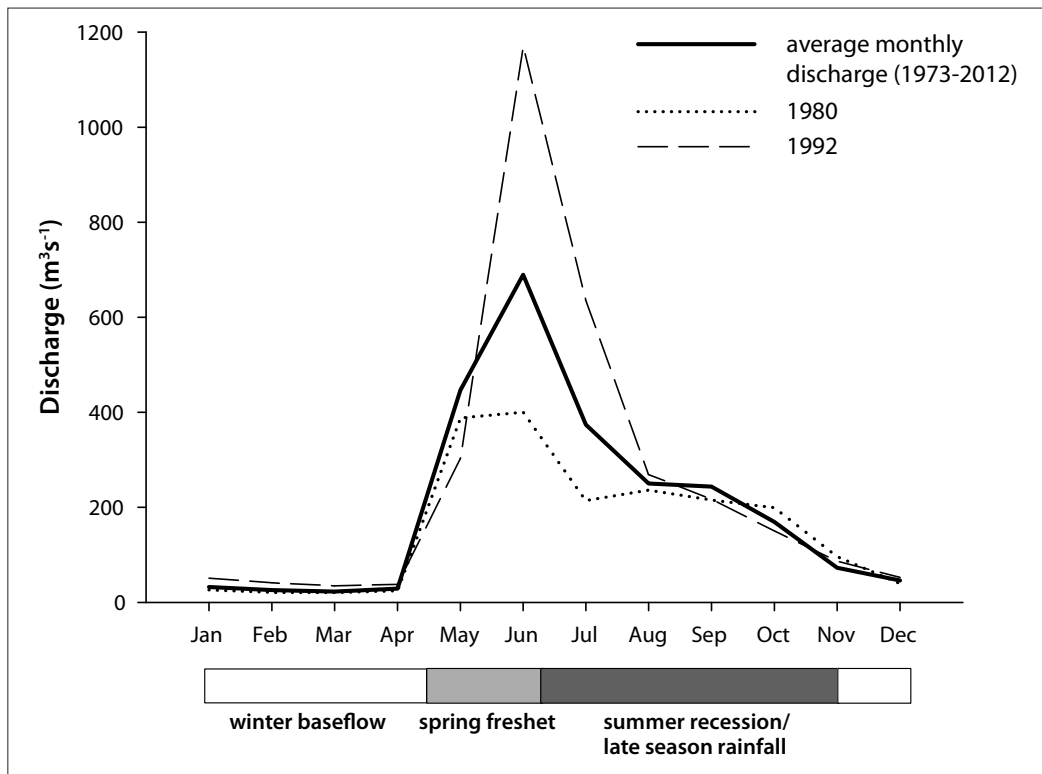


Figure 5. Average monthly discharge hydrograph for the Pelly River below Vangorda Creek (heavy solid line). Also shown are hydrographs for the years 1980 (dotted line) and 1992 (long-dashed line), demonstrating lowest and highest measured peak June discharge, respectively (Water Survey of Canada, 2015).

Peak yearly discharge also provides a basis for assessing the dynamics of surface water hydrology of the Ross River region. Figure 6 presents peak yearly discharge for all WSC stations with year-long data in the vicinity of Ross River (see Table 1 for details of WSC station locations; Rose Creek has been excluded because of its short duration, seasonal record). As previously described, peak discharge usually takes place during the spring freshet, when snowmelt inputs are high. Figure 6 clearly demonstrates that peak discharge events measured at headwater stations are mirrored in the discharge records of downstream stations, highlighting the importance of headwater snowmelt inputs to the Pelly River system (see NCE, 2011 for more details). It is also possible that those years in which headwater snowpacks are deep (producing high volumes of snowmelt and high, peak spring discharge events), downstream snowpacks are also deep. Thus, snowmelt contributions may continue to be significant along all reaches of the Pelly River and its tributaries, and act as a key input to discharge along the river system.

GROUNDWATER

Relatively little information is available regarding groundwater in the Ross River area. The water table is reported to be 1.0-3.2 m below the surface, within shallow deposits of sand and gravel that are likely hydraulically connected to the Pelly River (Gartner Lee Limited, 2003). There are four groundwater wells in Ross River - two domestic, one commercial/institutional, and one municipal/communal (installed in 1986 and considered to be the municipal well). The municipal well is in a deep aquifer, which occurs at 105-110 m below the ground surface (Gartner Lee Limited, 2003). Low-permeability silt and sand deposits are between the shallow water table and the deep aquifer in the area.

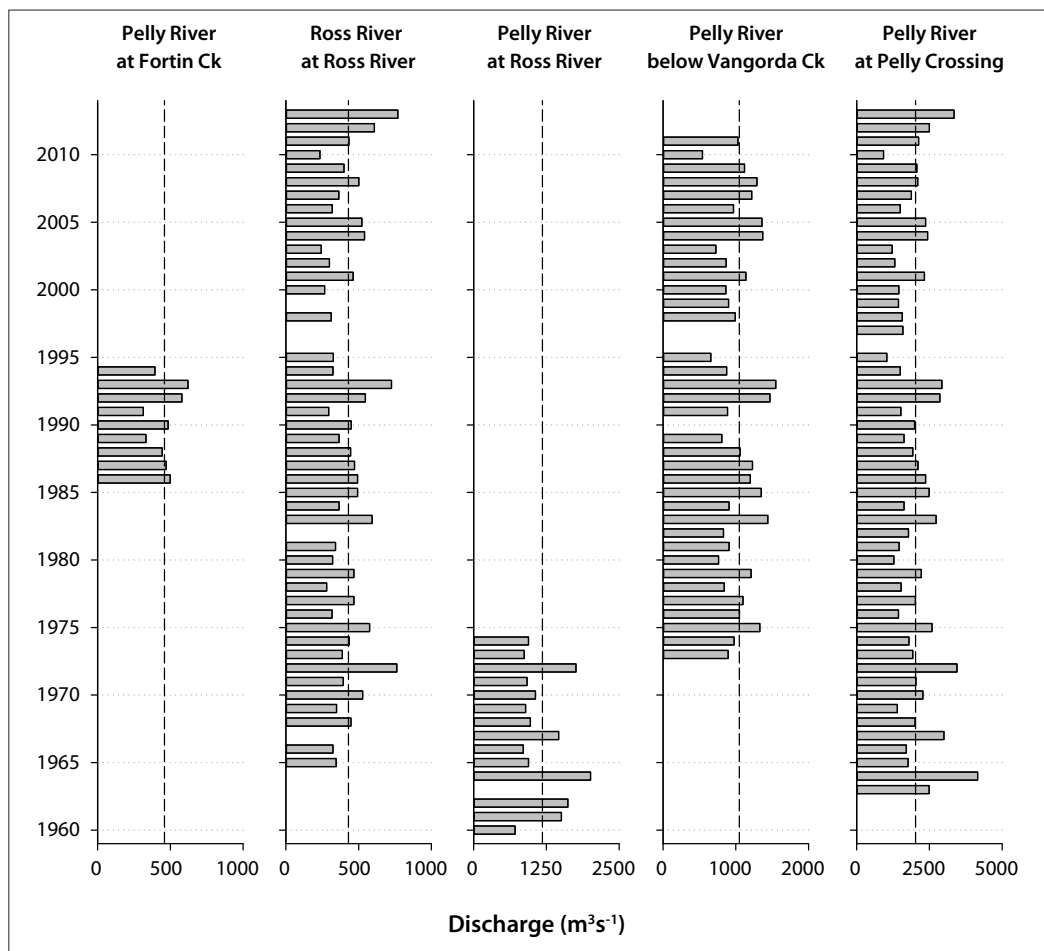


Figure 6. Peak discharge at WSC stations with full-year records, arranged generally upstream (left) to downstream (right). Vertical, long-dashed lines indicate average peak discharge for each station for its period of record (Water Survey of Canada, 2015).

ENVIRONMENTAL DISTURBANCE HISTORY

The majority of the environmental disturbance in the Ross River region has been the result of anthropogenic forces over the past several decades. These disturbances began around 1942, during the Second World War, with the construction of the Canol Road and pipeline.

The construction of the Canol pipeline was the source of many disturbances in the area, including its contribution to the migration of the commercial centre of Ross River from the north to the south bank of the Pelly River. Several factors, including project-related time pressures, led to the Canol pipeline being built directly on the ground surface. As a result of construction disturbance, permafrost under the pipeline began to thaw, causing the pipeline to sink into the ground beneath it (Government of Yukon, 1992). In turn, erosion and flooding resulted. Cracked pipes and repeated breaks in the pipeline, likely due to fast-tracked welding, were also the cause of several oil spills. There are reports that a storage tank on the banks of the Mackenzie River burst while two-thirds full, spilling its contents into the adjacent waterway.

The Canol pipeline operated for 13 months from 1944-1945 and was dismantled in 1949. In the late 1950s, the Canadian government launched a “Roads to Resources” program that encouraged natural resource development by supporting the creation of road networks (Weinstein, 1992). As

a result, the South Canol Road was re-opened, the Robert Campbell Highway between Ross River and Watson Lake was constructed, and the Nahanni Range Road to the pending CanTung tungsten mine was built (Weinstein, 1992; Dimitrov and Weinstein, 1984).

Since 1962, mining projects in the area have also contributed to landscape disturbance. In 1962, the CanTung mine, located in the Northwest Territories at the NWT/Yukon border, was opened. This mine ran on a fairly full-time basis until it closed in 1986 (Deklerk and Burke, 2008). In 2001, the CanTung mine was reopened and has operated intermittently since then (<http://www.natungsten.com/>). In 1965, in anticipation of the Faro mine site opening, the road between Carmacks and Ross River was constructed. In 1966, the Faro mine complex and town site were developed (Weinstein, 1992). The Faro mine site operated between 1969 and 1998, although between 1983 and 1998 the mine was operated by various owners and opened and closed several times. Ultimately, an interim receiver was appointed in 1998 to handle assets of the company operating the mine at the time, and to maintain the site.

Additionally, the Ketz River Mine operated just south of Ross River between 1988 and 1990, and the Sa Dena Hes mine, which is located 50 km northeast of Watson Lake, operated between 1991 and 1992 (Deklerk and Burke, 2008).

Forest fire disturbance has also impacted the Ross River area. As indicated in Figure 7, it was during the 1950s that the study area experienced the largest impact from forest fires. Environmental disturbance as a result of the forest fires includes changes in vegetation and re-establishment of early successional species. However, subsequent impacts on permafrost are also possible, including active layer deepening and degradation of the upper layers of permafrost. Because the organic mat on the forest floor acts as an insulator for permafrost, its disturbance can result in deepening of the active layer, alterations to surface albedo, and accelerated permafrost thaw or the development of taliks (an unfrozen layer between the seasonally thawed active layer and the permafrost) (Yoshikawa et al., 2003). Forest fire impacts on permafrost in the Ross River region will be discussed in more detail later in this report.

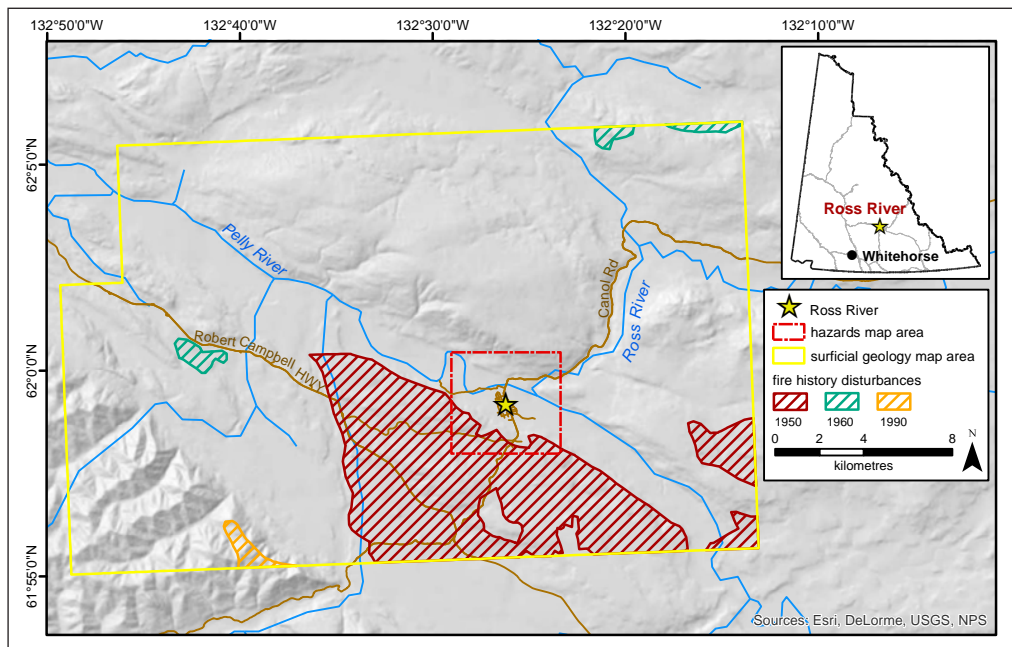


Figure 7. Fire history for the Ross River region, illustrating fire activity by relevant decade. Fire history records provided by Government of Yukon.

BEDROCK GEOLOGY

Regional mapping of bedrock geology in the study area was originally completed by Tempelman-Kluit (NTS 105F; 1977, 2012) and Gordey (NTS 105K; 1995, 2013a,b) at a 1:250 000 scale. These maps were compiled into the Yukon Digital Geology map, a compilation which is regularly updated (e.g., Gordey and Makepeace, 2003), most recently in 2015 (Colpron, 2015); Figure 8 is based on this most recent update.

Tintina fault is the most striking bedrock geological feature of the study area, roughly forming the southwest boundary of Tintina Trench (Figure 8). The fault has not been active since the early Tertiary time (~65 million years ago), when approximately 430-490 km of dextral strike-slip displacement occurred (Roddick, 1967; Tempelman-Kluit, 1980; Gabrielse, et al., 2006). The fault juxtaposes widely different geological domains on either side: rocks of the Cassiar terrane, a displaced fragment of the North American passive continental margin are to the southwest, whereas rocks of the Yukon-Tanana and Slide Mountain terranes, which originally formed in the Paleo-Pacific Ocean, are mapped to the northeast. Cretaceous and Tertiary igneous rocks are observed locally on both sides of the fault. Small basins bounded by normal faults occur near Ross River within a broader Tintina fault zone in which early Tertiary volcanic and sedimentary rocks were deposited.

Immediately southwest of the Tintina Trench, the Pelly Mountains are underlain by rocks of the St. Cyr assemblage, a component of the Cassiar terrane. Rocks of the poorly understood St. Cyr assemblage are Cambrian to Devonian in age (~540-360 Ma) and consist of marine slate and shale (CDS1, 3, 4 and 5 in Figure 8).

Yukon-Tanana and Slide Mountain terranes within and northeast of the Tintina fault zone comprise a wide diversity of rock types, mostly of upper Paleozoic age (360-250 Ma). Chert and cherty tuff (a fragmental volcanic rock) are found directly northeast of the Tintina fault (CK3 on Figure 8). A prominent light grey limestone (CK2) is found north of the Danger Creek fault and contains Late Pennsylvanian to Early Permian (~300 Ma) fossils. Dark grey metamorphosed shale (carbonaceous phyllite; DMF3) and pale green metamorphosed basalt (DMF1), both probably of Late Devonian age, are also found in this region. A belt of metamorphosed basalt and chert (CPSM2), possibly of Early Permian age (300-280 Ma), is found north of these rocks and extends to the Lapie River fault. Between the Lapie River fault and the northern limit of the Tintina Trench, metamorphosed sandstone, shale and mafic igneous rocks (PDS5) occur; these formed in a marine basin and were then dragged deep into the earth's crust in a Late Permian (~260 Ma) subduction zone.

South of the Ross River townsite, the Tintina fault zone is between the Tintina fault proper to the south, and the Lapie River fault to the north (Figure 8). In this region, Cretaceous (KS6; ~100 Ma) and Tertiary (ITR3; ~55 Ma) sedimentary and volcanic rocks are faulted against, and possibly locally deposited on, older metamorphosed and deformed sedimentary and volcanic rocks of Yukon-Tanana and Slide Mountain terranes. Near Whisker Lake, approximately 3 km south of the Ross River townsite, coal-bearing sandstone and conglomerate are faulted against the surrounding rocks of Yukon-Tanana and Slide Mountain terranes. This sequence contains dinosaur tracks and is mid-Cretaceous in age (Long et al., 2001; Gangloff et al., 2004). Coal within this sequence was mined to dry ore from the Faro mine prior to shipping to Skagway. Tertiary rocks occur mainly between the Tintina and Danger Creek faults. Tertiary volcanic rocks are primarily rhyolite with lesser basalt; the sedimentary rocks comprise mainly sandstone and conglomerate with local coal. The Tertiary rocks were deposited as the region between the Tintina and Lapie River faults dropped downward relative to surrounding rocks during the overall strike-slip displacement.

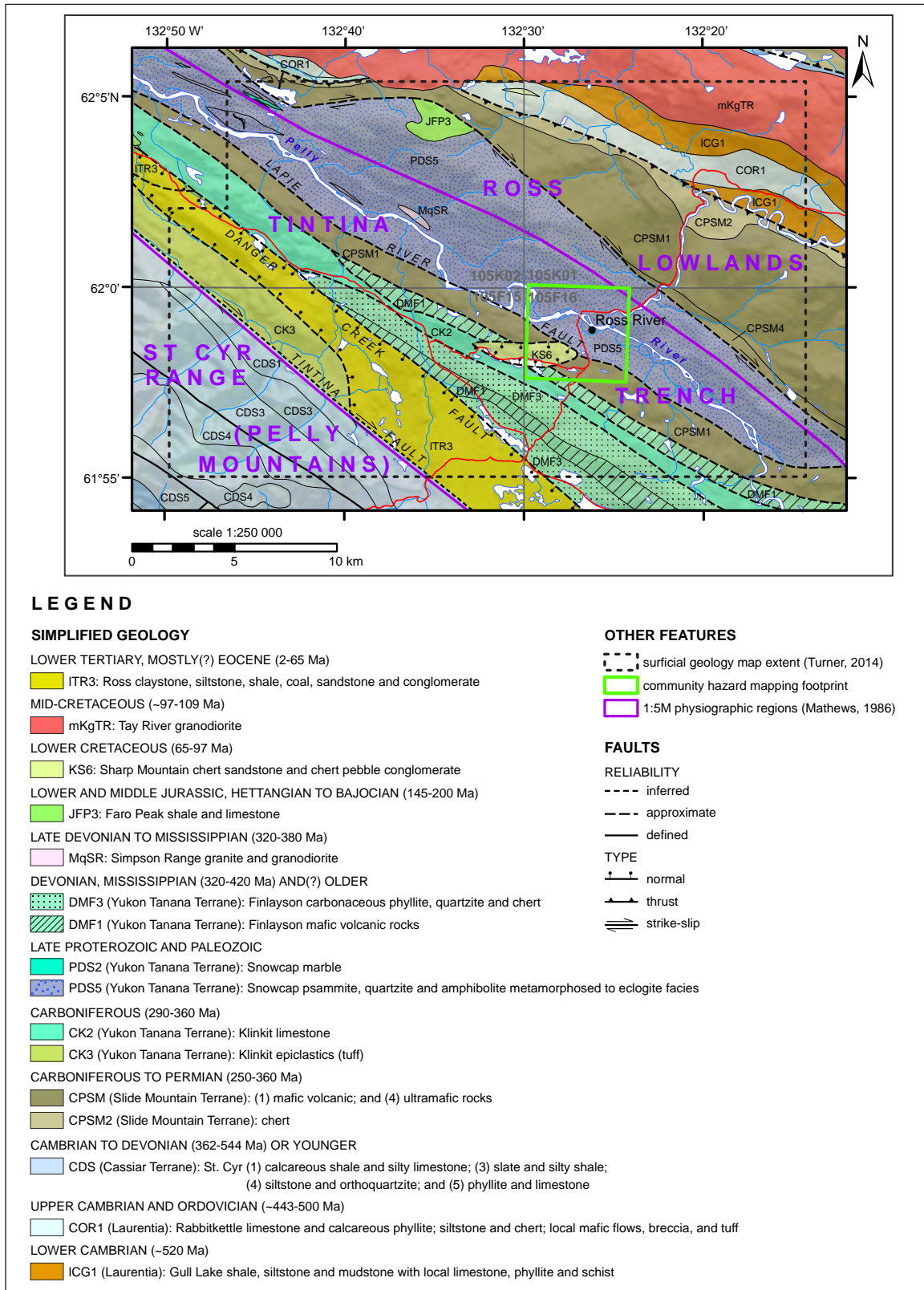


Figure 8. Simplified bedrock geology of the Ross River area based on Colpron's (2015) 1:250 000-scale compilation. Physiographic-region delineations are approximated based on Mathews (1986) 1:5 000 000-scale map.

The southwestern portion of the Ross Lowlands are primarily underlain by mafic volcanic rocks (e.g., basalt, gabbro and greenstone (CPSM1 KS6 on Figure 8); chert (CPSM2); and lesser ultramafic rocks (pieces of the earth's mantle; CPSM4) of the accreted Slide Mountain terrane. These rocks formed in an oceanic setting offshore of the ancient North American continental margin during the Carboniferous and Permian periods (360-250 Ma). Further to the north, the Ross Lowlands are underlain by ancient North American (Laurentian) sedimentary rocks (COR1 and ICG1), and mid-Cretaceous (~109-97 Ma) Tay River Suite plutonic rocks (mKgTR), including quartz monzonite and granodiorite.

LANDSCAPE EVOLUTION DURING THE PLEISTOCENE AND HOLOCENE EPOCHS

Following millions of years of tectonic activity (discussed in the previous bedrock geology section), the present-day landscape configuration of the study area is largely a product of glacial activity during the Pleistocene (2.6 million years to 10 thousand years (ka) before present), combined with more recent Holocene (10 ka to present) modification by fluvial (stream) erosion and deposition, as well as colluvial (gravity) and cryogenic (ground freezing) processes.

The study area was repeatedly glaciated during the Pleistocene. To the northwest, closer to Dawson, at least seven advances of the Cordilleran Ice Sheet and local, montane ice from the Ogilvie Mountains, filled the Tintina Trench with glacial sediment (Duk-Rodkin et al., 2010). The oldest of these occurred 2.64 million years ago in the Late Pliocene (Froese et al., 2000; Hidy et al., 2013). In the study area, however, most of the material deposited by these earlier glaciations has been eroded or buried. The oldest glacial sediment in the study area could be from either the early Wisconsinan Gladstone glaciation (ca. 75-60 ka) or the previous Reid glaciation (ca. 190-130 ka). These sediments are only exposed in a handful of stream cutbanks within the study area, where they are buried at depth beneath younger deposits (Plouffe, 1989; Jackson, 1994). Most of the surficial materials and glacial landforms that currently exist in the study area were deposited in the most recent, late Wisconsinan McConnell glaciation (ca. 25-10 ka).

During the onset of the McConnell glaciation, ice flowed from well-developed alpine cirques in the Pelly Mountains and down the Lapie River valley into the Tintina Trench (Plouffe, 1989). The influx of meltwater into the trench from these accumulating glaciers caused the Pelly River to develop a braided and rapidly aggrading "advance outwash" floodplain (Ward and Jackson, 2000). This initial phase of glaciation was followed by an advance of the Selwyn lobe of the Cordilleran Ice Sheet from its source region in the Selwyn Mountains (Jackson et al., 1991). During glacial maximum, an ice divide formed east of Finlayson Lake. Ice from this divide flowed southeast towards the Liard Lowland and northwest down Tintina Trench across the study area.

At its maximum, the Cordilleran Ice Sheet reached elevations between 1550 and 1900 m a.s.l. over Faro and Ross River (Jackson, 1994), covering all but the highest peaks. Despite its thickness, the ice sheet was never topographically independent in this area. Instead, it was composed of numerous ice streams that diverged and coalesced around, and out of, large topographic obstacles such as the Anvil Range (Jackson, 1989; Bond, 1999b). A radiocarbon date on a *Bison priscus* bone fragment at a site along the Ketz River, 30 km southeast of Ross River, yielded an age of 26,350 ± 280 before present (BP) (TO-393; Jackson and Harington, 1991). This provides a maximum age for the start of the McConnell glaciation in this area.

Deglaciation in the study area was likely a combination of active frontal retreat with re-advances and final stagnation of the ice sheet. Jackson (1994) made several observations that he used as evidence for a rapid rise in the equilibrium line and widespread stagnation and down wasting of the ice sheet: high-elevation stagnation features (e.g., ice-contact or kame features) in the Pelly Mountains; thick and highly disturbed supraglacial sediments infilling valleys; and progressively

lower lake elevations blocked by melting ice in the valley floor. However, others have found evidence that ice was still dynamically retreating during deglaciation, with multiple short re-advances of trunk ice flowing from Tintina Trench up-slope into the Lapie River valley and Pelly Mountains (Plouffe, 1989; Bond and Kennedy, 2005). One possible scenario is that the ice sheet initially actively retreated, before the equilibrium line rose above the ice elevation, causing wholesale starvation of the remaining ice.

The timing of deglaciation is not well known, and is the focus of research currently being undertaken by the Yukon Geological Survey and Simon Fraser University (J.D. Bond, pers. comm.). Ward (1989) radiocarbon dated a *Pisidium* sp. shell in the Glenlyon Range to the west of the study area, yielding an age of $12,590 \pm 120$ BP (TO-931). However, this date is likely too old due to hard water effects. Other ages from willow wood at the confluence of the MacMillan and Pelly rivers ($9,140 \pm 540$ BP; AECV-484C), and seeds from northeast of Faro ($10,550 \pm 40$ BP; Beta-128239) provide a minimum age for the establishment of upland vegetation across the study areas (Ward, 1989; Bond, 1999a; Beierle and Bond, 2002). Immediately following McConnell ice retreat, a large glacial lake formed in the Tintina Trench (Bond, 2001a; Jackson, 1994), depositing the thick glaciolacustrine sediments that are exposed in steep escarpments below the town of Faro and in many places along the banks of the Pelly River.

During the Holocene, a number of geomorphological adjustments occurred as the landscape transitioned from a glacial to a non-glacial regime. At the beginning of the Holocene, freshly exposed and unstable glacial deposits provided increased sediment loads for braided streams causing the rapid building or aggradation of alluvial fans and the Pelly and Ross river floodplains. Organic deposits began to accumulate at the surface as warmer and wetter climatic conditions returned, and vegetation and soil processes were re-established. As the rate of upland erosion and sediment supply gradually declined, streams transitioned from braided to meandering systems. Terraces (such as the glaciofluvial terrace at the mouth of Ross River) were formed as streams incised into the former fans, floodplains and glacial sediments. Based on radiocarbon dating, incision by the Pelly River approximately 100 km east of Ross River began at least 8000 years BP (Jackson, 1994). Incision continued until sometime before 1200 years BP, as indicated by the presence of White River tephra (volcanic ash) within modern floodplain deposits (Jackson, 1994).

Changes in climate through the Holocene had an impact on the development and degradation of permafrost. In general, permafrost may take decades to centuries to form, and equally long periods to degrade, although degradation can accelerate if surface ponding occurs or if ice within the ground is exposed. The surface organic mat can help preserve the permafrost for some decades during a warming phase, leading to what is termed ecosystem-protected permafrost (Shur and Jorgenson, 2007). Forest fire, which destroys the organic mat, may lead to the permanent loss of permafrost. The evolution of permafrost conditions in the Ross River area has not been studied in detail, but it can be inferred that permafrost existed beneath any exposed land during the last glacial period, and formed in newly exposed land during deglaciation. During the Holocene, it may have aggraded and degraded several times in response to cooling and warming, respectively. The latest phases of such changes are the cooler period of the Little Ice Age which lasted for several centuries up to the end of the 19th century, and the 20th century climatic warming which has continued through to present. Given lags in the reaction of permafrost, permafrost in the area is undoubtedly in a degrading phase.

SURFICIAL MATERIALS

Surficial materials in the Ross River area are depicted in an accompanying 1:25 000-scale map by Turner (2014; YGS Open File 2014-13). These materials are broadly classified into a variety

of genetic types, based on the physical processes they are derived from, including: organic (soil development); colluvial (downslope movement or creep); fluvial (rivers and streams); and glacial (ice, glacial streams and lakes). Each of these material types are described below based on their texture or grain size (e.g., gravel, sand, silt or clay); sorting (variety of grain sizes); structure (e.g., layering or bedding); association with permafrost; and the general distribution of the material.

ORGANIC MATERIALS

Organic materials are produced by the accumulation of decomposing vegetative matter and contain at least 30% organic matter by weight. They are generally found at the surface in low or flat-lying areas and in poorly drained depressions (especially in the swales between streamlined till and bedrock landforms within Tintina Trench; e.g., Figure 9a,b). Poor drainage associated with these deposits inhibits decomposition of organic material and results in fibric or peaty textures, although mesic and humic textures were also observed. Shallow permafrost is commonly encountered in, or beneath these materials due to their insulating capacity.

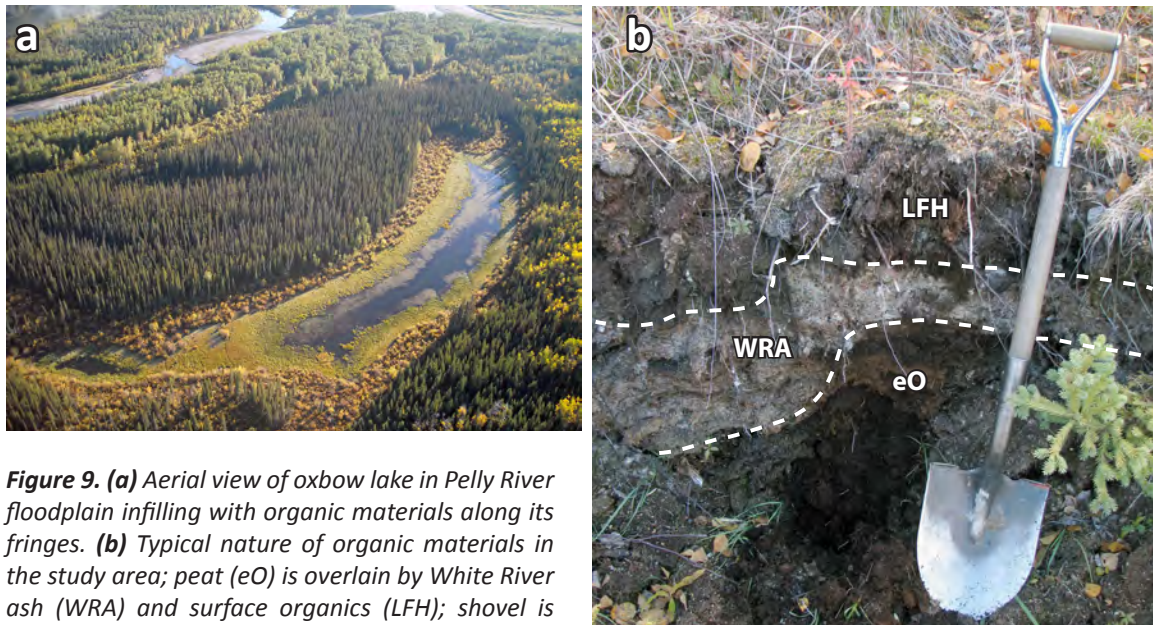


Figure 9. (a) Aerial view of oxbow lake in Pelly River floodplain infilling with organic materials along its fringes. (b) Typical nature of organic materials in the study area; peat (eO) is overlain by White River ash (WRA) and surface organics (LFH); shovel is 1 m.

VOLCANIC MATERIALS

A distinctive, white layer of volcanic ash known as the White River tephra is preserved near the ground surface in most areas (Figure 9b; also visible in Figures 39 and 42, shown later in this report), often immediately below the surface organic mat. However, it is generally not mapped because it is so thin (typically 10-20 cm thick in the map area). The source of the volcanic ash was near Mt. Bona-Churchill in the St. Elias Mountains, about 25 km west of the Yukon-Alaska border. The most recent eruption occurred approximately 1200 years ago (Lerbekmo and Campbell, 1969; Clague et al., 1995; Lerbekmo, 2008; Jensen et al., 2014).

COLLUVIAL MATERIALS

Colluvium (Figure 10a,b) is sediment transported and deposited on, or at the foot of slopes by gravity-driven processes such as creep, solifluction, landslides, and snow avalanches. Colluvium is common on moderately steep to steep slopes, and in areas of high relief such as the Pelly Mountains. It typically comprises poorly sorted sediment ranging in size from clay to boulders. The

texture of colluvium is directly related to the texture of the parent material that is entrained by the slope processes (e.g., morainal materials versus weathered bedrock). On gentle to moderate north-facing slopes, colluvium is commonly composed of fine-grained material and is deposited by periglacial processes such as sheetwash and active layer detachment slides. Coarse-grained colluvium is more typical on steeper slopes where larger landslides are the primary transport mechanisms. Colluvial fans, cones and aprons are also found at the base of slopes where they have been deposited by hazardous mass movement processes such as rockfall, rockslides, slumps, debris slides and debris flows. Permafrost presence in colluvium is highly variable and dependent on soil texture, topographic position, and surface expression.

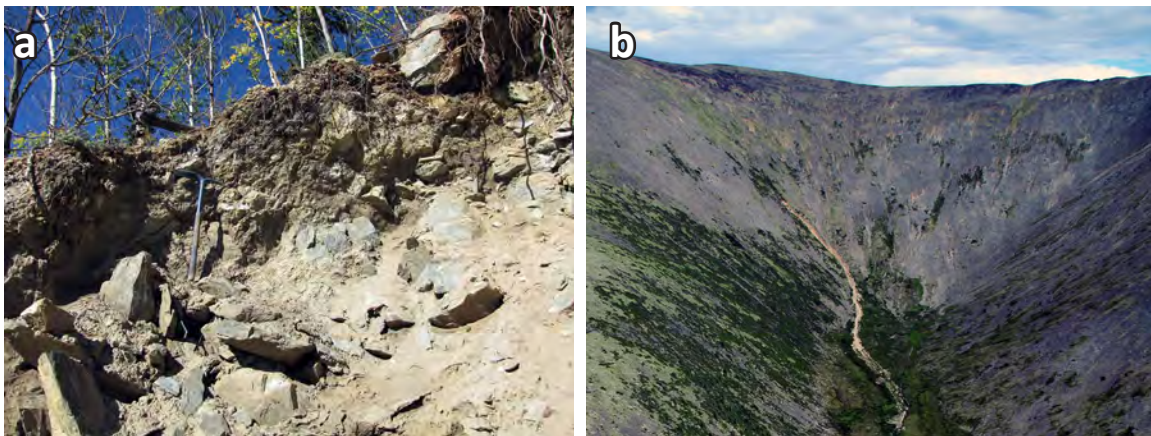


Figure 10. (a) Typical coarse, angular colluvium derived from weathered bedrock (station 13DT035; on the North Canal Road, approximately 2 km east of Tenas Creek). **(b)** Steep alpine slopes mantled with colluvial veneer derived from weathered bedrock. Debris flows (note fresh track in centre of photo) are a common transport mechanism in this environment. (This example is from outside the study area on Mt. Cockfield in the Dawson Range).

FLUVIAL MATERIALS

Fluvial sediments (Figure 11a,b) are transported by streams and rivers and deposited as floodplains, alluvial fans and terraces. They typically consist of well-sorted, stratified sand and rounded gravel with varying amounts of silt and organic materials. Silt, sand and organic materials make up thinly laminated or massive overbank deposits that are commonly interbedded with coarser gravel deposits. Floodplain sediments are widespread adjacent to the Pelly River and in and around Ross River townsite, where they reach thicknesses greater than 13 m (Environment Yukon, 1976). Fans are common where streams enter broad valleys. Higher elevation, narrow floodplains typically contain coarser-grained deposits compared to large, lower elevation floodplains where finer-grained sediments tend to accumulate. Steep bedrock canyons have also been cut along the Lapie River. Permafrost is uncommon in active fluvial deposits that have recently flooded or are subject to regular flooding, but may be found at depth in inactive floodplain areas.

GLACIOFLUVIAL MATERIALS

Glaciofluvial sediment (Figure 12a,b,c) exposed in the study area was deposited by glacial meltwater either directly in front of, or in contact with, late Wisconsin McConnell glacial ice. The sediment is typically poorly to well-sorted; clasts are rounded; and deposits tend to be stratified gravel and sand. Glaciofluvial materials in the study area were deposited as hummocky, ice marginal sediment, forming sub and englacial eskers, and kettled outwash plains that were subsequently eroded into terraces in the valley bottoms. Several large glaciofluvial fans were formed as sediment

was deposited from the Pelly Mountains into the Tintina Trench during, or immediately following, deglaciation. These fans are typically partly covered by smaller Holocene fans. The high porosity of glaciofluvial materials results in largely ice-free deposits or deep active layers. Sediments may be more ice-rich in areas with discontinuous, fine-grained sand and silt beds.

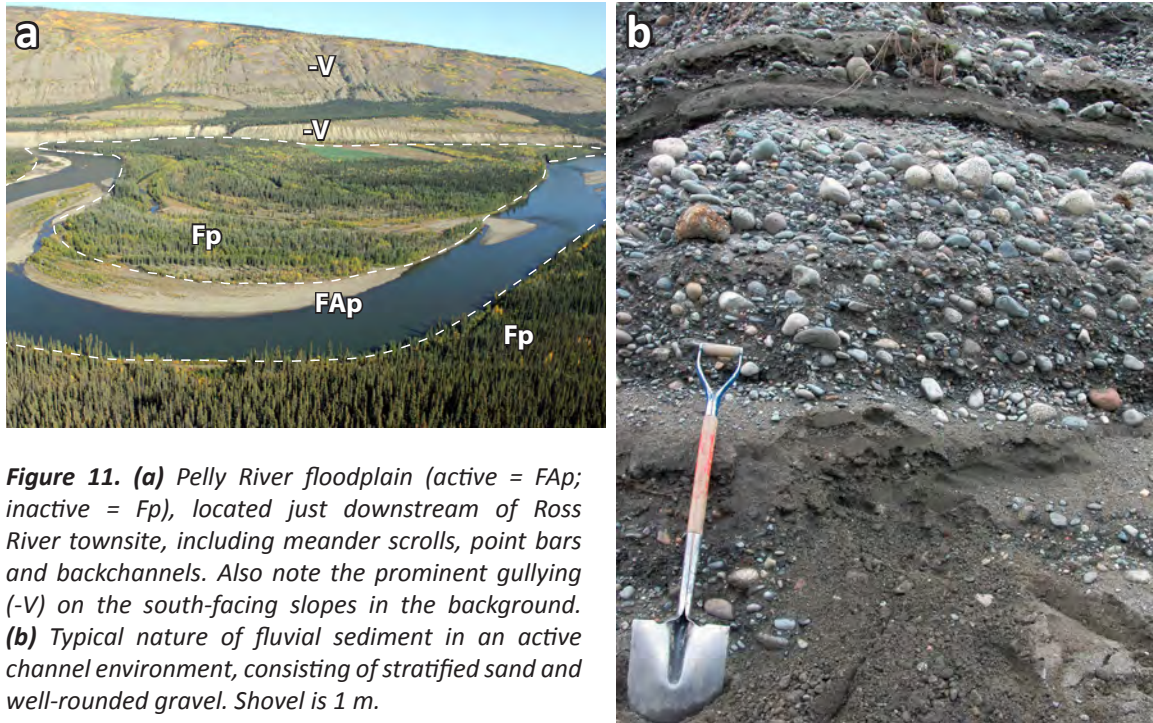


Figure 11. (a) Pelly River floodplain (active = FAp; inactive = Fp), located just downstream of Ross River townsite, including meander scrolls, point bars and backchannels. Also note the prominent gullying (-V) on the south-facing slopes in the background. **(b)** Typical nature of fluvial sediment in an active channel environment, consisting of stratified sand and well-rounded gravel. Shovel is 1 m.

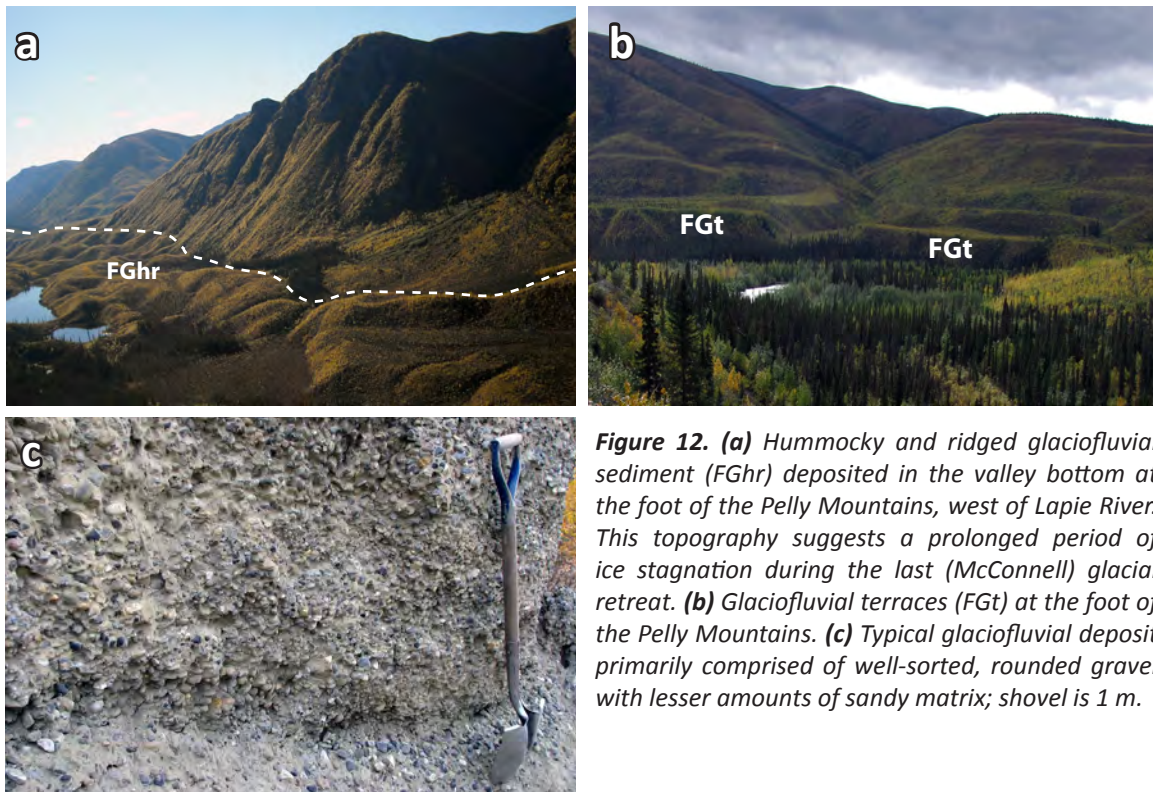


Figure 12. (a) Hummocky and ridged glaciofluvial sediment (FGhr) deposited in the valley bottom at the foot of the Pelly Mountains, west of Lapie River. This topography suggests a prolonged period of ice stagnation during the last (McConnell) glacial retreat. **(b)** Glaciofluvial terraces (FGt) at the foot of the Pelly Mountains. **(c)** Typical glaciofluvial deposit primarily comprised of well-sorted, rounded gravel with lesser amounts of sandy matrix; shovel is 1 m.

MORAINAL MATERIALS

Morainal deposits (Figure 13a,b) in the study area (also referred to as till) were deposited directly by late Wisconsin McConnell glacial ice without modification by any other transportation agent. These deposits are widespread, both in valley bottoms and across gentle to moderate slopes in the Tintina Trench. Till is typically a poorly sorted and consolidated mixture of silt, sand, and rounded to angular, pebble to boulder-sized clasts. Many of these clasts are heavily striated and have keels, lee-end fractures, and other evidence of glacial erosion. Till may be thin (less than 15 cm) in high-elevation areas, but reaches thicknesses of greater than 50 m across the study area (Environment Yukon, 1990). Morainal deposits are typically found as veneers or blankets that follow the underlying topography (Plouffe, 1989; Bond, 2001b). Streamlined drumlins, flutings, and crag and tails composed of heavily compacted basal till are abundant across the Tintina Trench (e.g., Figure 13a), which is attributed to rapid, unobstructed ice flow through the trench during glacial maximum (Bond, 2001a). The streamlined features were formed from sediment deformation at the ice-bed interface below the ice sheet, and are typically comprised of till deposits >5 m thick. Morainal deposits also form undulating and hummocky topography. Till is generally colluviated when found on slopes, and permafrost is commonly found within morainal deposits with varying amounts of ice.

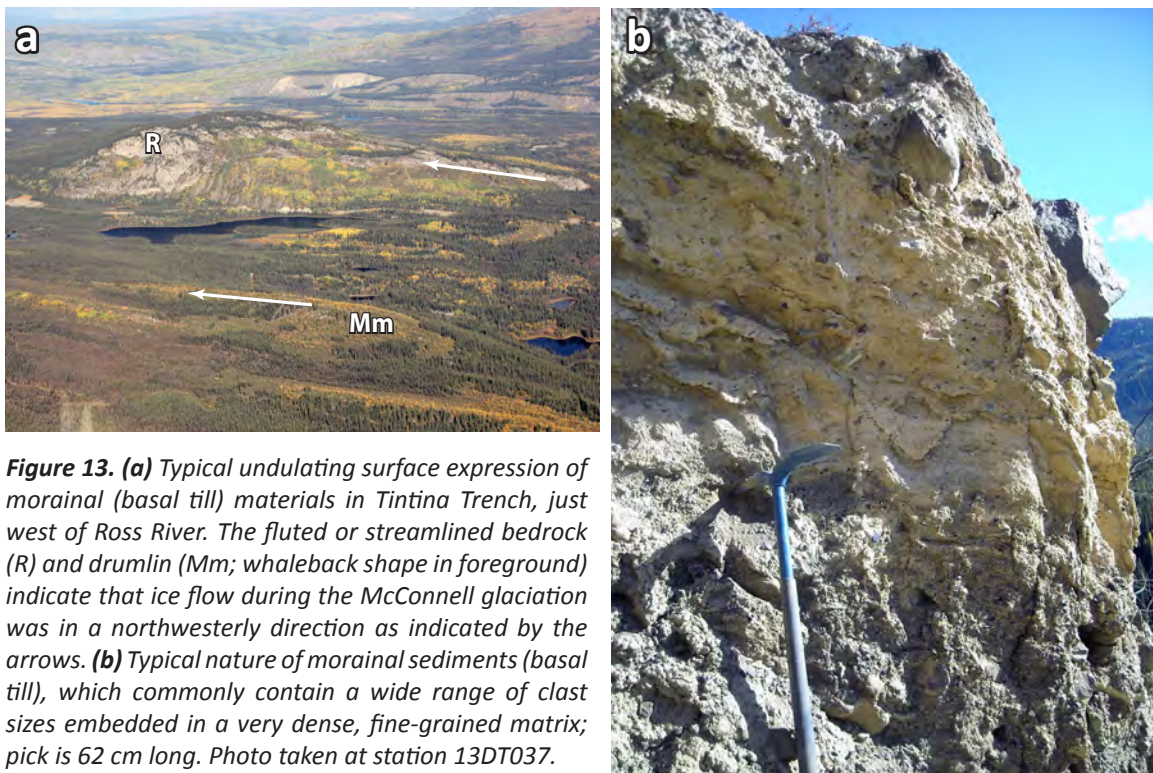


Figure 13. (a) Typical undulating surface expression of morainal (basal till) materials in Tintina Trench, just west of Ross River. The fluted or streamlined bedrock (R) and drumlin (Mm; whaleback shape in foreground) indicate that ice flow during the McConnell glaciation was in a northwesterly direction as indicated by the arrows. **(b)** Typical nature of morainal sediments (basal till), which commonly contain a wide range of clast sizes embedded in a very dense, fine-grained matrix; pick is 62 cm long. Photo taken at station 13DT037.

GLACIOLACUSTRINE MATERIALS

Glaciolacustrine materials (Figure 14a,b) primarily consist of interbedded and interlaminated clay, silt, and sand deposited in glacial lakes during late Wisconsin McConnell deglaciation. Glaciolacustrine deposits are widespread in the Tintina Trench, and reach thicknesses >10 m. Many of these deposits are covered by glaciofluvial, colluvial, lacustrine and organic sediment. A notable exception to this is the presence of large glaciolacustrine terraces on the southwest side of the Pelly River. These terraces are ~30 m above the Pelly River floodplain and have a plain

to undulating expression. Glaciolacustrine terraces also exist on the northeast side of the river, but they have been covered by 5-10 m of glaciofluvial sediment and are therefore mapped as glaciofluvial deposits. The low permeability of glaciolacustrine deposits promotes thin active layers. Thermokarst lakes and segregated ice lenses are common in these deposits, indicating the presence of ice-rich permafrost near the surface.

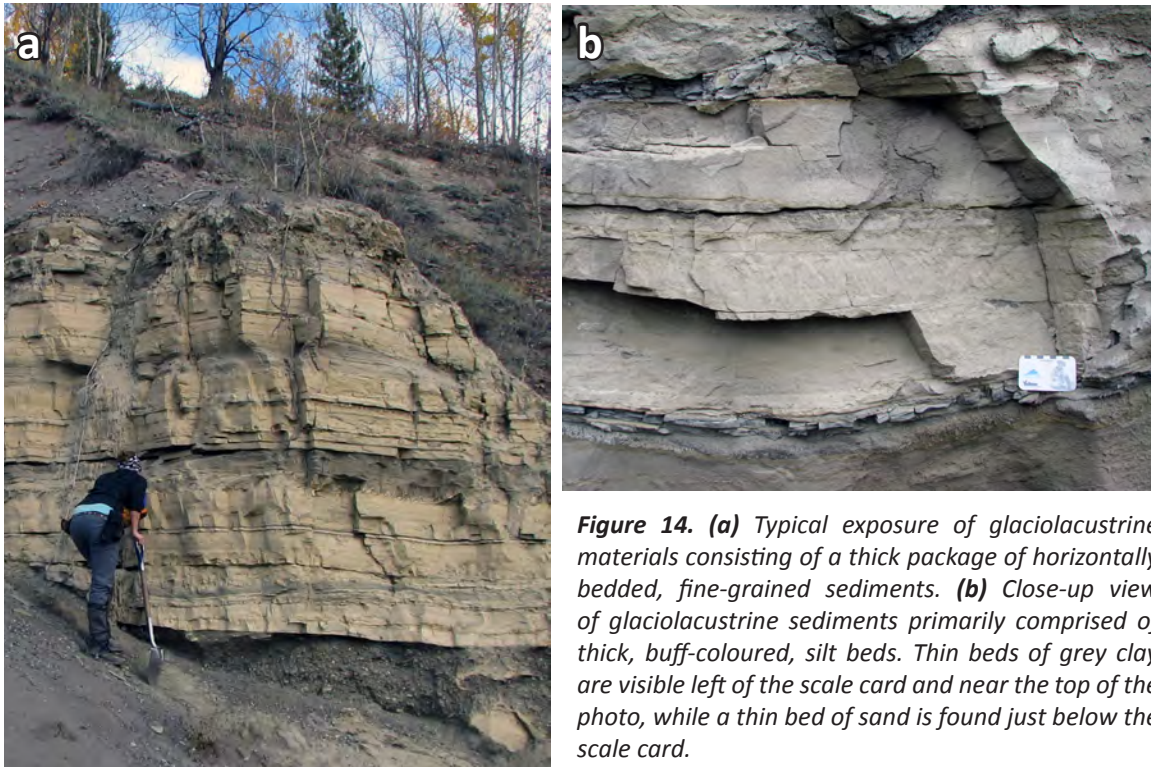


Figure 14. (a) Typical exposure of glaciolacustrine materials consisting of a thick package of horizontally bedded, fine-grained sediments. (b) Close-up view of glaciolacustrine sediments primarily comprised of thick, buff-coloured, silt beds. Thin beds of grey clay are visible left of the scale card and near the top of the photo, while a thin bed of sand is found just below the scale card.

STRATIGRAPHY

The stratigraphy of the Ross River area is complicated having large lateral variability (Figure 15), but generally reflects the glacial history and subsequent Holocene fluvial and colluvial activity as outlined above in the section titled *Landscape Evolution during the Pleistocene and Holocene Epochs*. Pre-McConnell till, as well as glaciolacustrine and glaciofluvial sediments have been documented at the base of a few scattered exposures along the Pelly and Lapie rivers (Plouffe, 1989; Jackson, 1993); however, most of the study area is blanketed by McConnell till up to 40 m thick (Turner, 2014) that is colluviated on slopes and escarpments. In some cases, the till is interbedded with glaciofluvial and/or glaciolacustrine sediments as a result of complex deglaciation processes and active ice retreat. During McConnell deglaciation, a large glacial lake formed in the Tintina Trench, depositing thick glaciolacustrine sediments in the valley bottom (Bond, 2001a); glaciofluvial sediments were also deposited in surrounding areas. After the lake drained, thick packages of fluvial sediments were deposited above the glaciolacustrine sediments in the Pelly River and major tributary valleys. Beneath the Ross River School, 6 m of these fluvial sediments were deposited on at least 20 m of glaciolacustrine clay, silt and sand (EBA Engineering Consultants, 2007, unpublished data).

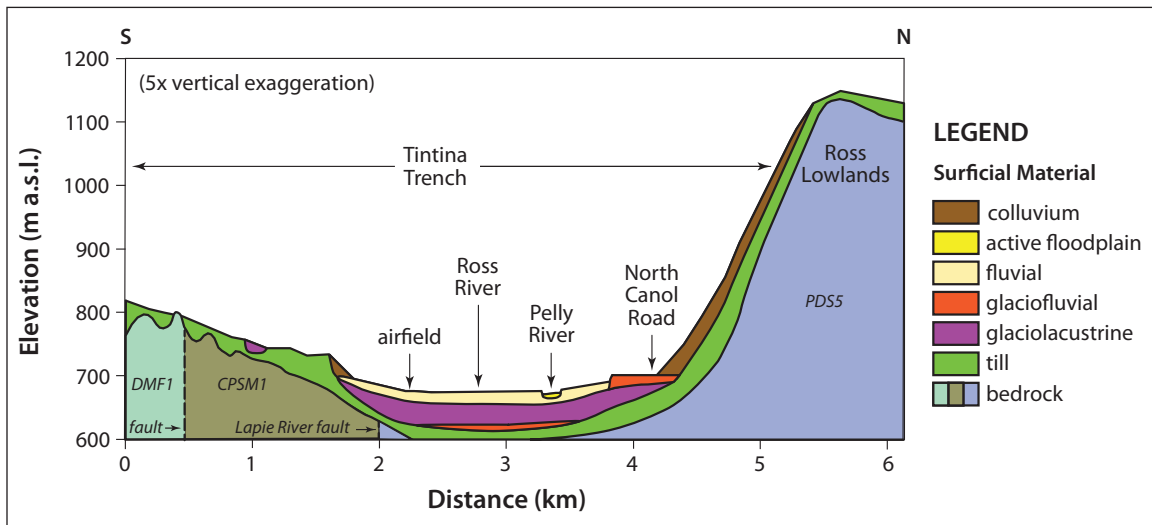


Figure 15. Hypothetical stratigraphy across Tintina Trench in the vicinity of Ross River. Unit thicknesses are exaggerated for visual clarity. Relative thicknesses are estimated based on aerial photo interpretation, borehole logs, and observation of stratigraphic exposures. Bedrock labels refer to units described in Figure 8.

PERMAFROST

In the study region, the permafrost profile is made up of several different components which must be considered collectively to accurately characterize local permafrost conditions. These components, and comments about their relevance to the Ross River region, are described in the following section.

ORGANIC COVER

The organic cover (i.e., peaty materials) is generally found at the top of the soil column; it has a very low thermal conductivity when dry, which reduces atmospheric heat transfer to lower sediment beds. Therefore, the thicker the organic cover, the cooler the ground. Under a thick organic mat, the active layer is thin and colder permafrost may develop. The high porosity of peat allows it to retain a significant amount of water or pore ice. Regardless of the presence of a visible cryostructure, peat is perfectly solid when frozen, but becomes highly compressible when thawed. If compression is applied, porosity and hydraulic conductivity decrease while thermal conductivity increases. Since it is one of the most significant drivers for ground ice sustainability, removing or compacting the organic cover can initiate degradation of the underlying permafrost by affecting its thermal regime. Additionally, high hydraulic conductivity in areas of groundwater flow can lead to preferential flow paths and discharge areas. When a flow pattern is disturbed by removal or compaction of the organic cover and degradation of the underlying permafrost, water accumulation may trigger further localized permafrost degradation by heat advection through groundwater and subsequent freeze-back (latent heat of water).

FOREST COVER

The forest cover keeps the ground cool by providing shade, increasing the soil moisture (increase in heat capacity), and increasing energy diffusion before it hits the ground surface. In the winter, trees retain snow, which locally reduces snow cover on the ground that is acting as an insulating layer between the atmosphere and the ground (Brown, 1963; Brown and Péwé, 1973). Clearing of the forest cover by machinery or forest fire usually leads to a deepening of the active layer and

degradation of the upper layers of permafrost. When the low-lying vegetation (e.g., bryophytes, grasses) is also removed, the effects are much more pronounced.

SURFACE MATERIAL TEXTURE

Four different surface material types were identified in the Ross River area based on the geotechnical characteristics of samples gathered during the permafrost drilling program. They were classified using the Unified Soil Classification System (USCS) as gravel, sand, silty sand and silt.

Gravel

The gravel surveyed in the project area is of fluvial origin. A sample from the old townsite of Ross River contains a layer composed of sub-rounded cobbles and pebbles, with little fine-grained matrix. Sediment dynamics in meandering and braided rivers change laterally, and along the length of the floodplain. These dynamics result in rapid, local changes in the stratigraphy, creating deposits of varying thickness with changing grain sizes, as the main fluvial channel migrates back and forth across the floodplain over time. Fluvial sediments are generally coarse-grained and well-drained, therefore generating deposits that are not frost-susceptible. Where permafrost is present, these sediments do not contain excess ice and are mechanically stable upon thawing. However, fluvial gravel sometimes contains a significant amount of fine-grained material such as silt in the matrix of the deposit, or as thin beds and interlayers. In these cases, the sediment has high ice-segregation potential. When contained in permafrost, these deposits display layers with ice-rich cryostructures and are characterized by strong, differential thaw settlement.

Sand

Sand layers are generally well-drained and do not contain excess ice. However, fine and very fine sand are frost susceptible, and may contain excess ice in the form of alternating ice lenses. Upon thawing, materials with excess ice will undergo thaw settlement and will drain slower than coarser sand deposits (i.e., medium to very coarse sand).

Silty sand

Where surficial hydrologic and thermal regimes allow, coarse silt and fine sand may contain a great amount of excess ice in various forms, because these two deposit types have significant ice segregation potential (Darrow et al., 2008).

Silt

Silt deposits documented in the study area are of fluvial and lacustrine origin. This fine-grained material is usually highly frost susceptible. If silt is present in the active layer, and if water is available, it leads to annual frost-heave and settlement of the ground. If a silty layer occurs at, or below the permafrost table, the upper part of the permafrost will be typically ice-rich and mechanically unstable upon thawing. Poor drainage characterizes these permafrost-degraded areas.

CONTEMPORARY PERMAFROST DISTRIBUTION

An assessment of the spatial pattern of current permafrost conditions in the Ross River region can be extracted from a model of permafrost probability developed for the southern half of Yukon (Bonnaventure et al., 2012). This model is essentially climatically based and takes into account the impacts of solar radiation and air temperature trends with elevation (Lewkowicz and Bonnaventure, 2011), but does not account for site-specific factors such as snow depth or surficial materials. The calculated probabilities are for typical snow cover conditions and there can be considerable sub-grid cell variability where sites are locally blown clear of snow (resulting in a higher probability of permafrost), or at sites that accumulate early and deep snow covers (resulting in a lower probability of permafrost; Lewkowicz and Ednie, 2004). Results portray the

broad spatial trends in permafrost conditions across the landscape but cannot be used for site-specific predictions. For example, if an area is shown as having a probability of 0.5 to 0.6, this means that 50-60% of the grid cells are predicted to be underlain by permafrost, but it does not indicate which of the cells may have permafrost and which may not.

Predictions from the regional model described above have been compared to the following: 1) field observations in the Sa Dena Hes region, which were not used in the derivation of the model (Lewkowicz and Bonnaventure, 2011); 2) permafrost zone boundaries from the national permafrost map of Canada (Heginbottom et al., 1995); 3) a database of Yukon rock glaciers (Page, 2009); and 4) temperature measurements in instrumented boreholes (Global Terrestrial Network for Permafrost, 2013). The results suggest that the model may slightly over-predict permafrost probabilities where values are >0.5 and slightly under-predict probabilities where values are <0.5. However, the overall trends reflect observed probability patterns documented in other regions of southern Yukon (Bonnaventure et al., 2012).

Model results for the Ross River region were extracted from the regional model (Figure 16) and indicate that permafrost distribution in the project area is largely consistent. Most of the terrain in the region exhibits permafrost probabilities of 60-70%. Permafrost probability on many south-facing slopes is lower (50-60%), while north-facing slopes exhibit values in the 70-80% range. This indicates that in the Ross River region, permafrost distribution is largely influenced by aspect. The influences of increases in mean annual air temperature on permafrost distribution shown in this model are discussed later in this report.

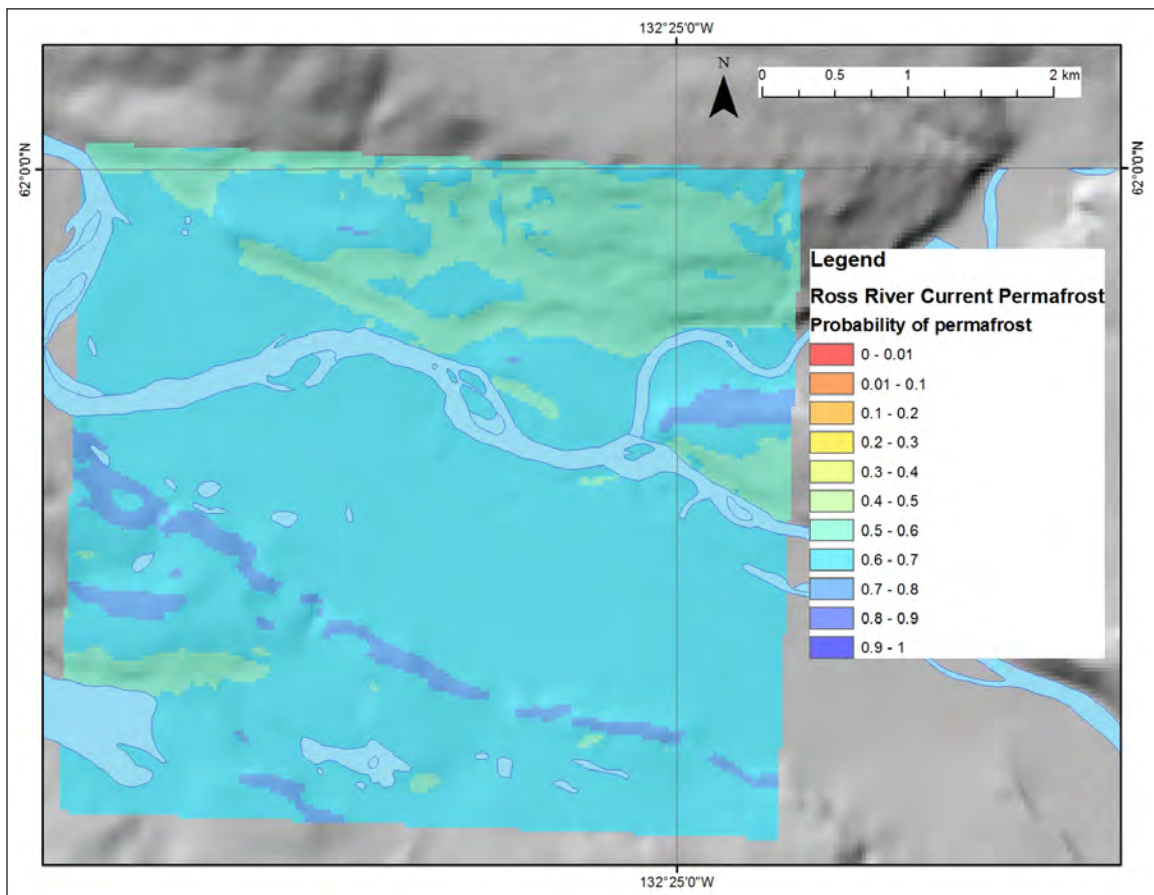


Figure 16. Permafrost probability under current climate conditions for the Ross River study area (based on Bonnaventure et al., 2012).

POTENTIAL HAZARD RISKS FOR THE ROSS RIVER REGION

LANDSLIDE PROCESSES

Landslides are created by the downslope movement (i.e., mass wasting) of surficial materials and/or bedrock fragments, often mixed with vegetative debris. They are generally triggered on moderate to steep slopes by a variety of factors including intense rainfall or snowmelt events, permafrost degradation, forest fires, river erosion, groundwater flow, and/or earthquakes. In many cases, several of these triggering factors act in combination.

Landslides range in size from metres to hundreds of metres. They may be restricted to very shallow surface layers, or they may be deep-seated and extend into thick sediments or bedrock. They may be rapid events that occur in seconds to minutes, or they may gradually creep or rotate over years to centuries. Depending on slope geometry and sediment water content, debris may free fall, slide, rotate and/or flow.

Large landslides are uncommon in the Ross River area, and extensive gully erosion is probably the most prominent form of mass wasting in the region, particularly in the till escarpments along the Pelly River floodplain, and on the colluvial/morainal south-facing slopes immediately north of Ross River (e.g., Figure 17; see also Fig. 11a). These slopes are particularly susceptible to gullying because the thick sediments have been over-steepened by Holocene fluvial erosion. Furthermore, the arid, south-facing slope aspect and steep slopes can only support very sparse vegetation, providing limited protection from erosion due to surface runoff.



Figure 17. Extensive gully erosion into a steep slope composed of till on the north bank of the Pelly River, approximately 4.5 km downstream from Ross River ferry.

The most common landslides mapped in the Ross River region are debris flows which are concentrated in steep gullies along the north and south walls of the Tintina Trench (Figure 18). Debris flows occur when saturated, loose sediment flows rapidly downslope in a slurry, and often occupies a pre-existing stream channel or gully. They are generally triggered by excessive runoff from intense rainfall and/or snowmelt events, especially where drainage is restricted by shallow bedrock. Debris flows are capable of entraining large trees and boulders and can therefore be potentially destructive. They are also one of the primary mechanisms by which colluvial fans are built in valley bottoms.

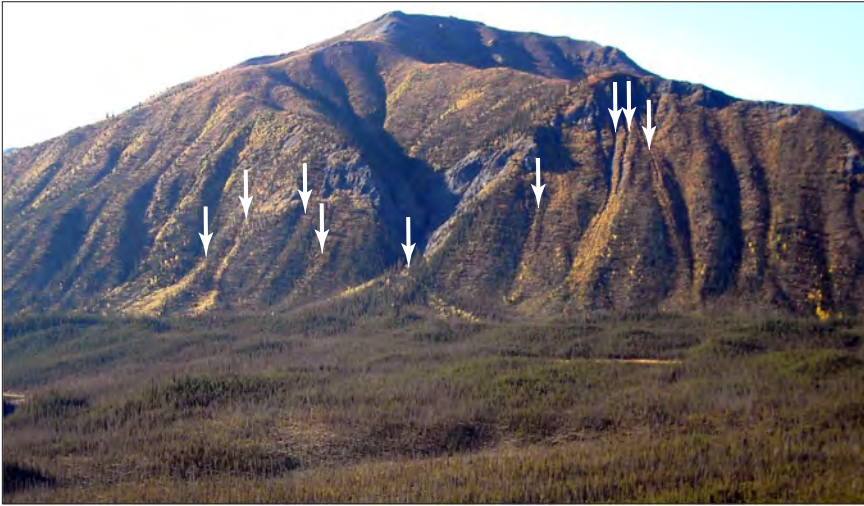


Figure 18. Numerous debris flow tracks (indicated by arrows) in steep gullies carved into the front ranges of the Pelly Mountains.

Other types of landslides in the area include small slides and slumps along river cutbanks, particularly along the Pelly River; scattered rockslides (Figure 19) and rockfalls (Figure 20) along the front ranges of the Pelly Mountains west of Lapie River (station 13DTS49); and a rotational slump located at km 9 of the North Canal Road (Figure 21).

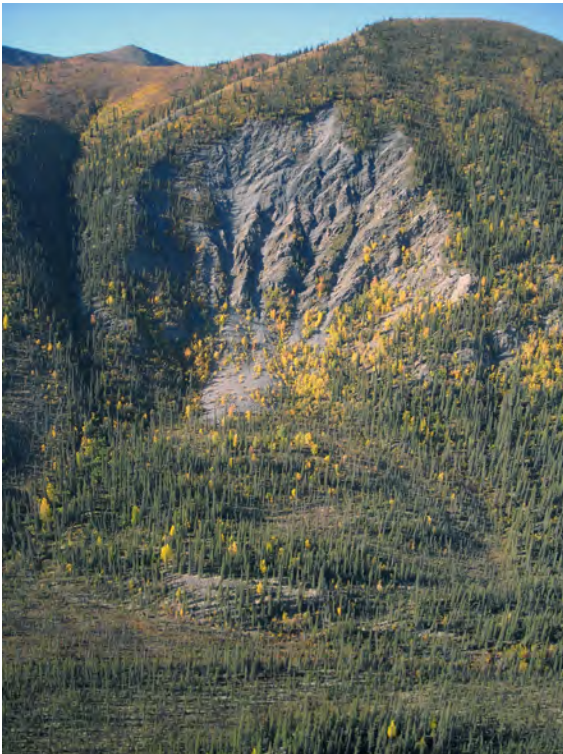


Figure 19. Rockslide along the front ranges of the Pelly Mountains (St. Cyr Range) south of Danger Creek (station 13DTS49).

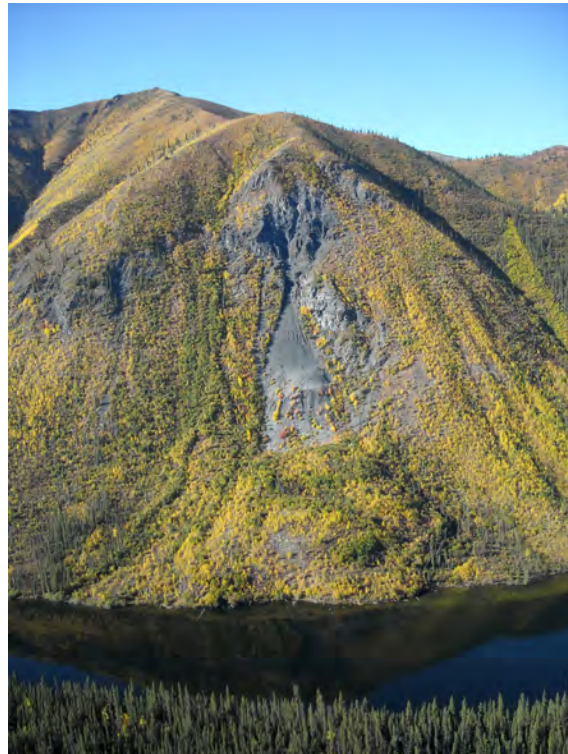


Figure 20. Rockfall along the front ranges of the Pelly Mountains west of Lapie River (~1 km southeast of station 13DTS49).



Figure 21. Rotational slump near km 9 of the North Canal Road (station 13DT37). Road construction and river erosion are undercutting the toe of the slide and contributing to instability. The slump is approximately 70 m tall, 250 m wide, and 180 m long.

PERMAFROST PROCESSES

Hazards related to permafrost have the potential to impact several elements such as ground stability, hydrology, and infrastructure integrity. The following section provides a general description of permafrost structure and characteristics, in order to present a more comprehensive picture of the risks associated with permafrost thaw.

PERMAFROST DEVELOPMENT

In permafrost regions, the distribution of ice in the surface material or soil (cryostratigraphy) is related to the manner in which permafrost has aggraded and degraded through time. The understanding of permafrost genesis at a given site is important because permafrost structure and composition is directly related to the type of permafrost development. Permafrost genesis can be divided into four main types: epigenetic, syngenetic, quasi-syngenetic, para-syngenetic and polygenetic (French and Shur, 2010; O'Donnell et al., 2012). Epigenetic permafrost forms in bedrock or in sediments following deposition. The ice content of epigenetic permafrost usually increases with depth, and the sediment layers in between ice features are usually ice-poor and over-consolidated or stiff (Stephani et al., 2010). The syngenetic growth of permafrost occurs when material is deposited at the surface while freezing is in progress. Thus, the permafrost is approximately the same age as the sediment in which it is found. The ice content of syngenetic permafrost is more likely to be uniform and ice-rich throughout the soil column. Quasi-syngenetic permafrost forms when the permafrost table shifts upward in response to vegetation growth at the surface, leading to the formation of an intermediate, ice-rich layer at depth. Para-syngenetic permafrost is defined by multidirectional refreezing of a talik zone (e.g., those areas of unfrozen ground under drained lakes). The ice content of para-syngenetic permafrost relates to the degree of saturation of the material prior to refreezing. If the permafrost has more than one origin, it can be defined as polygenetic (Lunardini, 1994; French and Shur, 2010).

GEOTECHNICAL PROPERTIES

The cryostratigraphy and geotechnical properties of the ground are important characteristics as they influence permafrost dynamics and the thermal and mechanical sensitivity of frozen ground. Cryostratigraphy is defined as the study of frozen layers in the Earth's crust and is used to reconstruct the deposition history of a given site, define the type of permafrost present, determine how ice developed, and how the ice is distributed within the permafrost. It is useful to predict the

rheology of surface and sub-surface terrains in the context of permafrost thaw (French and Shur, 2010). Cryostratigraphy is defined by cryofacies (e.g., ice-rich or ice-poor sediments), which are characterized by typical cryostructures.

Cryostructures are determined by the amount and distribution of ice within the pore structure, and by ice in excess of the porosity (e.g., lenses, layers of segregated ice; French and Shur, 2010). Table 2 presents typical cryostructures that may be observed in permafrost. Layered, lenticular, and microlenticular cryostructures are present in ice-rich permafrost. They are the result of ice segregation in the sediment and are typical of fine-grained syngenetic permafrost. When permafrost thaws, the water from the melting of excess ice is drained, leading to settlement of the ground. Porous visible and porous invisible cryostructures are ice-poor and result from in-situ freezing of water trapped in the soil pores with little to no migration of water to the freezing front (cryosuction) within the freezing soil. These types of cryostructures are common in coarse-grained sediments, but can also develop in fine-grained sediments that were originally ice-rich, thawed, drained, and subsequently refrozen (Stephani et al., 2010). Because there is no excess ice present, no significant subsidence of the ground is expected upon thawing.

Table 2. Cryostructure classification, from Stephani et al. (2014) and based on Murton and French (1994).

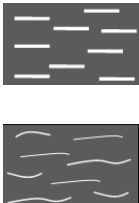
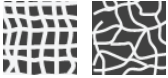
Name	Equivalent	Description	Sediment type	Illustration*
Lenticular	Lenticular ¹	<ul style="list-style-type: none"> • lens-shaped ice in sediment • generally continuously shaped • generally horizontal (parallel to freezing front) • may be straight, wavy, inclined, interlaced • may contain air bubbles • thickness: ≥1 mm Syngenetic permafrost: mm to cm thick Epigenetic permafrost: cm to dm thick • usually ice-rich sediment	silt to fine sand; silty clay	see Fig. 3.1A 
Microlenticular	Lenticular ^{1,2}	<ul style="list-style-type: none"> • lens-shaped ice in sediment • generally discontinuously shaped • generally horizontal (parallel to freezing front) • may be straight, wavy, inclined, interlaced • very few air bubbles • thickness: <1 mm • usually ice-rich sediment: Syngenetic permafrost: >50% by volume Epigenetic permafrost: 30-50% by volume	silt to fine sand; peat	see Fig. 3.1A 
Layered/belt-like structure	Layered ¹	<ul style="list-style-type: none"> • assemblage of lenticular cryostructures • thickness: centimetre to decimetre • usually ice-rich sediment 	silt to fine sand; peat	see Fig. 3.1C 

Table 2. Cyrostructure classification, from Stephani et al. (2014) and based on Murton and French (1994), *continued*.

Name	Equivalent	Description	Sediment type	Illustration*
Ice veins		<ul style="list-style-type: none"> • ice-filled crack or fissure in sediment • thickness variable (millimetre to centimetre) Frost crack: 1-5 mm thick Dilation/extension cracks: cm-dm thick	all types	
Reticulate	Reticulate ^{1,2}	<ul style="list-style-type: none"> • net-like cryostructure of interconnected sub-horizontal ice lenses and sub-vertical ice veins • usually ice-rich to very ice-rich sediment (~35-95% by volume) 	silt to fine sand	see Fig. 3.1F 
Suspended	Suspended ¹ ; Ataxitic ²	<ul style="list-style-type: none"> • suspended aggregates in ice • usually very ice-rich sediment (up to 90-95% by volume) • common in upper part of permafrost 	silt to fine sand; occasionally peat; silty clay	see Fig. 3.1E 
Crustal	Crustal ^{1,2}	<ul style="list-style-type: none"> • ice-coating around rock fragments, aggregates or wood fragments • usually partial coating, occasionally total • common just beneath permafrost table • thickness: few millimetres to centimetre-thick coating 	gravel/rock fragments; diamicton	see Fig. 3.1D 
Porous visible	Ice cement ¹ ; Massive ²	<ul style="list-style-type: none"> • pore ice that is visible to the unaided eye • usually ice-poor sediment (<30% by volume) 	gravel/rock fragments; diamicton	see Fig. 3.1F 
Porous invisible	Ice cement ¹ ; Massive ²	<ul style="list-style-type: none"> • pore ice not visible to the unaided eye • usually very ice-poor sediment (<10-30% by volume) 	all types	see Fig. 3.1F 

*Illustrations modified from Murton and French, 1994

¹ Murton and French (1994); ² Kudryavtsev (1979)

Legend: grey = sediment; dark grey = aggregates or wood fragments; white = ice.

Generally, dry or unsaturated frozen sediments do not present a high risk upon thawing, as the water will remain in the soil porosity, or will drain away. In contrast, when a saturated material thaws, it presents a much higher risk of settlement, mass movement, or ponding in response to poor drainage. Hazards related to the thawing of ice-rich deposits are affected by factors such as stratigraphy and the grain size distribution of the stratigraphic layers, as well as external factors such as slope, surface roughness, and vegetation.

For thaw-settlement hazard assessments, cryostratigraphy is used to locate ice-rich and ice-poor layers, and determine the geometry and distribution of massive ice (e.g., patterns of ice wedges). Generally speaking, the presence of ice-rich deposits raises concern in terms of hazard potential. Where ice-rich deposits overlie ice-poor layers, the thaw-settlement hazard is high on the short

term and the rate of change is fast. Conversely, where ice-poor deposits overlie ice-rich sediment, the thawing of the upper layer is rapid but with minimal thaw settlement; this will be followed by the slow, but constant thawing of the underlying ice-rich layer resulting in differential thaw settlement.

The grain-size distribution of sediments determines the porosity and hydraulic conductivity of the ground. Coarse material (medium sand and coarser) has a high hydraulic conductivity and readily drains as ice melts, whereas fine-grained material drains poorly once it thaws due to its low hydraulic conductivity. Furthermore, fine-grained sediments often contain excess ice (i.e., the volume of ice in excess of the total pore volume of the ground when unfrozen) and may form ice lenses or layers by ice segregation. On flat terrain, ground with excess ice will undergo severe thaw settlement; likewise, on slopes, silt and clay deposits may experience mass movement when the pore water pressure created by melting ice is high. For deposits on slopes, the plastic and liquid limits of the material are used to evaluate the potential of ground failure.

PERMAFROST AS A HAZARD RISK

The ground thermal regime of permafrost is influenced by climate, surface conditions, and the complex interactions of geophysical factors such as hydrography, topography, vegetation, soil texture and ground-ice content (Jorgenson and Osterkamp, 2005). As a result, variations in climate or terrain conditions (e.g., environmental changes or human interventions) can both have a great impact on permafrost stability. Higher surface temperatures, variation in snow cover depth, active-layer hydrology variations, infrastructure, and fire disturbances are good examples of changes that can play, at various scales, a major role in permafrost degradation (Stephani et al., 2014). Additionally, since it is closely linked to local factors, permafrost response to environmental change can be spatially and temporally heterogeneous and can respond differently to geomorphic processes due to different terrain conditions. Therefore, permafrost landscapes will have a dynamic response to environmental change and must be considered holistically, at diverse spatio-temporal scales.

Because permafrost stability is essentially maintained by the bonding between ice and the ground particles, when ice melts, cohesion is lost and soil stability is diminished (French, 2007). Following an increase in air temperature, the active layer is expected to deepen as the ice contained in the upper part of the permafrost (right below the bottom of the active layer) melts. If the volumetric water content of the ground is lower than the volume of soil pores, the ground is not saturated. Thawing of this type of ice-poor soil results in moderate surface settlement and is essentially due to the loss of volume upon ground ice melting and subsequent soil consolidation. If the volumetric water content of the ground is equal to, or slightly above the volume of soil pores when unfrozen, the soil is saturated. Thawing of this type of ice-rich soil results in poorly drained surface conditions, and the soil will be unable to consolidate due to the high pore-water pressure. If the volumetric water content of the ground is higher than the volume of soil pores, the ground is super-saturated and contains excess ice in its frozen state. Thawing of this type of ground results in severe surface settlement, and is essentially due to the loss of volume upon ground ice melting and soil drainage (Nelson et al., 2002). In gently sloping areas, water ponding is frequent; on steep slopes, the release of water builds excess pore water pressure in the soil pores, which is conducive to rapid mass movements (e.g., slides, slumps and debris flows). When the material is coarse-grained, soil water is drained according to the hydraulic conductivity of the material and there is minimal settling or movement of the sediment. When the material is fine grained, the drainage is slow and pore water pressure may trigger slow mass movement (e.g., solifluction). Depending on the nature of the soil material and the amount of ground ice present, significant hazards may

develop. Permafrost-related hazards represent some of the principal challenges for planning and development in northern environments.

To assess permafrost stability for land-planning purposes, an estimation of the maximum thaw depth that could be reached under changing climatic conditions is essential, mainly to evaluate the potential deformation that the soil may undergo in the future (Instanes, 2003). The rate and type of deformation (rheology) is closely linked to the type of surficial deposits, the ground ice content and its distribution, the ground temperature, and the soil hydrological regime.

Permafrost-related landslides such as active-layer detachments and retrogressive thaw flows are documented in the study area (Lipovsky and Huscroft, 2007). Permafrost influences slope stability by strongly affecting drainage (which is restricted by the permafrost table), soil moisture (which may increase in response to rapid thaw of ground ice), and soil strength (through bonding of frozen soil particles). Active-layer detachments (Figure 22) are triggered by rapid thaw of the active layer, which is often caused by forest fires. These landslides are generally relatively small and shallow (<1 m deep), but can occur on very gentle slopes and in large numbers, which may affect local sedimentation rates (Lipovsky et al., 2006). Retrogressive thaw slumps occur where thawing material continually flows away from a steep exposure of ice-rich permafrost. These slides gradually grow in size over years to decades as new ice-rich sediment is exposed and subsequently thaws. Retrogressive thaw slumps are especially common where river erosion exposes ice-rich glaciolacustrine sediments along cutbanks.

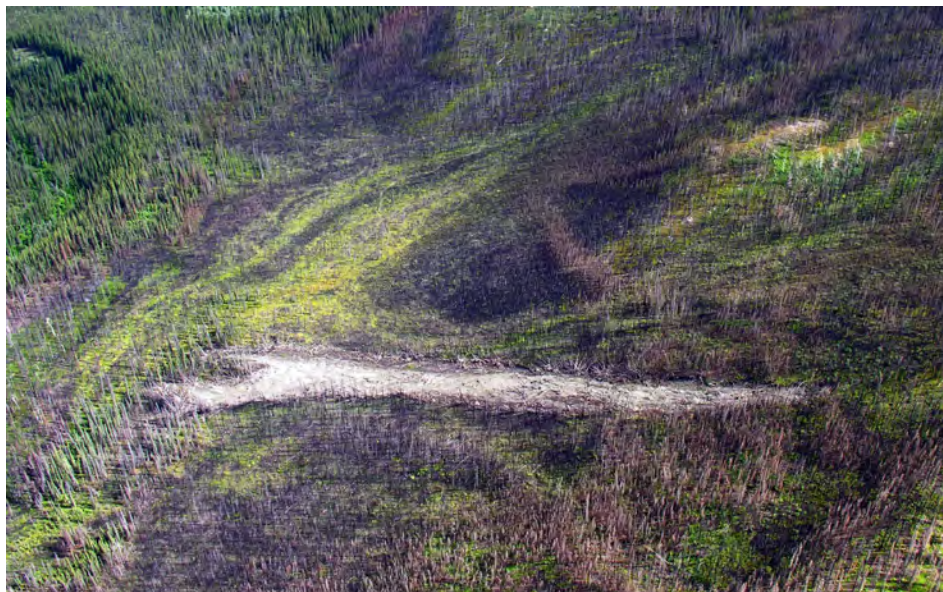


Figure 22. Large active-layer detachment slide (estimated to be 300 m long) which initiated on a gentle, north-facing slope near the confluence of Excell Creek and Pelly River (approximately 23 km upstream of the Faro bridge) following a 2004 forest fire.

Thermokarst collapse features, generally occupied by small ponds or lakes, occur in scattered locations around the map area, particularly near the southern margin of the Pelly River floodplain approximately 1.5 km west of Ross River (Figure 23). Thermokarst depressions result from the thaw of ground ice and subsequent settlement of the ground surface. Ice-rich glaciolacustrine sediments are most susceptible to thermokarst collapse following some kind of surface disturbance which exposes ground ice. Thermokarst depressions may grow in size for decades until the supply of ground ice is exhausted.



Figure 23. Thermokarst collapse ponds visible on a 2007 air photograph (National Air Photo Library A28547-233) are highlighted by white arrows. Comparison with historical air photographs shows that at a new pond has developed since 1967 (see point 1), while an old pond that was present in 1967 has since filled in with organic materials (see point 2).

Sheetwash or slope wash occurs where surface water flows in sheets along a shallow impermeable frost table. It is recognized by a very distinctive surface pattern, where subtle vegetation differences give the land surface a distinctive, flowing appearance when viewed from the air (Figure 24). This process is most common on gentle to moderate north-facing slopes and contributes to the gradual downhill transport of fine sediment to valley bottoms.



Figure 24. Typical surface expression indicating the presence of sheetwash on a north-facing slope underlain by permafrost.

Where the active layer is thin, surface soils are commonly saturated because the permafrost table is impermeable. Slopes with thin active layers are susceptible to creep through the processes of solifluction (gradual downhill movement of saturated soil) and frost creep (development of needle ice and subsequent heaving of freezing ground). The combined effects of sheetwash, solifluction and frost creep may produce very subdued topography and cause ongoing sedimentation at the base of the affected slopes.

SEISMICITY

Seismic hazard in the Ross River area is relatively low (Figure 25), although minor earthquakes do occasionally occur. Thirty-four earthquakes have been recorded within 50 km of Ross River since 1980 (Natural Resources Canada, 2010), and of these, the largest was magnitude 4.6, while the remainder were all below magnitude 4. Although the town is situated very close to the Tintina fault which is a major structural feature, the fault has not been active since the early Tertiary (Tempelman-Kluit, 1980) over 50 million years ago.

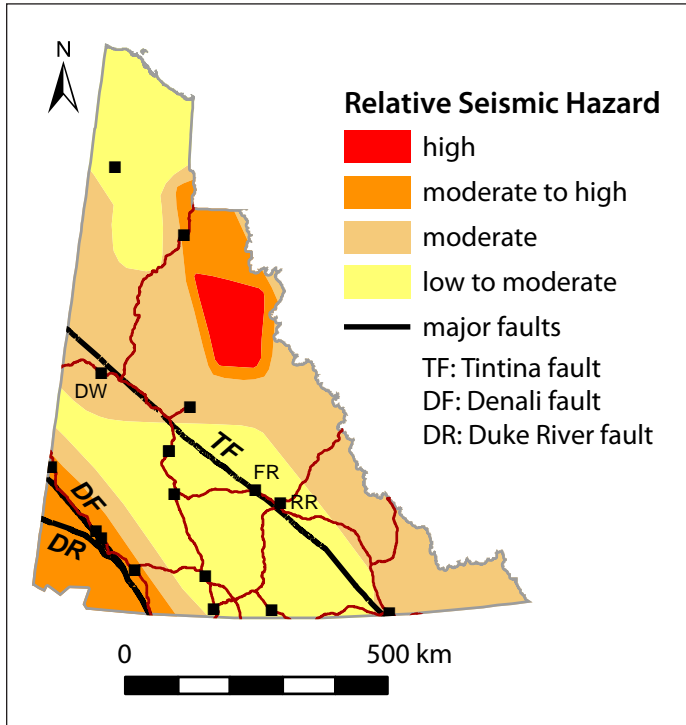


Figure 25. Simplified version of the National Building Code of Canada's 2010 seismic hazard map (for spectral acceleration at a 0.2 second period (5 cycles per second)), depicting the relative likelihood of experiencing earthquakes strong enough to potentially damage some, but not all, single family (one and two-story) dwellings (Natural Resources Canada, 2010). Ross River (RR) is located in the low to moderate hazard zone, where there is a 1-5% chance that significant damage will occur every 50 years. FR = Faro; DW = Dawson.

ASSESSING CURRENT HAZARDS FOR THE ROSS RIVER REGION

CASE STUDY SITES

To assess the risk of the hazards described above for the Ross River region, the research team focused on several case study sites. Findings from case study sites were then used to assess risk on a regional scale.

The case study sites for Ross River were determined in consultation with the community – they reflect areas where there are hazards-related concerns, or where future development may take place. Case study sites were also chosen to cover a variety of landscape types. Case study sites are: 1) central Ross River (Ross River school, arena, pool and vicinity); 2) a designated area surrounding the rifle range; 3) a site near the north end of Kulan Street; and 4) the former Ross River townsite (herein referred to as “Old Ross”). The locations of case study sites are shown in (Figure 26). At each site, researchers used geophysical approaches (ERT and GPR), permafrost borehole and soil pit observations, and examined exposed surficial material where possible. Results from each case study site are described below.

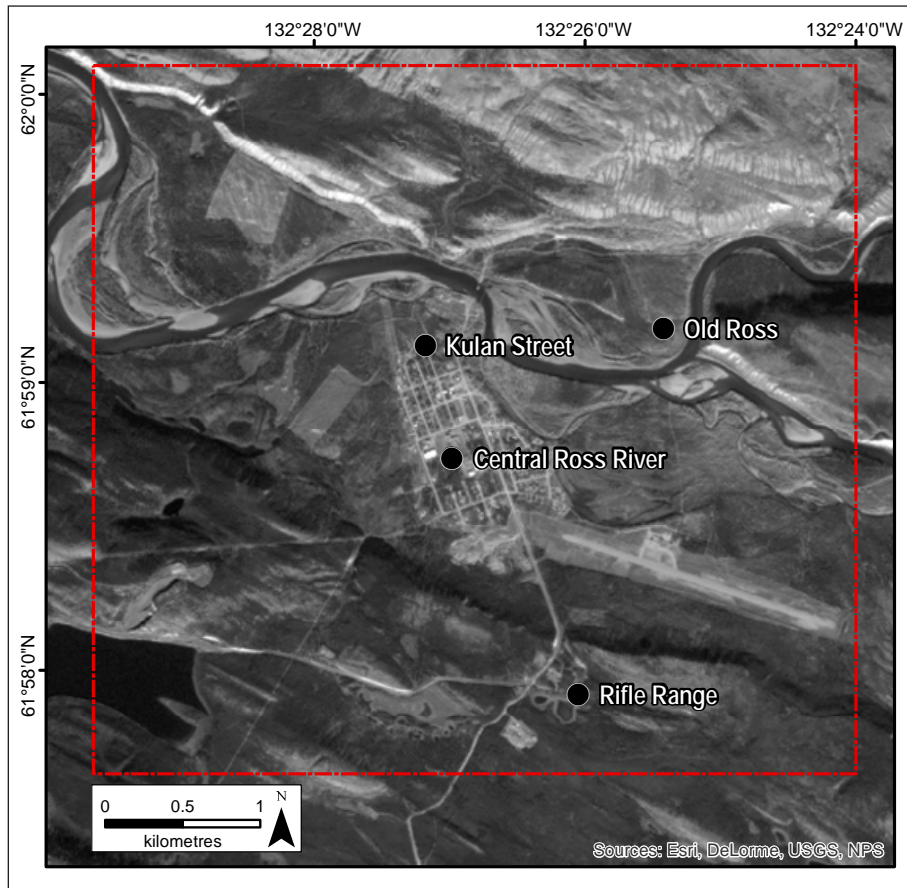


Figure 26. Map illustrating locations of all case study sites for the Ross River project area.

CENTRAL ROSS RIVER

The entire town of Ross River is located on a fluvial terrace of the Pelly River which is comprised of interbedded silt, sand and gravel. Fine (silt and clay), laminated sediments likely represent slackwater overbank flood deposits, whereas coarse deposits of sand and gravel were originally deposited by moving water on active floodplains and bars. Based on unpublished borehole logs (R. Trimble, TetraTech EBA, pers. comm.), the fluvial sediments beneath much of the town are up to 6 m thick, and are underlain by at least 20 m of fine-grained glaciolacustrine material. These glaciolacustrine sediments of silt and clay were deposited in a large glacial lake that filled the Tintina Trench at the end of the McConnell glaciation.

Laminated and bedded, compact, fine-grained sand and silt deposits were encountered in a 55-cm pit dug in a mature forest behind Ross River School (Figures 27 and 28; station 13DT045). The surface material at this site was weakly gleyed (sticky and clay-rich) and oxidized suggesting it has been subjected to flood events in the recent past. Three metres of fluvial sediments were exposed in a nearby borehole (*RR_BH01*; see Figure 29 for location), drilled at the boundary between the forest and the school yard. Textures ranged from gravel near the base of the borehole to silty sand near the surface, and thin beds of medium to coarse sand in between.

A deep borehole drilled in the Ross River School yard in 2007 (approximately 150 m north of the previous site) encountered 4 m of sand overlying 2 m of gravel and 21 m of glaciolacustrine clay, silt and sand (EBA Engineering Consultants, unpublished data). At that time, the thawed layer

was approximately 7 m thick, and the permafrost was over 14 m thick. Subsequent permafrost monitoring at this site indicated that the active layer was approximately 9.5 m thick (based on a year of data collected between 2007 and 2008; Lipovsky and Yoshikawa, 2009). By 2013, the active layer thickness had decreased to 8.7 m and the permafrost was very warm (-0.5°C at 13 m; data averaged over the time period 2008-2013; Lipovsky, 2015). Other sources have reported a depth to the base of permafrost to be 15-18 m (Stanley Associates Ltd., 1986), and a mean annual ground temperature of -0.4°C (Hoggan Engineering and Testing, 1989) for the area. The glaciolacustrine sediments at this location are very ice-rich in places, and degradation of this permafrost since the school was built in 2000 has caused thaw settlement which has resulted in damage to the building. The frost table depth encountered in several other boreholes located near the school varied from 3.5 m to 5.5 m in late summer or early fall (R. Trimble, TetraTech EBA, pers. comm.).



Figure 27. Fine-grained fluvial sediments exposed in a 55 cm-deep soil pit dug near Ross River School (station 13DT045).

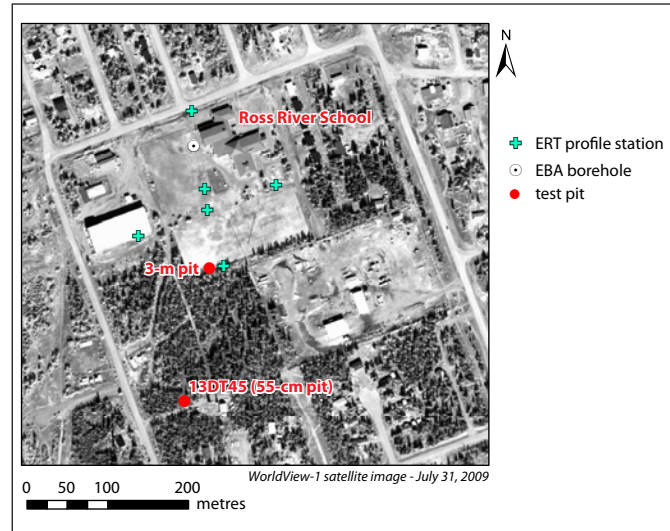


Figure 28. Map depicting locations of soil and permafrost investigation sites near Ross River School.

Borehole *RR_BH01* (Figure 29) was drilled south of the school at the limit between the school yard and a forested area, approximately 20 m along the ERT profile *RR_ERT02*. The ground was covered with 10 cm-high grass and 30 cm-high shrubs (*carex* sp.) in the school yard, and by 8 m-tall aspen and 15 m-tall black spruce in the open, regenerated forest. A pit was dug into the active layer and the frost table was encountered at a depth of 170 cm. The stratigraphy (measured from ground surface at 0 cm) was composed of layers of medium to fine sand (-15 to -74 cm) interlaced with layers of coarser sand (-74 to -190 cm). Once frozen ground had been reached, a borehole was drilled to a depth of 207 cm, until a gravel layer impeded further coring. At this depth, the permafrost had an excess ice content of 51% by volume. The material was composed predominantly of sand (87%), and the profile exhibited a homogeneous porous-invisible cryostructure. Thaw settlement potential of the permafrost was relatively low and had only 8% total settlement under a stress load of 150 kPa. The complete borehole log is shown in Appendix B, and ice content and grain size analysis results are shown in Appendix C.

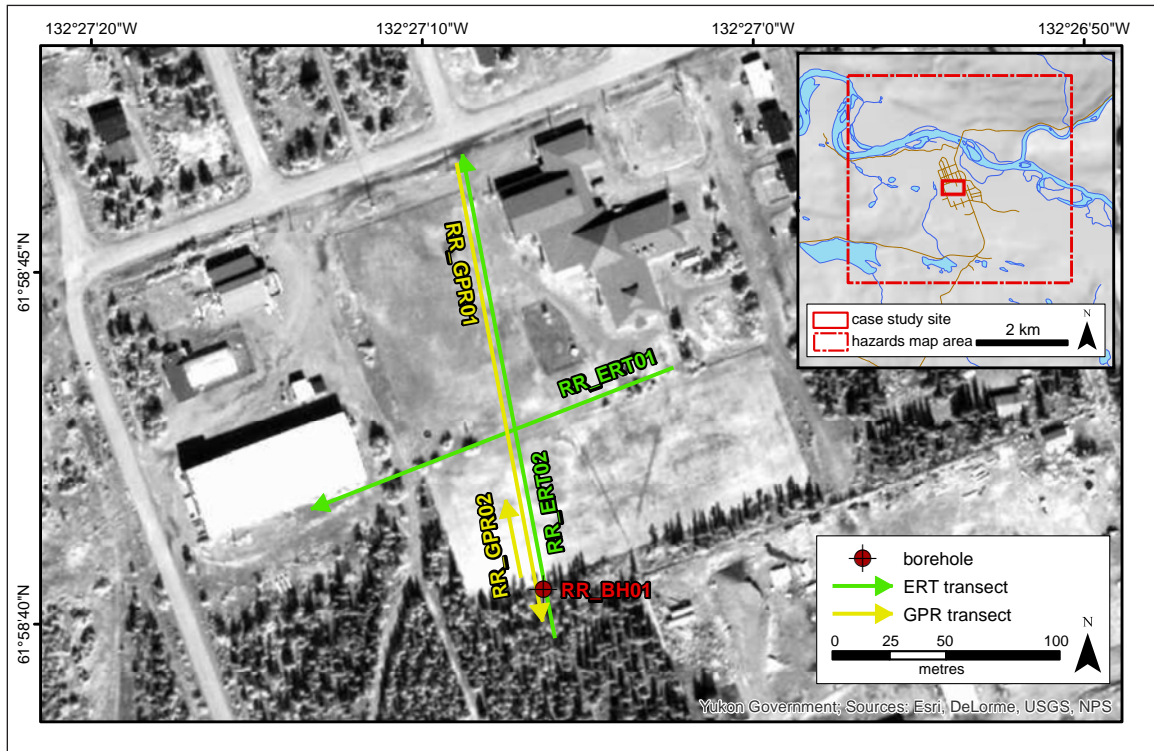


Figure 29. Map illustrating locations of detailed site investigations for Central Ross River. Refer to Figure 26 for all other case study locations within the study area boundary.

Two ERT profiles were completed near the school. The first (*RR_ERT01*; see Figure 29 for location) was 160 m long and was run from east to west across almost flat terrain from the arena parking lot, to the play structure that was built on sand and gravel. Frost probing was not possible at this site due to the widespread presence of coarse gravel. The ERT profile illustrates a low resistivity surface layer up to 2 m thick over a higher resistivity layer across most of the profile (Figure 30). This is inferred to represent a thick active layer overlying permafrost that extends to depths of 10-12 m. The base of the permafrost is not represented by a sharp change in resistivities across most of the profile and it may extend to greater depths than those depicted in the profile. A break (i.e., a through-going talik) occurs in the permafrost body from 108-112 m, and to the west of this, the permafrost is only about 5-6 m thick. The ERT profile indicates that permafrost has persisted beneath most of the transect, but given the disturbed terrain, the talik, and the thinner body at the west end of the profile, it is plausible that the permafrost may be gradually thawing.

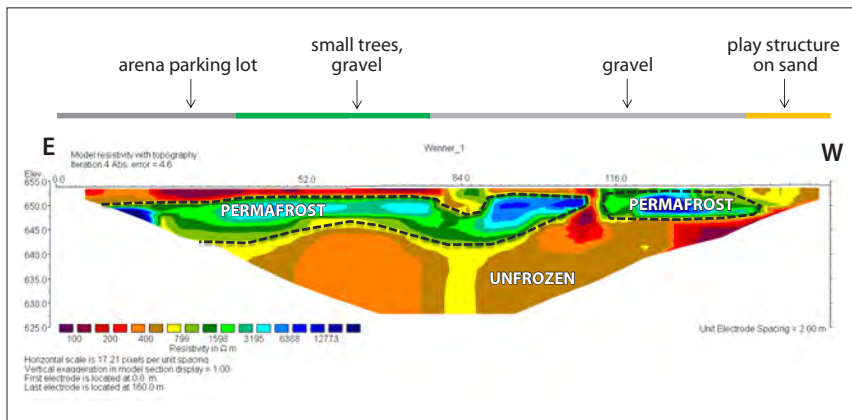


Figure 30. ERT profile *RR_ERT01*, which is 160 m long and was run east to west from the arena parking lot to the play structure near the Ross River School (see Fig. 29 for location). The profile has a maximum penetration depth of ~30 m. Likely areas of permafrost are outlined by black dashed lines.

The second ERT profile (*RR_ERT02*) was 200 m long and was run from south to north, beginning immediately west of the school, across the sports field, and up to the road ditch, which is oriented east-west (Figure 31). It is not as detailed as the first ERT profile (*RR_ERT01*) because it was undertaken using an electrode spacing of 5 m in order to penetrate to greater depths. The general pattern is a three to four-layered system, with a discontinuous low resistivity layer overlying a higher resistivity layer, and a lower resistivity layer that extends to near the base of the profile. At the base of the central part of the profile, there is an additional high resistivity layer. Resistivities are particularly high at depths below 5 m at the southern end of the profile (i.e., exceeding 10 ohm m). At the northern end, the high resistivity body terminates at 170 m along the profile.

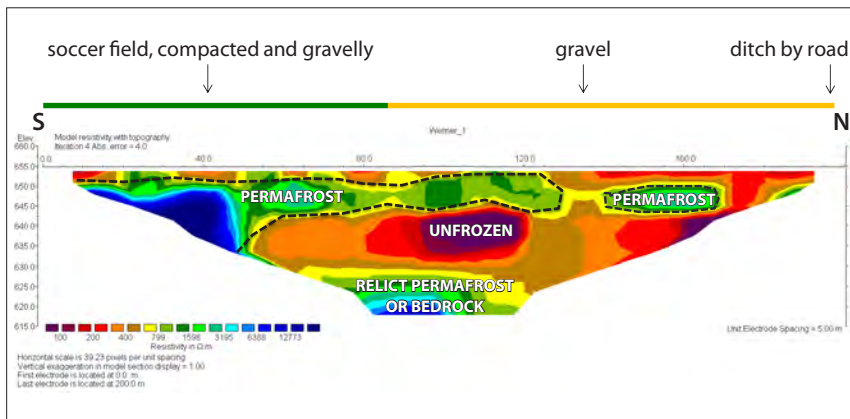


Figure 31. ERT profile *RR_ERT02*, which is 200 m long and was run south to north on the west side of the Ross River School (see Fig. 29 for location). The profile has a maximum penetration depth of ~30 m. Likely areas of permafrost are outlined by black dashed lines.

Based on the ERT profile depicted (*RR_ERT02*), permafrost is believed to reach depths of up to 20 m at the southern end of the transect, decreasing to less than 10 m at about 80 m along the profile (near the transition with the surface gravel), and possibly disappearing or being overlain by a supra-permafrost talik within 30 m of the road. The 80 m point on ERT profile *RR_ERT02* marks the intersection with ERT profile *RR_ERT01* and occurs 70 m along this profile. Both ERT profiles exhibit a 7 m-thick permafrost body at this location. The high resistivities at depth at the southern end of the profile (*RR_ERT02*) may represent high ice contents or a stratigraphic change. The high resistivities below 30 m depth in the centre of the profile may be deep permafrost that is gradually thawing or a bedrock contact beneath the glaciolacustrine sediments.

Two GPR surveys were performed at this site. The first (*RR_GPR01*; Figure 32), was 185 m long and was run parallel to ERT profile *RR_ERT02*, although in the opposite direction (i.e., from north to south; see Figure 29). The signal penetrated to a depth of ~4 m with a speed of 0.1 m/ns. An irregular layer is evident at a depth of ~170 cm at the beginning of the profile. The layer gets deeper towards the forest, reaching a maximum depth of ~3 m, and rises again to a depth of ~2 m under the forest cover. According to the borehole data (*RR_BH01*) and ERT profiles (*RR_ERT01*, *RR_ERT02*) from this location, this layer likely corresponds to the permafrost table, located at the interface between the sand and gravel units in the stratigraphic profile. A strong reflective layer is also located at a distance of 98 m along the transect. The GPR signal is stronger and penetrates more deeply between 30 and 75 m along the transect, which could be related either to frozen ground, or the intersection with a metallic object. (Underground services are present in the area, so the presence of an underground metallic structure is plausible.)

A second GPR transect (*RR_GPR02*) was run parallel to GPR survey *RR_GPR01* but in the opposite direction (i.e., from south to north; see Figure 29). This survey depicts a stratigraphic reflection at a depth of ~160 cm (Figure 33), which likely represents the contact between the active layer and permafrost noted in the Ross School borehole (*RR_BH01*; see Appendix B for complete borehole

logs). There are grey areas in the profile which may correspond to areas of saturated soil, where moisture has attenuated the GPR signal. The hummocky appearance of the layers may correspond to the sand and gravel fill used in the construction of the playing field. This strong reflection could correspond to the change in resistivity visible on the south side of the ERT profile *RR_ERT02* (see Figure 31).

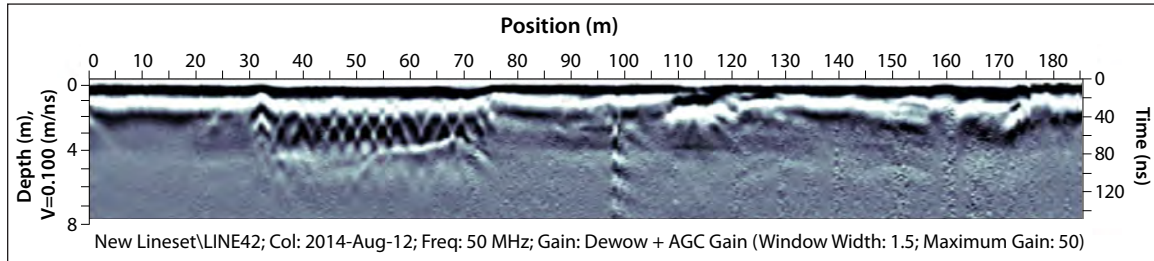


Figure 32. GPR profile (*RR_GPR01*) from the field next to the Ross River School, illustrating a strong horizontal reflection at ~170 cm, likely corresponding to the top of the permafrost table.

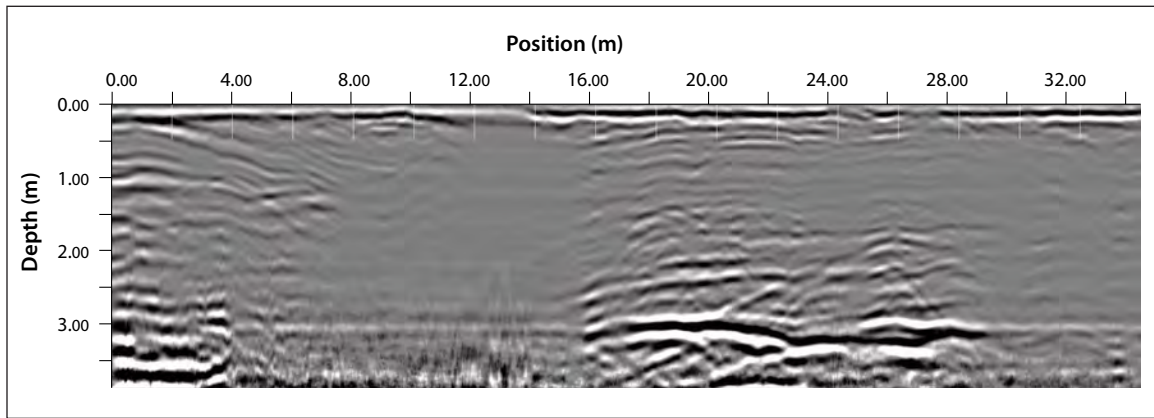


Figure 33. GPR profile (*RR_GPR02*) from the field adjacent to the Ross River School and running parallel to GPR survey *RR_GPR01* (see Fig. 32), showing a stratigraphic reflection at 1.6 m, likely corresponding to the top of the permafrost table.

The Ross River School exhibits many signs of structural damage that is potentially related to permafrost degradation (e.g., cracks, notable settlement, etc.). This could be a result of the top of the permafrost table lowering into icerich silt deposits underlying the gravel, causing subsequent melting of the excess ice contained within these sediments, and eventual thaw settlement. Based on results described above, the undisturbed ground appears to be stable, and the permafrost table is located in ice-poor material. However, any future ground surface thermal regime disturbances (e.g., vegetation clearing, an increase in snow accumulation, and/or an increase in mean annual air temperature) could lead to further permafrost degradation and thaw settlement at this site.

RIFLE RANGE

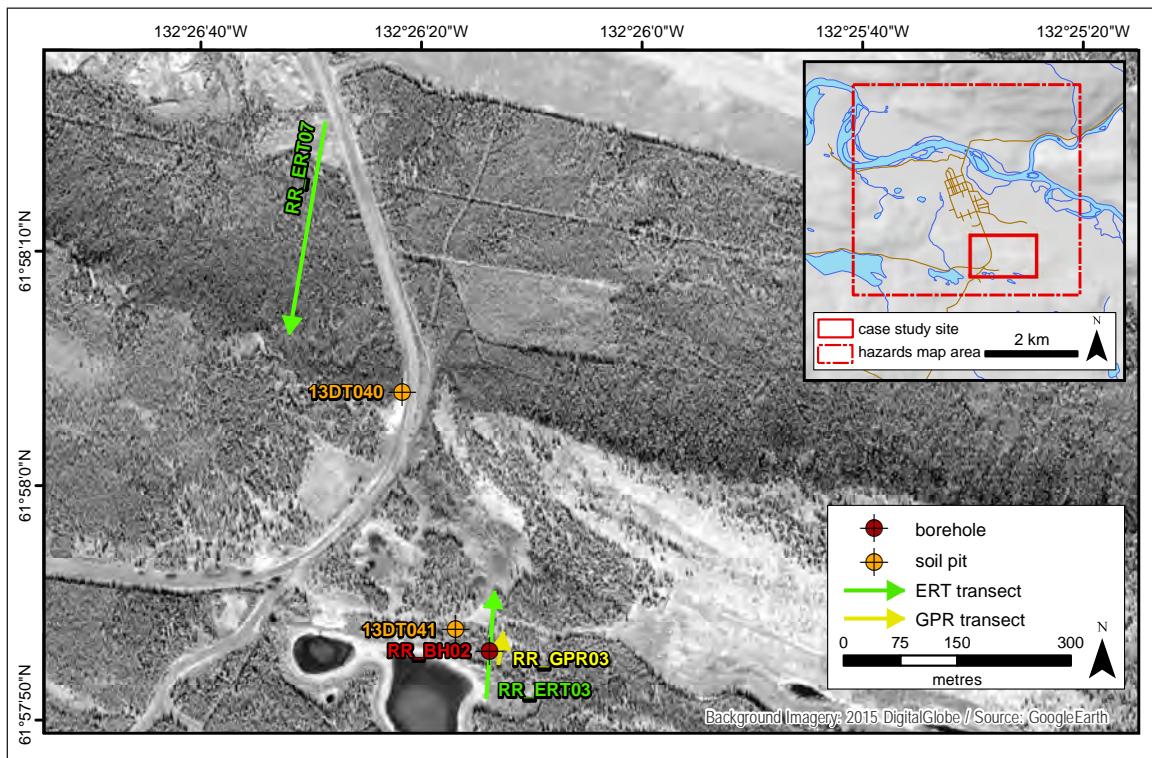
This site is located on a glaciolacustrine plain. Surface sediments exposed in a 60-cm test pit (Figure 34; station 13DT041) consisted of weakly stratified, very well-sorted, medium-grained sand containing two buried organic beds approximately 5 cm thick. Borehole *RR_BH02* (drilled approximately 40 m east of this pit; Figure 35) contained 5.4 m of coarse sand and fine gravel

underlain by 2 m of ice-rich silt and clay; the active layer was ~2 m thick. Five metres of bedded and laminated sand and silt were also exposed in a pit (station 13DT040) 350 m north of this site.



Figure 34 (left). Glaciolacustrine sand exposed in a 60 cm-deep soil pit dug at the Lacustre/Gun Range site (station 13DT041).

Figure 35 (below). Map illustrating locations of detailed site investigations for the area near the Ross River rifle range. Refer to Figure 26 for all other case study locations within the study area boundary.



Borehole *RR_BH02* is located 68 m along ERT profile *RR_ERT03* in an open, mesic, black spruce forest (see Figure 35). The black spruce trees averaged 20 m in height, and branches and spruce needles composed the forest floor litter. The borehole was drilled down to 717 cm, and the permafrost table was encountered at a depth of 201 cm. The stratigraphy was composed of a thin organic layer (13 cm thick) composed of moss, humus and tephra overlying layers of medium and

coarse sand (9 and 24 cm thick, respectively). Below these units, a thick layer of grey and brown coarse fluvial sand (151 cm thick) marked the bottom portion of the active layer. The water table was noted at a depth of 197 cm, directly on top of the permafrost table, which indicates that there was only 4 cm of saturated material at the bottom of the active layer. The first 330 cm of the permafrost (from 201 cm to 531 cm) comprised coarse to very coarse fluvial sand (98%) interlaced with small layers (13 to 54 cm thick) of fine gravel (clasts averaging 7 mm in diameter). This unit had a porous invisible cryostructure (i.e., structureless), typical of ice-poor permafrost, with an excess ice content of 8% by volume. At 530 cm, the stratigraphy changed, from coarse sand to clayey silt (86% silt, 11% clay), and was interpreted as a glaciolacustrine deposit. Here, the permafrost had an ice-rich microlenticular cryostructure and the volumetric excess ice content was in the range of 30%. Although the stratigraphy of each of the borehole sections was very different, they both exhibited some vulnerability to thaw settlement. During the first compaction test, a stress load of 15 kPa was applied. The upper section of the profile experienced a settlement of 6%, whereas settlement in the bottom section was measured at 18%. During the second compaction test, under a stress load of 150 kPa, the upper section of the profile exhibited a settlement of 15%, and settlement for the bottom section of the profile was 23%. The complete borehole log is shown in Appendix B, and grain size analysis and ice content results are shown in Appendix C.

A 160 m-long ERT profile (*RR_ERT03*; see Figure 35) was run at this site. At this location, the terrain is almost flat and the ERT profile shows a strong relationship between the degree of disturbance to the vegetation cover and the characteristics of the underlying permafrost (Figure 36). Frost tables were within 120 cm of the surface from the start of the profile through to 32 m, and again from 72-88 m along the profile. At the southern end of the profile, a thin body of permafrost, 5-7 m thick, is present beneath grasses and shrubs and adjacent to the pond. A through-going talik is present in a clearing from 48-56 m, dividing the thin permafrost from the main body. This permafrost extended to the edge of a dirt road at 116-136 m, and its depth reached the base of the ERT profile at about 25 m. Permafrost appears to be present beneath the road and its upper surface is noted at a depth of about 10 m, indicating that a supra-permafrost talik is present. Permafrost is again inferred at the north end of the profile beneath open forest, and one frost table depth of 70 cm was measured along this section of the profile. The thick active layer shows up clearly in the southern end of the ERT profile but not in the northern end. Borehole *RR_BH02*, located at 68 m along the profile, corresponds to a section where the permafrost is inferred to extend to a depth of at least 25 m, well below the depth of 7.2 m reached by the drill.

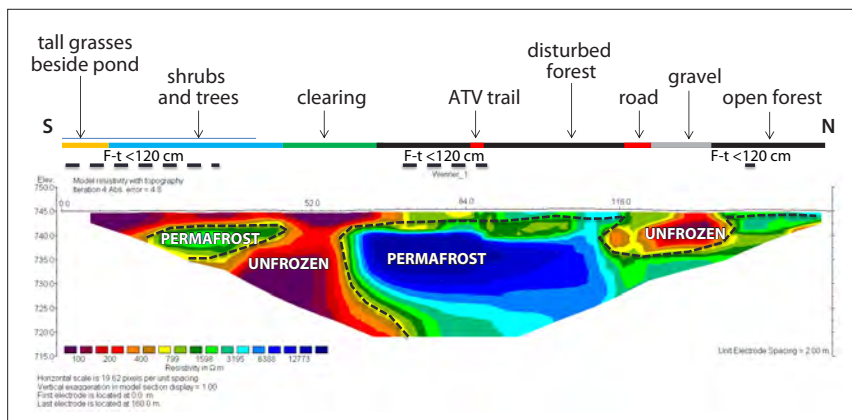


Figure 36. ERT profile *RR_ERT03*, which is 160 m long and runs south to north and intersecting borehole *RR_BH02* (see Fig. 35 for location). The profile has a maximum penetration depth of about 25 m. Likely areas of permafrost are outlined by black dashed lines. F-t = frost table.

A second ERT profile (*RR_ERT07*) was run northwest of ERT profile *RR_ERT03* (Figure 37). The survey was completed on a north-facing slope about 500 m northwest of *RR_ERT03*. This

400 m-profile was run down a gentle forested slope and into the valley bottom. There is a continuous, high-resistivity layer of variable thickness (8-30 m) just below the surface that overlies a lower resistivity layer. Tall deciduous shrubs from 310-340 m along the profile, which likely accumulate snow, correspond to an area of lower resistivity in the near-surface which may represent deeper seasonal thaw or a talik. A similar anomaly is present from 210-230 m along the profile where the forest is more open. There is a stratigraphic change (according to surficial mapping) at about 220 m along the profile and together with changes in drainage, this probably accounts for the highest resistivities observed within the lowest segment of the profile.

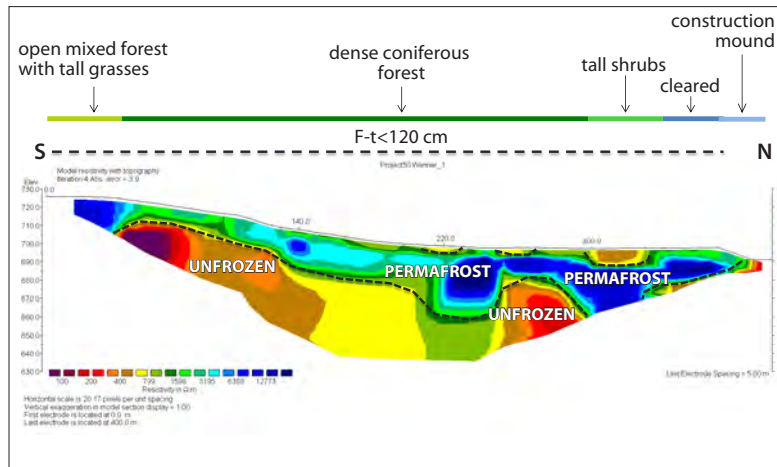


Figure 37. ERT profile RR_ERT07, which is 400 m long and located on a north slope about 500 m northwest of RR_ERT03 (see Fig. 35 for location). The profile has a maximum penetration depth of about 100 m. Likely areas of permafrost are outlined by black dashed lines. F-t = frost table.

A GPR transect (RR_GPR03) was also undertaken at this site. The penetration speed used for this survey was 0.914 m/ns. The permafrost table was identified in borehole RR_BH02 at a depth of 201 cm (see Appendix B for the complete borehole log), and appears as a strong horizontal reflection on the GPR profile, oscillating between depths of 1.5 and 2 m (Figure 38).

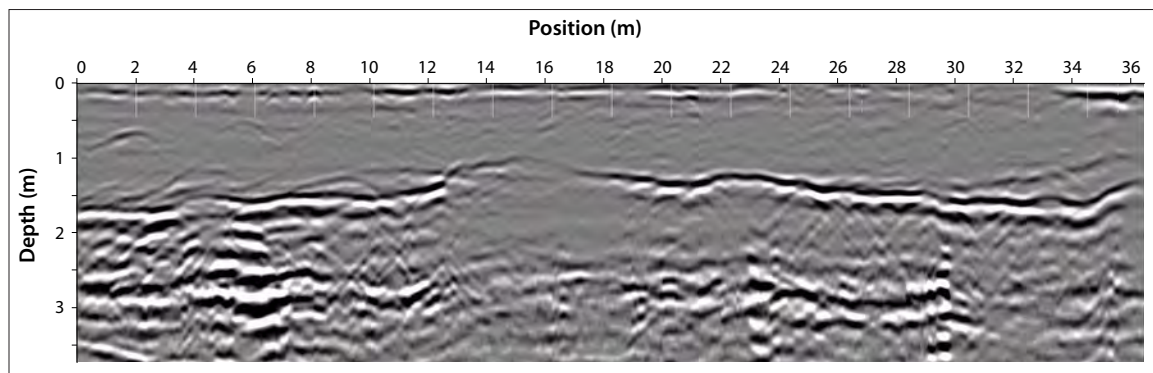


Figure 38. GPR profile from the gun range near Ross River, illustrating a strong horizontal reflection at ~197 cm, likely corresponding to the top of the water table.

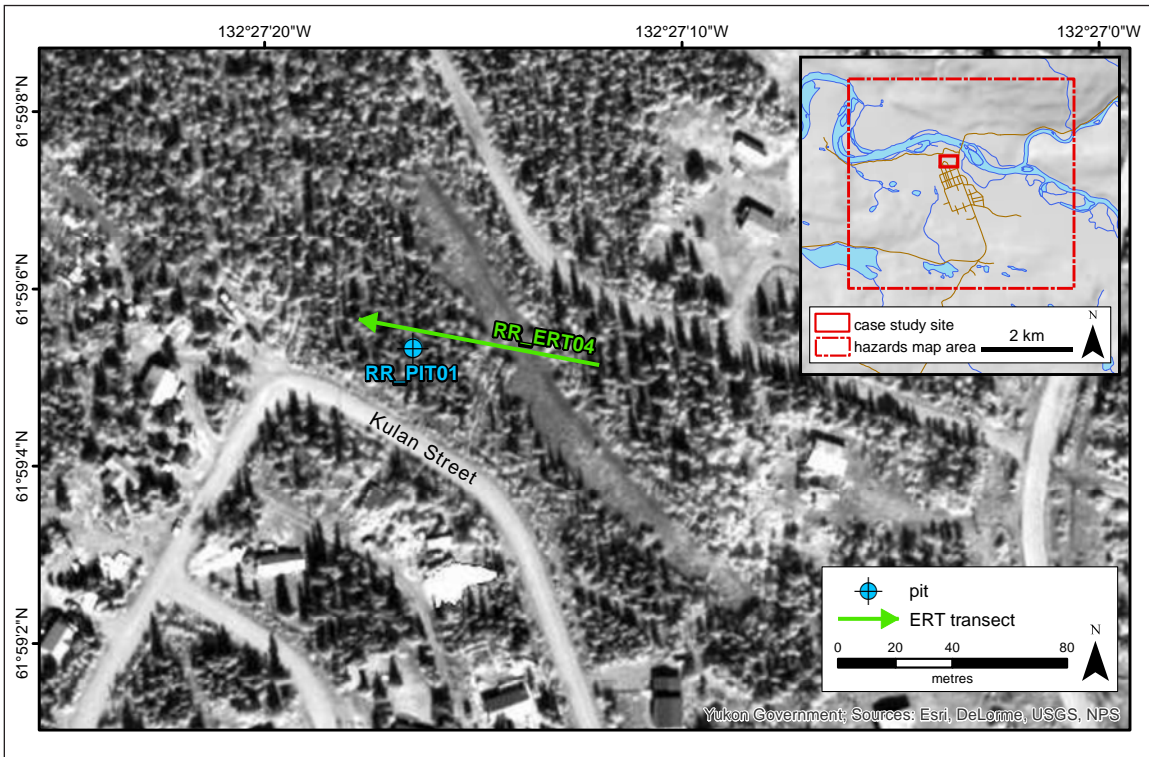
KULAN STREET

This site is located on the same fluvial terrace as the Ross River School. Interlaminated and bedded silt, and fine and medium-grained sand with mild to moderate oxidation were observed in an 80-cm test pit (Figure 39; station 13DT046), dug approximately 5 m from the road in a mature, mixed forest. One metre of coarser sand deposits were encountered at the top of an adjacent pit (RR_PIT01; see Figure 40), underlain by 0.8 m of cross-bedded gravel.



Figure 39 (left). Fine-grained fluvial sediments exposed in an 80 cm-deep soil pit dug at the Kulan Street site (station 13DT046). Pockets of White River ash are visible just below the brown surface organic layer.

Figure 40 (below). Map illustrating locations of detailed site investigations near Kulan Street. Refer to Figure 26 for all other case study locations within the study area boundary.



To investigate permafrost characteristics at this site, a shallow soil pit was excavated. *RR_PIT01* is located in a mesic, open, black spruce (up to 7 m high) and poplar (average of 15 m high) forest, along ERT *RR_ERT04* (Figure 40). There were no signs of past disturbances at the site, and a thin (1-cm thick) moss layer covered the ground. Although the site was located about 15 m from a drainage channel, the sandy nature of the sediments resulted in relatively dry surface conditions. A temperature of 1.7°C was recorded in situ at a depth of 200 cm. The stratigraphy consisted of a very thin organic layer (17 cm thick) mainly composed of slightly decomposed sandy humus

and tephra overlying medium to coarse sand, and dry sand mixed with gravel from 122 cm down to the base of the pit (at 204 cm). The complete log is shown in Appendix B. No permafrost was encountered, and the water table was not reached.

The ERT profile *RR_ERT04* was run over a distance of 80 m and extended to a depth of approximately 12 m (Figure 41). The eastern third of the profile is in a depression, while the remainder is slightly raised and better drained. Permafrost is absent at both ends of the profile and there is a single permafrost body in the centre, extending to a depth of about 10 m. Probing was possible across the profile but no frost tables were encountered within 120 cm of the surface. The ERT also suggests a relatively thick active layer where the permafrost is present. The pit *RR_PIT1* at 56 m along the profile did not encounter frozen ground to a depth of 2 m, but the ERT profile shows that it is present at greater depths.

No GPR transects were completed at this site.

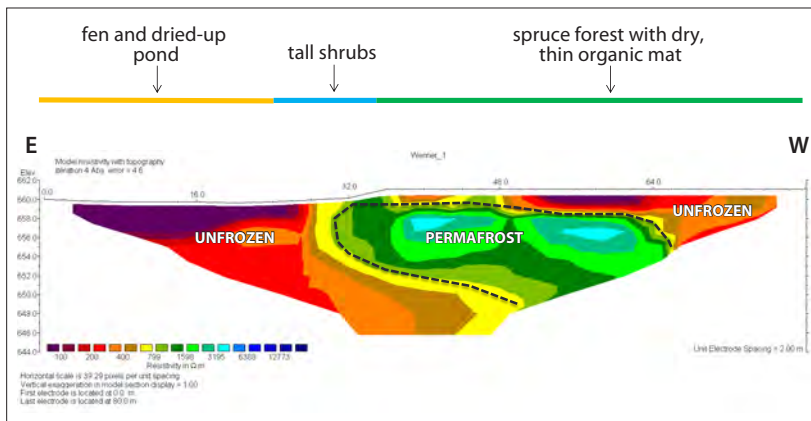


Figure 41. ERT profile *RR_ERT04*, which is 80 m long and runs east to west, just north of *RR_PIT01* (see Figure 40 for location.) The profile has a maximum penetration depth of 12 m. Likely areas of permafrost are outlined by black dashed lines.

OLD ROSS

The Old Ross site is also situated on a fluvial terrace of the Pelly River. Overbank flood deposits consisting of interbedded silt, fine and medium-grained sand with some organics were exposed in a shallow, 65-cm test pit (Figure 42; station 13DT031). Gravel is likely more abundant at depth, and was noted at surface in adjacent areas.



A stratigraphic cut (*RR_CUT01*) was prepared at the Old Ross site and was located in an open field, about 50 m north from the bank of the Pelly River (Figure 43). The ground is predominantly covered with moss and tall grasses up to 10 cm high. The surface material was slightly humid to dry to the bottom of the stratigraphic cut section (104 cm). No borehole was drilled at this site due to the shallow gravel deposits encountered 40 cm below the surface. A thin organic layer (16 cm thick) composed of fibric, undecomposed humus with roots and tephra mixed with fine sand was underlain by silty sand deposits (24 cm thick). No water or permafrost table was reached. Below this, a layer of clean, subrounded gravel

Figure 42. Fine-grained overbank flood sediments exposed in a 65 cm-deep soil pit at the Old Ross site (station 13DT031). White River ash is visible at the surface.

(clasts with a diameter of 0.5 to 30 cm), oriented but not sorted, marked the remaining section of the profile. The complete stratigraphic cut section is shown in Appendix B.

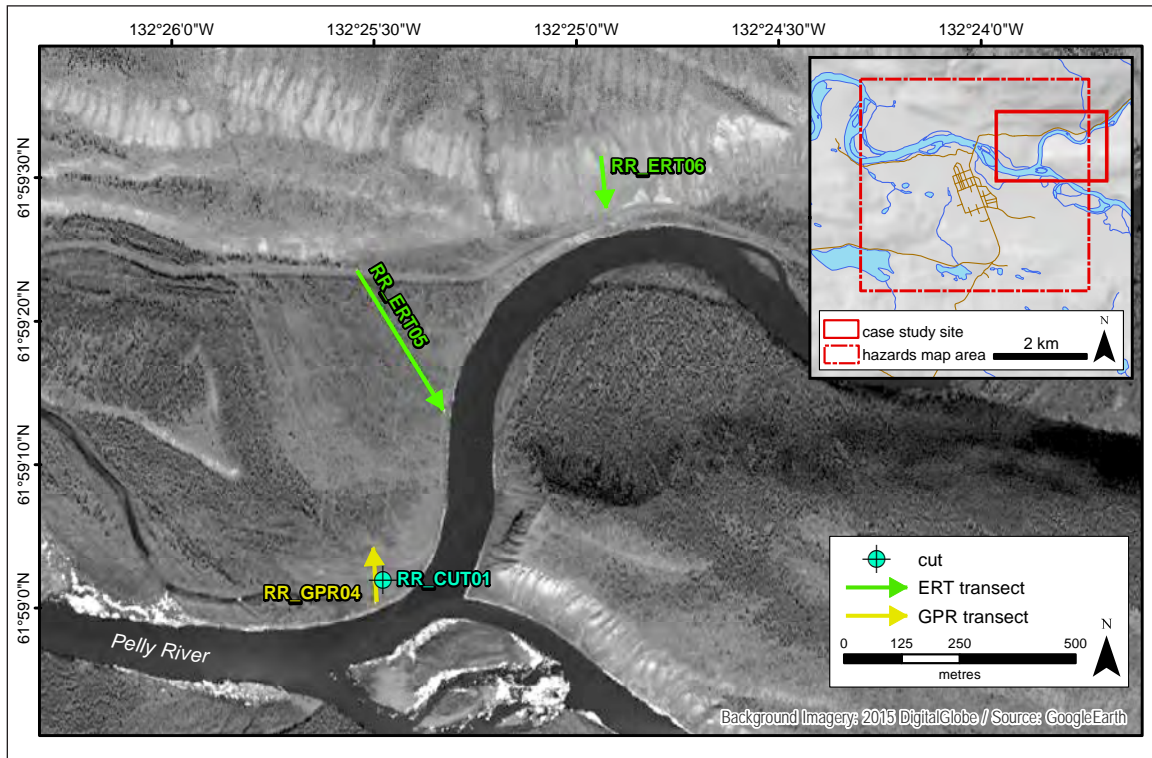


Figure 43. Map illustrating locations of detailed site investigations at the Old Ross case study site. Refer to Figure 26 for all other case study locations within the study area boundary.

Two ERT transects were run at this site. The first was a 300 m-long ERT transect (RR_ERT05) located about 200 m north of the cut described above (Figure 44). The profile runs from a cut bank on the river through forest regrowth, consisting largely of aspen and spruce trees. The ERT profile shows a high resistivity layer to a depth of about 8 m overlying a lower resistivity layer extending to the base of the profile at a depth of 50 m. This is interpreted as permafrost to 8 m overlying unfrozen ground. The active layer is not evident in the ERT profile because an electrode spacing of 5 m was used to obtain a deeper penetration. No frost table results could be obtained at this site because of the gravel or stiff clay layers.

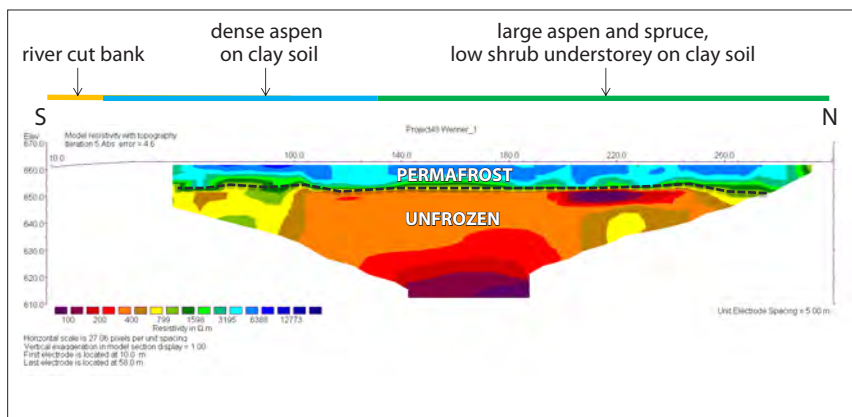


Figure 44. ERT profile RR_ERT05, which is 300 m long and runs south to north towards the river (see Figure 43 for location). The profile reaches a maximum penetration depth of 50 m. Likely areas of permafrost are outlined with black dashed lines.

A second ERT profile (*RR_ERT06*), 120 m in length, was undertaken on a steep (27-35°) south-facing slope. The survey was run from north to south at the Old Ross townsite on the north side of the Pelly River (Figure 45). The ground is covered by tussocks of grass with patches of exposed mineral soil. The ERT profile illustrates a moderate resistivity layer over a lower resistivity layer across the central part of the profile; the lower resistivity layer reaches the surface at both ends. This is interpreted as a body of permafrost, approximately 8 m thick, with unfrozen sediment at the upper and lower ends of the profile. The resistivities in the permafrost layer are typically 1000-3000 ohm m and these moderate values probably reflect warm or ice-poor permafrost.

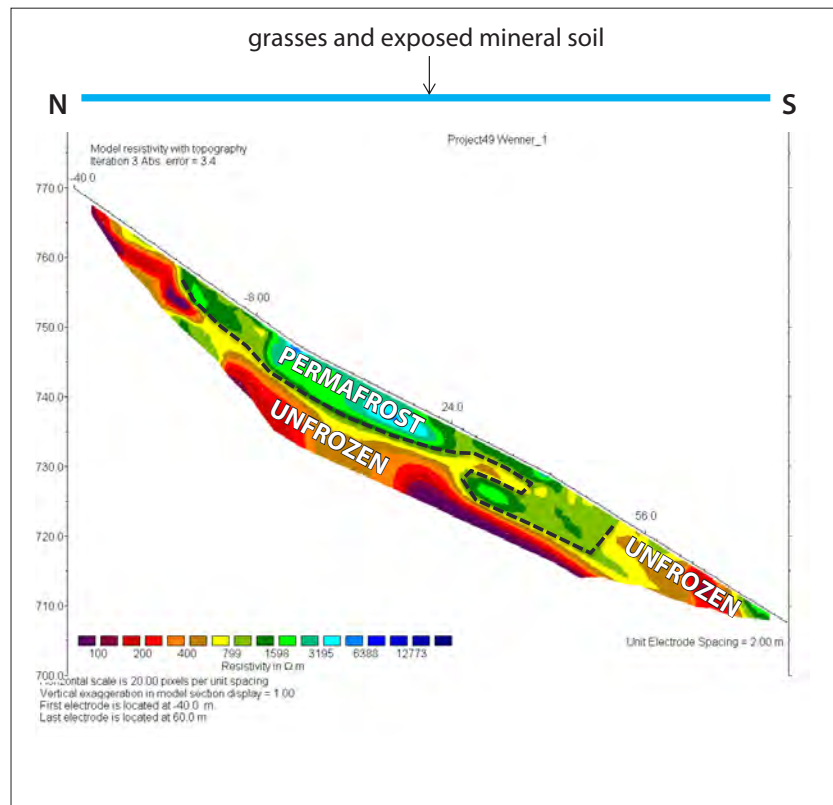


Figure 45. ERT profile *RR_ERT06*, which is 120 m long and runs north to south down a steep, south-facing slope near the Pelly River (see Figure 43 for location). The profile reaches a maximum penetration depth of about 15 m. Likely areas of permafrost are outlined by black dashed lines.

A 120 m-long GPR survey (*RR_GPR04*) was completed at this site. The survey was run northward from a bank of the Pelly River, across an open field where buildings once stood, to within a few metres of *RR_CUT01* (see Figure 43). The penetration speed used for this transect was 0.11 m/ns. The first 6 m of the profile were located in a forested zone, ~2 m below the level of the field. A strong and continuous contact is visible at a depth of ~2 m, and a second layer (strong but irregular) is evident at a depth of ~4.5 m (Figure 46). Although no permafrost was encountered at *RR_CUT01*, the nearby ERT profiles did detect permafrost. Because of the nature of the ground at cut *RR_CUT01*, and the presence of many parabolic features forming the reflected lines in the GPR profile, it is likely that layers of coarse material, such as boulders and cobbles, are present in the subsurface at this site.

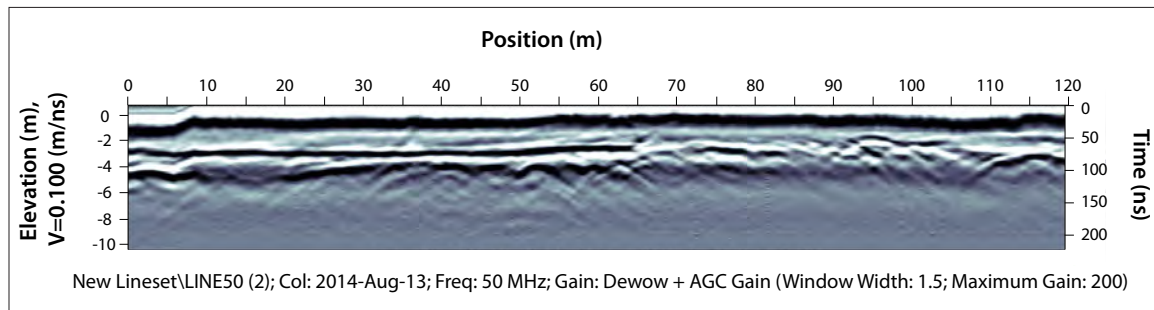


Figure 46. GPR profile from the Old Ross case study site, illustrating a strong horizontal reflection at ~2 m and a strong but irregular reflection at ~4.5 m, possibly reflecting layers of coarse material.

PROJECTING HAZARD RISKS IN A CHANGING CLIMATE

PROJECTED CLIMATE CHANGE FOR THE ROSS RIVER REGION

Climate projections for the Ross River area were integrated into this project in order to evaluate how current environmental conditions may pose risk in the future as a result of changes in climate. Predicting future climate change around the globe has become a critical component in climate change science and adaptation. Scientists use a variety of Global Climate Models in combination with discrete scenarios in order to make a range of projections for numerous climate variables (e.g., temperature and precipitation).

GLOBAL CLIMATE MODELS

Global Climate Models (GCMs) – also referred to as Atmosphere-Ocean General Circulation Models – are mathematical representations of atmospheric and oceanic circulation in the world. There are several types of GCMs; however, three-dimensional global atmosphere and ocean models are most commonly used to generate future climate projections. GCMs are complex mathematical models that incorporate a wide range of climate variables including radiation, energy transfer by winds, cloud formation, evaporation and precipitation of water, and transport of heat by ocean currents (CCRUN, 2011). The model calculations are based on a complex grid system that covers the globe in both a horizontal and vertical dimension on the order of 200-500 km. Data for each grid box is input into the model equations to solve for atmosphere, land surface and oceans (CCRUN, 2011).

CLIMATE CHANGE SCENARIOS

In order to generate future climate projections, the Intergovernmental Panel on Climate Change – the leading international body for the assessment of climate change – developed several scenarios that outline a range of possible emission futures. There are a total of six scenario groups, each making different assumptions about the release of greenhouse gases (e.g., carbon dioxide (CO₂), methane (CH₄), nitrous oxide (N₂O) etc.; see Nebojša et al., 2000 for details). Projections used for Ross River were derived from regionally downscaled climate data provided by the Scenarios Network for Alaska Planning (SNAP) at the University of Alaska Fairbanks (SNAP, 2013). For the purpose of this project, SNAP applied three scenarios that best represented the possible shifts in climate for the Yukon communities. The three scenarios used are defined as follows (SNAP, 2013):

The B1 scenario – low to moderate degrees of climate change

- rapid economic growth (as in A1B), but with rapid changes towards a service and information economy

- population rising to 9 billion in 2050 and then declining as in A1 (see Nebojša et al., 2000)
- reductions in material intensity and the introduction of clean and resource-efficient technologies
- an emphasis on global solutions to economic, social and environmental stability

The A1B scenario – medium to high degrees of climate change

- rapid economic growth
- a global population that reaches 9 billion in 2050 and then gradually declines
- the quick spread of new and efficient technologies
- a convergent world, i.e., income and way of life converge between regions
- extensive social and cultural interactions worldwide
- a balanced emphasis on all energy sources

The A2 scenario – high degree of climate change

- a world of independently operating, self-reliant nations
- continuously increasing population
- regionally oriented economic development
- slower and more fragmented technological changes and improvements to per-capita income

The climate projections developed by SNAP were then enhanced to reflect local landscape heterogeneity (like mountainous terrain, which can create local temperature inversions that are not typically captured in models; see Appendix D for more details). Climate projections for three time periods (the 2020s, 2050s and 2080s) were produced, and maps of all projections are included in Appendix D.

Based on climate normal data measured at the Faro Airport meteorological monitoring station (the closest long-term monitoring station to Ross River) for the period 1980-2010 (Environment Canada, 2014a), mean annual air temperature for the region is -2.7°C (Table 3). Interestingly, back-cast temperatures were hindcasted for the period 1950-1979 using the modelling approaches described above, and indicate that mean annual air temperature for this period was -4.0°C . This suggests a warming of 1.2°C has already taken place over the region in the past ~50 years.

Projections of mean annual air temperatures in the Ross River region show continued warming over the next several decades. All three scenarios predict temperatures in the 2020s that are comparable to climate normal conditions. By the 2050s, the B1 scenario predicts the lowest mean annual air temperature (-1.9°C), while A2 predicts the highest (-1.6°C). However, by the decade of the 2080s, both the A1B and A2 scenarios predict mean annual air temperatures to exceed 0°C (0.1°C and 0.3°C , respectively). Even B1, the most conservative scenario applied, predicts a mean annual air temperature of -0.9°C by the 2080s, which is 1.8°C warmer than present. However, as discussed in earlier sections of this report, warming in the region will not be uniform – lapse rates (i.e., changes in temperature with elevation gain) are variable and differ significantly from the global average (Lewkowicz and Bonnaventure, 2011). Regardless of scenario, continued increase in mean annual air temperature has the potential to exacerbate hazards in the Ross River region in ways that will be described below.

Table 3. Statistics generated for the B1, A1B and A2 climate scenarios, displaying mean, minimum and maximum air temperature in the 2020s, 2050s and 2080s.

Projection	Air Temperature (°C)		
	Mean	Minimum	Maximum
Current MAAT	-2.7	-3.1	-2.6
1950 - 1979	-3.8	-4.2	-3.7
B1 2020s	-2.5	-2.9	-2.4
B1 2050s	-1.9	-2.4	-1.8
B1 2080s	-0.9	-1.4	-0.8
A1B 2020s	-2.6	-3.0	-2.4
A1B 2050s	-1.3	-1.7	-1.2
A1B 2080s	0.1	-0.4	0.2
A2 2020s	-2.6	-3.1	-2.5
A2 2050s	-1.6	-2.0	-1.5
A2 2080s	0.3	-0.1	0.4

LANDSCAPE SENSITIVITY TO CLIMATE CHANGE

Under the projected climate scenarios presented in this report, risks associated with surficial materials and terrain stability are variable and primarily related to the effects of changing soil moisture and surface runoff. In general, terrain stability declines with increased soil moisture and/or surface runoff, both of which can be caused by thawing of ice-rich permafrost, and changing hydrological regimes (including streamflow, flooding, groundwater flow, seasonal precipitation patterns, and extreme snowmelt and rainfall events).

Changes in permafrost strongly affect surface and groundwater drainage and can cause near-surface materials to become either wetter or drier depending on site conditions. In ice-rich permafrost, active layer thickening may increase soil moisture and decrease slope stability, whereas in ice-poor permafrost, deepening of the active layer may improve local drainage capacity and increase surface slope stability. Increases in regional moisture delivery could also raise stream and lake levels which, in turn, may enhance incision or aggradation rates, and erosion on stream banks and lake shores. Changes in the amount or seasonal timing of precipitation, snowmelt and sediment supply may also increase stream channel instability and migration, undercutting and oversteepening of cutbanks and initiation of landslides. Extreme rainfall and snowmelt events will also trigger landslides by rapidly saturating soils, especially in areas where groundwater concentrates, such as in gullies or depressions, or where drainage is limited by shallow permafrost or bedrock. With climate amelioration, retrogressive thaw slumps could become more frequent, especially in areas where water comes in contact with ice-rich glaciolacustrine material.

Flooding is an ongoing concern near Ross River. Although the floodplain in this area is not currently active, test pits and water wells show that the Pelly River regularly floods the area around Ross River. With climate change, the intensity and frequency of flooding will likely be less predictable. In addition, thermokarst development and channel migration may also present significant hazards to the town site, due to the presence of ice-rich glaciolacustrine deposits at depth. The projected degradation of near-surface permafrost will increase the hazard associated with periglacial processes, including active layer detachment slides, sheetwash, and thermokarst erosion. Most of these processes occur on north-facing slopes, but can also occur on other aspects.

SENSITIVITY OF LOCAL SURFACE MATERIAL TYPES

The case study sites investigated in the Ross River area are located on an alluvial plain (Old Ross, Central Ross River and the Kulan Street area) or contain lacustrine deposits (the Rifle Range case study site). The stratigraphy in the project area mainly comprises ice-poor, coarse-grained material (gravel or sand) overlying ice-rich, fine-grained material (glaciolacustrine deposits). To evaluate the stability of a specific location in the study area, it is recommended that deep boreholes be drilled to determine the complete stratigraphy. If a fine-grained layer was to be encountered, appropriate mitigation techniques would be required. In the absence of a fine-grained layer, risks of permafrost thaw and ground settlement are low and constructed infrastructure is most likely to remain stable.

Nonetheless, the superposition of different surface material layers can change the behavior of a given deposit type (e.g., its frost susceptibility, hydraulic response, etc.). The following scenarios of deposit types were commonly observed in the Ross River area during drilling investigations.

Silt on gravel

Silt is a frost-susceptible, thaw-sensitive material that should be avoided for land-use planning involving buildings and transportation infrastructure. The impact of a layer of silt over a layer of gravel depends on the thickness of the silt layer. When the active layer is entirely composed of silt, significant frost heave and thaw settlement of the surface will occur, especially if the area is poorly drained. When the bottom of the active layer is composed of gravel and the silt is drained when freezing occurs, the material can be expected to remain stable. Active layer deepening in gravel without fines does not create significant thaw settlement. This stratigraphy is present in the upper part of the soil profile at the Old Ross case study site.

Gravel or sand on silt

A layer of non-frost susceptible, coarse-grained material (sand or gravel) can become problematic if it overlies a fine-grained layer. Even if the coarse layer is ice-poor and not frost-sensitive, this dry material could quickly transfer heat to an ice-rich, fine-grained layer beneath. Thus, following surface disturbances (e.g., vegetation clearing, excavation), the active layer could quickly reach the silt layer and cause settlement problems. This stratigraphic scenario is present in the Central Ross River and Rifle Range case study sites, and the boundary between the gravel and sand/silt layer is located at a depth of ~5-6 m. It is likely that this scenario is present at other sites where fluvial deposits are present; however, the depth to the silt layer may vary. Attention must be given to the identification of glaciolacustrine deposits, which are generally ice-rich and may be present at depth below coarse fluvial deposits.

Sand on gravel

A stratigraphy of sand over gravel is usually well drained, not frost-susceptible, and mechanically stable upon thawing. This stratigraphic scenario is present in the upper part of the soil profile at the Kulan Street case study site.

PROJECTED CHANGES IN PERMAFROST DISTRIBUTION

Increases in mean annual air temperature will affect permafrost distribution in the Ross River area. To assess potential future permafrost distribution in the study area, contemporary permafrost distribution must first be examined. A detailed assessment of the spatial pattern of current permafrost conditions in the Ross River region can be extracted from a model of permafrost probability developed for the southern half of Yukon (Bonnaventure et al., 2012). Model results for the Ross River region were extracted from the regional model (see Figure 16 on page 26 of this report).

To map future permafrost distribution, the contemporary permafrost probability model is perturbed by altering the input variable of equivalent elevation which represents mean annual air temperature. This effectively simulates a uniform regional temperature change, which is used to predict the probability of permafrost occurrence in the study area under differing degrees of warming. A range of mean annual air temperature increases from +1°C to +5°C were imposed, based on widely accepted projections of change for the next several decades (e.g., see IPCC, 2015). A scenario approach was favoured over applying global or regional climate model predictions, because the latter tends to provide inadequate representations from the effects of topography in the Yukon (see Burn, 1994).

The goal of imposing climate change scenarios on the regional permafrost probability model is to examine the sensitivity of permafrost to changes in mean annual air temperature over time. It is important to note that modelling is done for equilibrium conditions and therefore does not take into account the rate at which the change in climate might occur, nor the lag times associated with permafrost thaw. Still, it is a useful indication of potential changes in the spatial distribution of permafrost regionally, under a changing climate.

Increases in mean annual air temperature were simulated in the spatial model by uniformly decreasing the values of equivalent elevation in the transformed digital elevation model (Janke, 2005; Lewkowicz and Bonnaventure, 2011; Bonnaventure et al., 2012), and then running the model to produce an altered basal temperature of snow surface. This affects the predicted permafrost probabilities that are calibrated with the non-linear logistic regression coefficients determined for 1971-2000 climate normal conditions. An increase of 1°C is represented by a decrease in the equivalent elevation surface of 154 m. Even though the change is uniformly applied across the region, it results in differential responses that depend on the surface lapse rates below treeline. This methodology has the advantage of preserving all elements of the spatial model for a given area such as aspect, shading and slope, as well as the specific relationships that exist between changes in elevation and basal temperature of snow values. Although other environmental factors, such as snow and vegetation, significantly influence permafrost distribution in the discontinuous zones (e.g., Smith and Riseborough, 2002) and are expected to change in the future (e.g., IPCC, 2015), the model cannot take such changes into account, as they are not part of the input variables.

As with contemporary permafrost probability modelling presented above, results show probabilities on a scale of 0 to 1. If an area has a probability value of 0.6, this means that 60% of the grid cells in the area are likely to be underlain by permafrost. However, the model is not capable of distinguishing which grid cells in the area have permafrost; rather, it identifies local probabilities given local conditions.

The results of the perturbed permafrost probability modelling (see Figures 47-51) show that a relatively small increase in air temperature (1-2°C) is likely to have an impact on permafrost probability in Ross River. Under current conditions, the probability of permafrost occurring at any point in the region (defined by the boundaries of the hazards map; see Figure 1 for map area) is 60%. With a mean annual air temperature increase of +1°C, the probability of permafrost declines to 40%. With subsequent increases, permafrost probability continues to decline, so that with a mean annual air temperature increase of +5°C, the probability of permafrost in the map area is 20% (Table 4).

It is important to note that given the very significant thicknesses of permafrost in the case study sites demonstrated by the ERT profiles, there may be lag times of decades or even centuries in response to climate change that may affect predictions of future distribution of permafrost in the study area. However, sites with thinner, warmer permafrost, or sites subject to severe disturbance, can be expected to respond more rapidly. Where permafrost is ice-rich at depth (e.g., in buried

glaciolacustrine deposits), thaw settlement can persist for years, particularly where ice-rich deposits are thick. Potential declines in permafrost extent as a result of increases in mean annual air temperature should be factored into adaptive planning decisions, since there is a continual hazard risk to infrastructure as long as permafrost is in the process of thaw and degradation.

Table 4. Statistics displaying the probability of permafrost presence in the hazards map area under current and future scenarios of temperature increase.

Mean annual air temperature	Probability of permafrost presence		
	Mean	Minimum	Maximum
Current	0.6	0.5	0.8
+1°C	0.4	0.4	0.7
+2°C	0.3	0.3	0.5
+3°C	0.3	0.2	0.4
+4°C	0.2	0.2	0.3
+5°C	0.2	0.2	0.2

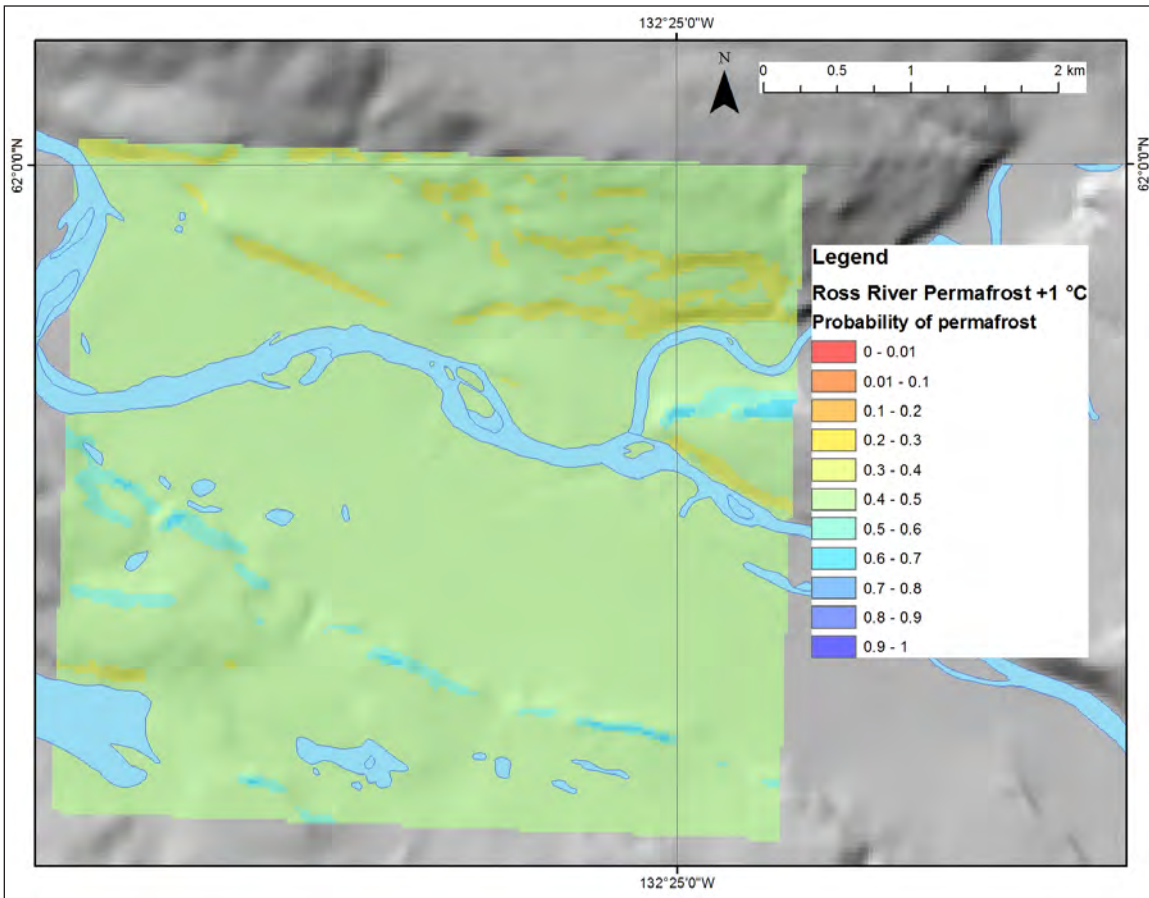


Figure 47. Projected permafrost probability for the Ross River region under an increase in mean annual air temperature of 1°C.

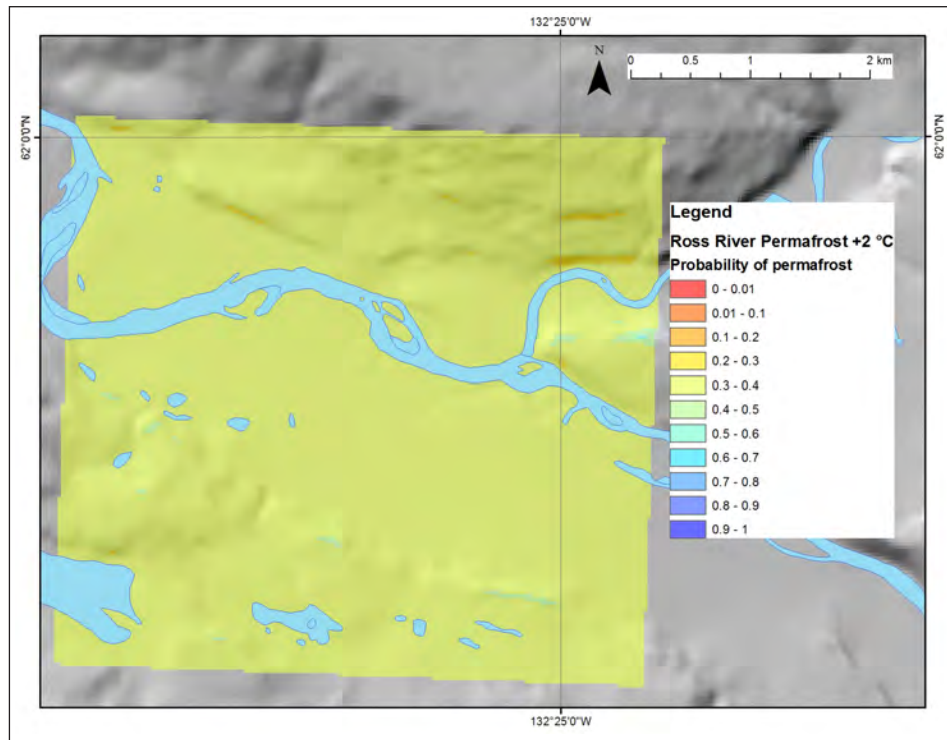


Figure 48. Projected permafrost probability for the Ross River region under an increase in mean annual air temperature of 2°C.

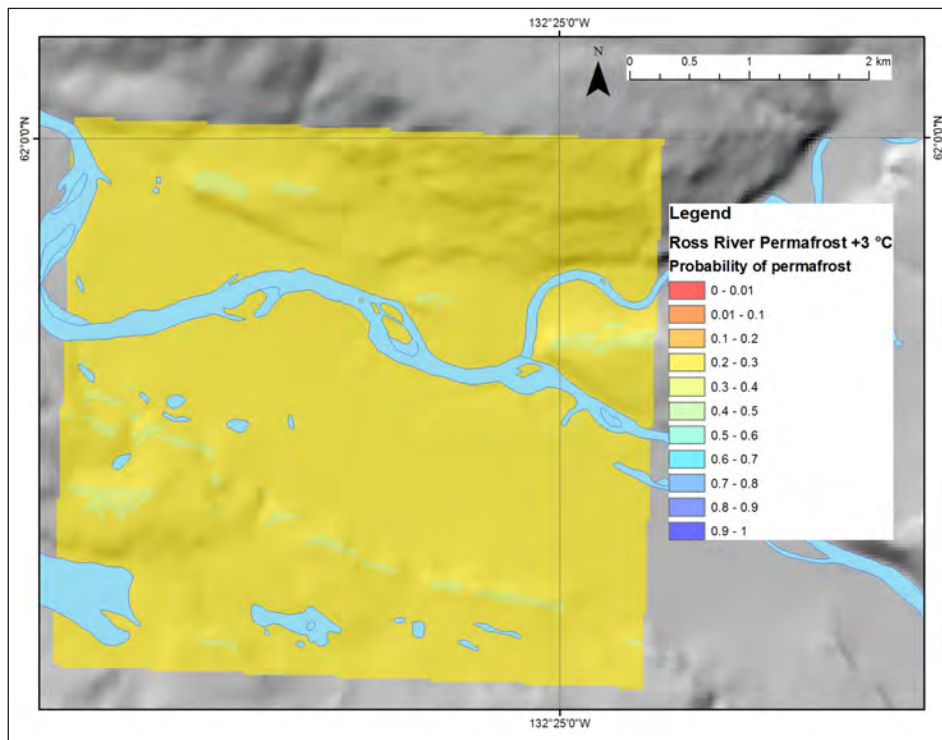


Figure 49. Projected permafrost probability for the Ross River region under an increase in mean annual air temperature of 3°C.

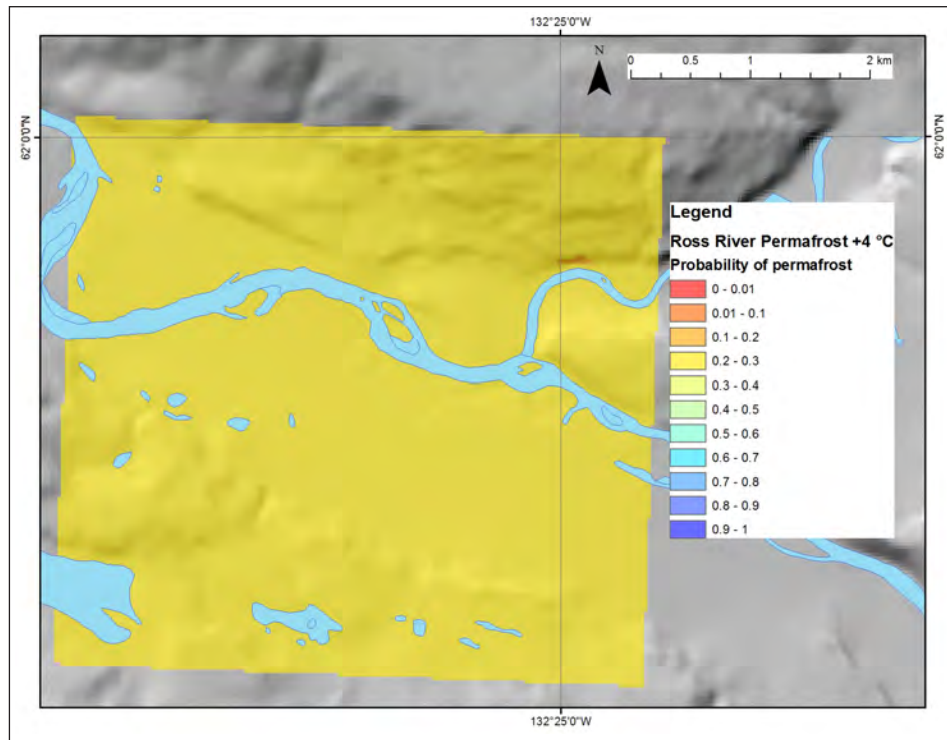


Figure 50. Projected permafrost probability for the Ross River region under an increase in mean annual air temperature of 4°C.

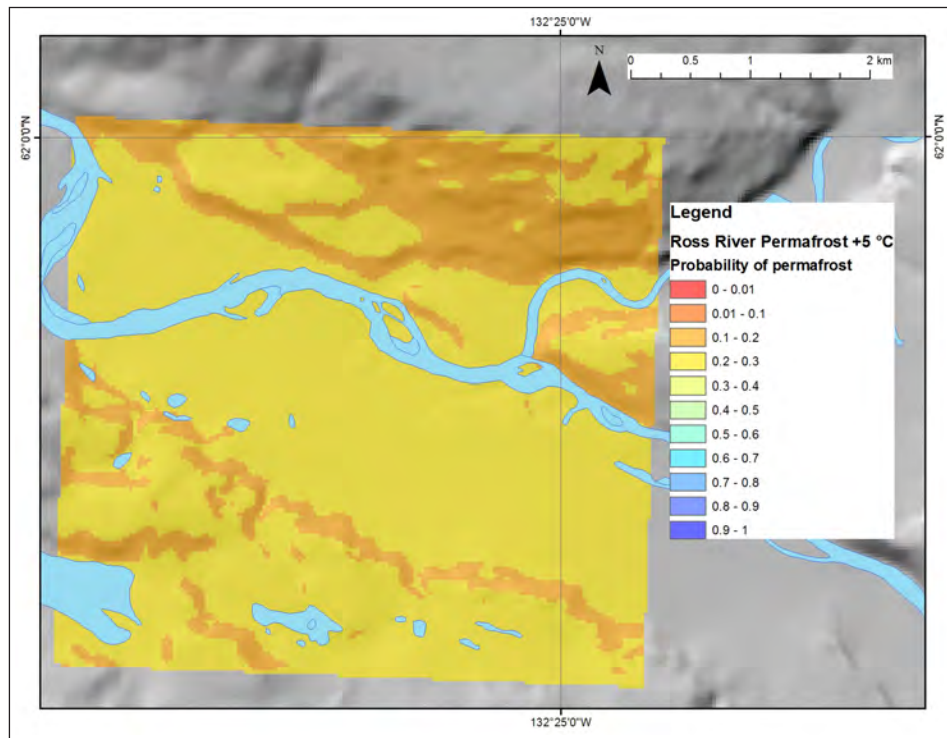


Figure 51. Projected permafrost probability for the Ross River region under an increase in mean annual air temperature of 5°C.

INTEGRATING RISK IN A LANDSCAPE HAZARDS MAP FOR THE ROSS RIVER REGION

To develop a landscape hazards map for the Ross River region that integrates current and future hazard risks in a changing climate, results from study region characterization, case study site investigations, laboratory analyses, climate projections, and contemporary and future permafrost probability modelling were integrated. All these geoscience parameters were combined to develop a risk ranking matrix specific to the Ross River region, as follows:

-  **Green: low** risk of hazards following permafrost degradation **or low** risk of geomorphic hazards.
-  **Yellow: moderate** risk of hazards following permafrost degradation (e.g., moderate thaw settlement) **or moderate risk** of geomorphic hazards.
-  **Red: high** risk of hazards following permafrost degradation (e.g., high thaw settlement, water ponding, and slow to rapid mass movement on slopes) **and/or high** risk of geomorphic hazards (e.g., gullying, flooding, steep slopes).

This risk matrix was then applied to each of the surficial geology polygons in the hazards map footprint (see Figure 1), and a risk ranking was assigned based on the geoscience characteristics of each polygon. It is important to note that in classifying polygons, we have taken a precautionary approach and applied a category of higher risk where we are not confident in lower categories. However, every polygon will contain zones of lower and higher risk than the overall polygon classification. It is for this reason that this map should serve as an initial guide for planning purposes. Any development will still require detailed site investigations. It is also important to note that hazard rankings are based on general observations of surface materials, drainage, slope angle, vegetation, and the presence of permafrost. Additionally, subsurface information provided by ERT and GPR profiles, drilling and probing of permafrost, and textural analyses of surficial and borehole samples are also used in determining hazard rankings. This has resulted in a projected risk ranking that will require geotechnical and/or engineering analyses to quantify.

The hazards map for the Ross River region is 22 km² and is presented in Figure 52, as well as in a larger print version in the back pocket of this report. As described earlier, the hazards map area is a subset of the surficial geology map created as part of this project (Turner, 2014; included in back pocket of this report), and each of the surficial geology polygons within the hazards map area has been assigned a hazard risk ranking. Appendix E details the hazard classification assigned to each numbered polygon in the map area, and outlines its associated hazard(s).

A total of 63 polygons fall within the map area and were ranked based on current and perceived hazard risks. Of these, 26 polygons (representing 6.7 km² of the map area) were assigned a low hazard risk ranking, 13 polygons (7.8 km² of the map area) were assigned a moderate hazard risk ranking, and 24 polygons (6.2 km² of the map area) were assigned a high hazard risk ranking. (Water bodies make up an additional 1.3 km² of the map area.) Generally, low-risk polygons are in the southwestern portion of the map area, where surficial deposits are composed mainly of morainal deposits (e.g., polygons 4, 5, 6, 13 and 23), whereas moderate and high-risk polygons are noted along the Pelly River and in the northeastern portion of the map area, where inactive floodplains and variable slopes are present (e.g., polygons 15, 21, 51, 54). The most common hazards associated with moderate and high hazard risk polygons are related to geomorphological factors, including active and moderately steep slopes, debris flows, and gullying. These factors affect 20 polygons in the map area. Fourteen polygons were designated moderate or high-risk

rankings due to the potential for flooding or because they are composed of inactive floodplains. Eight polygons were associated with ice-rich permafrost or thermokarst and were assigned a moderate or high-risk ranking as a result, and a single polygon was ranked as having a moderate hazard risk due to the presence of mine pit walls. (Note that polygons may be subject to more than one risk factor; for example, a polygon may be subject to both flood and ice-rich permafrost hazard risk.)

Investigations at case study sites in the Ross River area allow for a more detailed assessment of hazard risk at each location. The Kulan Street and Central Ross River case study sites are both located on fluvial deposits (polygon 16) and were classified as having a moderate hazard risk because of the potential presence of ice-rich, fine-grained deposits (e.g., glaciolacustrine, gravelly to sandy silt) below gravel and sand layers, resulting in risk associated with permafrost degradation. If permafrost degraded to the point where the active layer reached the silty layer, notable thaw settlement could take place. In fact, the Ross River School, which shows several signs of damage attributed to permafrost thaw (e.g., cracks, settlement), is affected by such a situation – results from case study investigations demonstrate that the permafrost table is located close to, or just below, the silty layer. Associated thaw settlement will likely continue to be problematic in this area. Thaw settlement could be augmented in the next decades if the ice-rich glaciolacustrine sediments in the area are thick. However, in undisturbed ground (e.g., forested areas) the permafrost table tends to be closer to the surface. Nonetheless, it is likely that clearing of undisturbed areas will result in permafrost degradation and subsequent risk due to sustained, multi-year (or multi-decadal) thaw settlement. There is a low risk of hazards as a result of mass movement or drainage, because of the coarse-grained nature of near-surface deposits, and the low-relief, gently-sloping landforms found in much of this area.

Adjacent to the Kulan Street and Central Ross River case study sites, polygons 19 and 22 were classified as having a high hazard risk based on past flood events and due to the potential for flooding by the Pelly River during spring break-up or summer high flows.

The Rifle Range case study site (polygon 27) has been classified as having a moderate hazard risk. However, it is important to note that ice-rich, fine-grained glaciolacustrine deposits were found at a depth of about 5 m, underneath an ice-poor, fluvial sand layer. Although the first 5 m of surface material in this area have low settlement potential, if the permafrost degraded to a point that the active layer reached the ice-rich layer, settlement potential could greatly increase, and the associated thaw settlement would become problematic. Because the sand overlying the ice-rich layer is ice-poor and has low heat capacity, a thermal disturbance at the surface (e.g., site clearing, increase in mean annual air temperature) could lead to rapid thawing of the underlying, ice-rich silt layer. There is also the potential for poor drainage at this site, particularly if the silt layer thaws, contributing to its moderate risk ranking. Note that adjacent polygons 24, 53 and 62 have been ranked as having a high hazard risk, because these polygon areas are made up of organic deposits that already exhibit poor drainage conditions, and contain thaw-sensitive, ice-rich permafrost.

The Old Ross case study site (polygon 54) was ranked as having a moderate hazard risk due to flood risk, as it is located on a fluvial plain at the confluence of the Ross and Pelly rivers. No permafrost was encountered in a shallow pit excavated 50 m from the river on the fluvial plain; however, geophysical surveys detected thin, near-surface permafrost at nearby sites away from the river. Gravel at depth may prevent thaw settlement at this site, should permafrost degradation occur. At this site (and at nearby polygons 15, 33 and 41), flood risk is considered more notable than risks associated with permafrost degradation, although gravel deposits present at the site prevented a more thorough investigation of permafrost by drilling. As a result, additional work to characterize

permafrost conditions at this site is recommended if development of the Old Ross River townsite is considered in the future.

It is important to note that no matter the classification, all future development projects must be preceded by thorough engineering investigations prior to construction. The higher the hazard-risk ranking, the more notable and potentially problematic hazard risks at this site will likely be. Nonetheless, a moderate or high hazard risk ranking does not preclude the possibility of development, should suitable engineering and mitigation techniques be employed. Special attention must be given to the detection of ice-rich glaciolacustrine deposits at depths exceeding 5 m south of the Pelly River. Additionally, Appendix F describes of types of foundation techniques that may be suitable for buildings in permafrost environments similar to those of Ross River, and may assist in mitigating permafrost thaw.

GENERATING ACTION FROM SCIENCE

The knowledge and data generated by the Ross River hazards mapping project can be used to inform planning and policy development and establish a baseline from which future science can be generated. It is the hope of the authors that the information contained herein informs planning and decision-making processes in the Ross River area.

This project has contributed to the assessment of vulnerability for the Ross River region. In particular, this project has characterized the local landscape and assessed local hazards, while advancing our understanding of potential climate change impacts in the region. This information may serve as a basis for evaluating how community infrastructure, security and well-being may be influenced by climate variability, and how the community might take action to respond. By integrating variability into decision-making through multiple scenarios, robust and responsive adaptation strategies can be developed. In this way, the science of hazards assessment is an important foundation from which to build action.

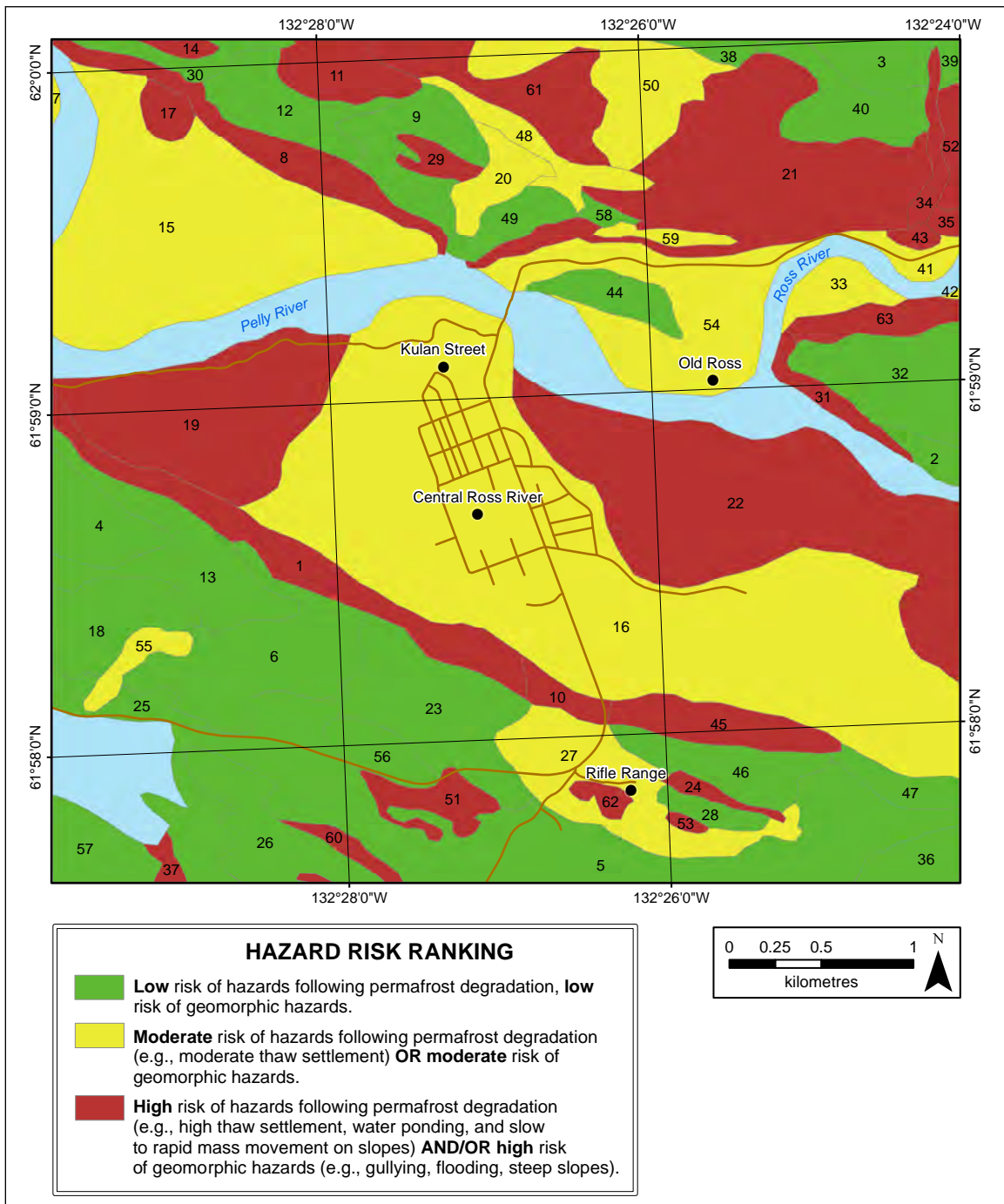


Figure 52. Map depicting hazard risk ranking for the Ross River area (see Figure 1 for location of the map boundary). Specific hazards associated with each numbered polygon are listed in Appendix E. A larger fold-out version of this map is included in the map pocket in the back of this report.

REFERENCES

- Beierle, B. and Bond, J.D., 2002. Density-induced settling of tephra through organic lake sediments. *Journal of Paleolimnology*, vol. 28, p. 433-440.
- Bond, J.D., 1999a. Surficial geology map of Mount Mye and Faro (105K 3&6 W), central Yukon. Exploration and Geological Services Division, Yukon Region, Indian and Northern Affairs, Canada, Open File 1999-8. 1:25 000 scale.
- Bond, J.D., 1999b. McConnell ice-flow map of the Anvil District (105K), central Yukon. Exploration and Geological Services Division, Yukon Region, Indian and Northern Affairs, Canada, Open File 1999-14. 1:250 000 scale.
- Bond, J.D., 2001a. Quaternary geology and till geochemistry of the Anvil district (parts of 105K/2, 3, 5, 6 and 7), central Yukon Territory. Exploration and Geological Services Division, Yukon, Indian and Northern Affairs Canada, Bulletin 11, 39 p.
- Bond, J.D., 2001b. Surficial geology and till geochemistry of Weasel Lake map area (105G/13), east central Yukon. *In: Yukon Exploration and Geology 2000*, D.S. Emond and L.H. Weston (eds.), Exploration and Geological Services Division, Yukon, Indian and Northern Affairs Canada, p. 73-96.
- Bond, J.D. and Kennedy, K.E., 2005. Late Wisconsinan McConnell ice-flow and sediment distribution patterns in the Pelly Mountains, Yukon. *In: Yukon Exploration and Geology 2004*, D.S. Emond, L.L. Lewis and G.D. Bradshaw (eds.), Yukon Geological Survey, p. 65-82.
- Bonnaventure, P.P., Lewkowicz, A.G., Kremer, M. and Sawada, M., 2012. A regional permafrost probability model for the southern Yukon and northern British Columbia, Canada. *Permafrost and Periglacial Processes*, vol. 23, p. 52-68, doi:10.1002/ppp.1733.
- Brown, R.J.E., 1963. Influence of vegetation on permafrost. First International Conference on Permafrost, Lafayette, PA.
- Brown, R.J.E. and Péwé, T.L., 1973. Distribution of permafrost in North America and its relationship to the environment: A review, 1963-1973. Second International Conference on Permafrost, Yakutsk, USSR.
- Brown, J., Ferrians, O.J. Jr., Heginbottom, J.A. and Melnikov, E.S., eds., 1997. Circum-Arctic map of permafrost and ground-ice conditions. Washington, DC; US Geological Survey in Cooperation with the Circum-Pacific Council for Energy and Mineral Resources, Circum-Pacific Map Series CP-45, scale 1:10 000 000, 1 sheet.
- Burn, C.R., 1994. Permafrost, tectonics, and past and future regional climate change, Yukon and adjacent Northwest Territories. *Canadian Journal of Earth Sciences*, vol. 31, p. 182-191.
- CBC, 2013. Ross River, Yukon, homes flooded a second time. <http://www.cbc.ca/news/canada/north/ross-river-yukon-homes-flooded-a-second-time-1.1332252>.
- Clague, J.J., Evans, S.G., Rampton, V.N. and Woodsworth, G.J., 1995. Improved age estimates for the White River and Bridge River tephras, western Canada. *Canadian Journal of Earth Sciences* vol. 32, p. 1172-1179.
- Colpron, M. (compiler), 2015. Update of the Yukon bedrock geology map. Yukon Geological Survey, http://www.geology.gov.yk.ca/update_yukon_bedrock_geology_map.html.

- Consortium for Climate Risk in the Urban Northeast (CCRUN), 2011. What methods do scientists use to make projections about future climate change and its impacts? CCRUN, Fact Sheet #4, Columbia University, New York, NY, 3 p. http://ccrun.org/ccrun_files/attached_files/FactSheet4.pdf.
- Darrow, M.M., Huang, S.L., Shur, Y. and Akagawa, S., 2008. Improvements in frost heave laboratory testing of fine-grained soils. *Journal of Cold Regions Engineering*, vol. 22, p. 65-78.
- De Grandpré, I., Fortier, D. and Stephani, E., 2012. Degradation of permafrost beneath a road embankment enhanced by heat advected in groundwater. *Canadian Journal of Earth Sciences*, vol. 49, p. 953-962. doi: 10.1139/e2012-018.
- Deklerk, R. and Burke, M. (compilers), 2008. Yukon Mineral Property Update 2008. Yukon Geological Survey, 94 p.
- Dimitrov, P. and Weinstein, M., 1984. So That the Future Will Be Ours, Volume 2. Ross River Indian Impact Report, prepared by the Ross River Indian Band, Ross River, YT, 190 p.
- Duk-Rodkin, A., Barendregt, R.W. and White, J.M., 2010. An extensive late Cenozoic terrestrial record of multiple glaciations preserved in the Tintina Trench of west-central Yukon: stratigraphy, paleomagnetism, paleosols, and pollen. *Canadian Journal of Earth Science*, vol. 47, p. 1003-1028.
- EBA Engineering Consultants Ltd., 2007. Borehole W14101031-BH01 drill log. Report prepared for the Government of Yukon.
- Environment Canada, 2014a. Historical Climate Data. Environment Canada, Ottawa, Ontario, http://climate.weather.gc.ca/index_e.html.
- Environment Canada, 2014b. Climate Trends and Variations. Environment Canada, Ottawa, Ontario, <http://ec.gc.ca/adsc-cmda/default.asp?lang=En&n=F3D25729-1>.
- Environment Yukon, 1976. Groundwater Information Network water well 211030018. <http://gw-info.net/>.
- Environment Yukon, 1990. Groundwater Information Network water well 211030017. <http://gw-info.net/>.
- French, H., 2007. *The Periglacial Environment*, 3rd edition. John Wiley and Sons, West Sussex, England, 478 p.
- French, H. and Shur, Y., 2010. The principles of cryostratigraphy. *Earth Science Reviews*, vol. 101, p. 190-206.
- Froese, D.G., Barendregt, R.W., Enkin, R.J. and Baker, J., 2000. Paleomagnetic evidence for multiple Late Pliocene – Early Pleistocene glaciations in the Klondike area, Yukon Territory. *Canadian Journal of Earth Sciences*, vol. 37, p. 863-877.
- Gabrielse, H., Murphy, D.C. and Mortensen, J.K., 2006. Cretaceous and Cenozoic dextral orogen-parallel displacements, magmatism, and paleogeography, north-central Canadian Cordillera. *In: J.W. Haggart, R.J. Enkin and J.W.H. Monger (eds.), Paleogeography of the North American Cordillera: Evidence For and Against Large-Scale Displacements*. Geological Association of Canada, Special Paper 46, p. 255-276.
- Gangloff, R.A., May, K.C. and Storer, J.E., 2004. An early Late Cretaceous dinosaur tracksite in central Yukon Territory, Canada. *Ichnos*, vol. 11, issue 3-4, p. 299-309.

- Gartner Lee Limited, 2003. Yukon Groundwater and Ground Source Heat Potential Inventory. Prepared for Energy Solutions Centre, Report # 22-680, Whitehorse, YT, 258 p.
- Global Terrestrial Network for Permafrost, 2013. <http://www.gtnp.org/>
- Gordey, S.P., 1995. Geology, Tay River map area, Yukon Territory (105K). Geological Survey of Canada, Map 19-1987, Sheet 2, 1:250 000 scale.
- Gordey, S.P., 2013a. Geology, Selwyn Basin (Sheldon Lake and Tay River), Yukon. Geological Survey of Canada, "A" Series Map 2149A, 3 map sheets, scale 1:250 000 and 1 sheet of cross-sections, 1:100 000 scale.
- Gordey, S.P., 2013b. Evolution of the Selwyn Basin region, Sheldon Lake and Tay River map areas, central Yukon. Geological Survey of Canada, Bulletin 599, 190 pages and 5 sheets.
- Gordey, S.P. and Makepeace, A.J. (compilers), 2003. Yukon digital geology, version 2.0. Geological Survey of Canada, Open File 1749, and Yukon Geological Survey, Open File 2003-9(D), 2 CD-ROMs.
- Government of Yukon, 1992. Canol Project. In *The Alaska Highway: A Yukon Perspective*. Retrieved from <http://www.alaskahighwayarchives.ca/en/chap5/index.php>.
- Government of Yukon, 2014. Ross River. Yukon Community Profiles – Ross River. Retrieved from <http://www.yukoncommunities.yk.ca/ross-river>.
- Hauck, C., Isaksen, K., Vonder Mühll, D. and Sollid, J.L., 2004. Geophysical surveys designed to delineate the altitudinal limit of mountain permafrost: An example from Jotunheimen, Norway. *Permafrost and Periglacial Processes*, vol. 15, p. 191-205. doi:10.1002/ppp.493.
- Heginbottom, J.A., Dubreuil, M.A. and Harker, P.T., 1995. Permafrost Map of Canada. *In: The National Atlas of Canada, 5th Edition, (1978-1995)*, published by Natural Resources Canada, sheet MRC 4177, 1: 7 500 000 scale.
- Hidy, A.J., Gosse, J.C., Froese, D.G., Bond, J.D. and Rood, D.H., 2013. A latest Pliocene age for the earliest and most extensive Cordilleran Ice Sheet in northwestern Canada. *Quaternary Science Reviews*, vol. 61, p. 77-84.
- Hilbich, C., Hauck, C., Hoelzle, M., Scherler, M., Schudel, L., Voelksch, I., Vonder Muehll, D. and Maüsbacher, R., 2008. Monitoring mountain permafrost evolution using electrical resistivity tomography: A 7-year study of seasonal, annual, and long-term variations at Schilthorn, Swiss Alps. *Journal of Geophysical Research-Earth Surface*, vol. 113, F01S90. doi:10.1029/2007JF000799.
- Hilbich, C., Maescot, L., Hauck, C., Loke, M.H. and Maüsbacher, R., 2009. Applicability of electrical resistivity tomography monitoring to coarse blocky and ice-rich permafrost landforms. *Permafrost and Periglacial Processes* vol. 20, p. 269–284. doi:10.1002/ppp.652.
- Hoggan Engineering and Testing, 1989. Geotechnical investigation, Ross River roads and sanitary sewer development, Ross River, Yukon Territory. Report to Department of Community and Transportation Services, Yukon Territorial Government, Whitehorse, YT, 11 p.
- Huntington, H. and Weller, G., 2005. Chapter 1: An Introduction to the Arctic Climate Impact Assessment. *In: Arctic Climate Impact Assessment Scientific Report*, C. Symo, L. Arris and B. Heal (eds.), Cambridge University Press, p. 1-20.

- Instanes, A., 2003. Climate change and possible impacts on Arctic infrastructure. Proceedings of the Eighth International Conference on Permafrost, Zurich, Switzerland, June 2003, p. 461-466.
- Intergovernmental Panel on Climate Change (IPCC), 2015. Fifth Assessment Report. IPCC, Geneva, Switzerland, <https://www.ipcc.ch/index.htm>.
- Jackson, L.E. Jr., 1989. Paleoglaciology of the Selwyn Lobe of the Cordilleran Ice Sheet and Quaternary stratigraphy of east-central Yukon. In: Late Cenozoic History of the Interior basins of Alaska and the Yukon, L.D. Carter, T.D. Hamilton and J.P. Galloway (eds.), U.S. Geological Survey, Circular 1026, p. 60-65.
- Jackson, L.E. Jr., 1993. Surficial geology, Bruce Lake, Yukon Territory. Geological Survey of Canada, Map 1791A, 1:100 000 scale.
- Jackson, L.E. Jr., 1994. Terrain inventory and Quaternary history of the Pelly River area (105 F, G, J, K), Yukon Territory. Geological Survey of Canada, Memoir 437, 41 p.
- Jackson, L.E. Jr. and Harington, C.R., 1991. Pleistocene mammals, stratigraphy, and sedimentology at the Ketza River site, Yukon Territory. *Géographie Physique et Quaternaire*, vol. 45, p. 69-77.
- Jackson, L.E. Jr., Ward, B., Duk-Rodkin, A. and Hughes, O., 1991. The latest Cordilleran ice sheet in southern Yukon Territory. *Géographie Physique et Quaternaire*, vol. 45, p. 341-354.
- Janke, J.R., 2005. Modelling past and future alpine permafrost distribution in the Colorado Front Range. *Earth Surface Processes and Landforms*, vol. 30, p. 1495-1508, doi: 10.1002/esp.1205.
- Janowicz, R., 2008. Apparent recent trends in hydrologic response in permafrost regions of northwest Canada. *Hydrology Research*, vol. 39, p. 267-275.
- Jensen, B.J., Pyne-O'Donnell, S., Plunkett, G., Froese, D.G., Hughes, P.D., Sigl, M., McConnell, J.R., Amesbury, M.J., Blackwell, P.G., van den Bogaard, C., Buck, C.E., Charman, D.J., Clague, J.J., Hall, V.A., Koch, J., Mackay, H., Mallon, G., McColl, L. and Pilcher, J.R., 2014. Transatlantic distribution of the Alaskan White River Ash. *Geology*, vol. 42, no. 10, p. 875-878.
- Jorgenson, M.T. and Osterkamp, T.E., 2005. Response of boreal ecosystems to varying modes of permafrost degradation. *Canadian Journal of Forest Research*, vol. 35, p. 2100-2111.
- Kneisel, C., Hauck, C. and Vonder Mühl, D., 2000. Permafrost below the timberline confirmed and characterized by geoelectrical resistivity measurements, Bever Valley, eastern Swiss Alps. *Permafrost and Periglacial Processes*, vol. 11, p. 295-304. doi:10.1002/1099-1530(200012)11:4<295::AID-PPP353>3.0.CO;2-L.
- Kneisel, C., Hauck, C., Fortier, R. and Moorman, B., 2008. Advances in geophysical methods for permafrost investigations. *Permafrost and Periglacial Processes*, vol. 19, p. 157-178.
- Kudryavtsev, V.A., 1979. Method of permafrost survey. Moscow State University Publication, Moscow, Russia.
- Lerbekmo, J.F., 2008. The White River Ash: Largest Holocene Plinian tephra. *Canadian Journal of Earth Sciences*, vol. 45, p. 693-700.
- Lerbekmo, J.F. and Campbell, F.A., 1969. Distribution, composition and source of the White River Ash, Yukon Territory. *Canadian Journal of Earth Sciences*, vol. 6, p. 109-116.

- Lewkowicz, A.G. and Bonnaventure, P.P., 2011. Equivalent elevation: A method to incorporate variable lapse rates into mountain permafrost modeling. *Permafrost and Periglacial Processes*, vol. 22, p. 153-162.
- Lewkowicz, A.G., Etzelmüller, B.E. and Smith, S.L., 2011. Characteristics of discontinuous permafrost from ground temperature measurements and electrical resistivity tomography, southern Yukon, Canada. *Permafrost and Periglacial Processes*, vol. 22, p. 320-342.
- Lewkowicz, A.G. and Ednie, M., 2004. Probability mapping of mountain permafrost using the BTS method, Wolf Creek, Yukon Territory, Canada. *Permafrost and Periglacial Processes*, vol. 15, p. 67-80.
- Lipovsky, P.S., 2015. Summary of Yukon Geological Survey permafrost monitoring network results, 2008-2013. *In: Yukon Exploration and Geology 2014*, K.E. MacFarlane, M.G. Nordling and P.J. Sack (eds.), Yukon Geological Survey, p. 113-122.
- Lipovsky, P.S., Coates, J., Lewkowicz, A.G. and Trochim, E., 2006. Active-layer detachments following the summer 2004 forest fires near Dawson City, Yukon. *In: Yukon Exploration and Geology 2005*, D.S. Emond, G.D. Bradshaw, L.L. Lewis and L.H. Weston (eds.), Yukon Geological Survey, p. 175-194.
- Lipovsky, P. and Huscroft, C., 2007. A reconnaissance inventory of permafrost-related landslides in the Pelly River watershed, central Yukon. *In: Yukon Exploration and Geology 2006*, D.S. Emond, L.L. Lewis and L.H. Weston (eds.), Yukon Geological Survey, p. 181-195.
- Lipovsky, P.S. and Yoshikawa, K., 2009. Initial results from the first year of the Permafrost Outreach Program, Yukon, Canada. *In: Yukon Exploration and Geology 2008*, L.H. Weston, L.R. Blackburn and L.L. Lewis (eds.), Yukon Geological Survey, p. 161-172.
- Long, D.G.F., Lowey, G. and Sweet, A.R., 2001. Age and setting of dinosaur trackways, Ross River area, Yukon Territory (105F/15). *In: Yukon Exploration and Geology 2000*, D.S. Emond and L.H. Weston (eds.), Exploration and Geological Sciences Division, Yukon Region, Indian and Northern Affairs Canada, p. 181-198.
- Lunardini, V.J., 1994. Heterogenetic and syngenetic growth of permafrost. Ground Freezing '94, Proceedings of the Seventh International Symposium on Ground Freezing, Nancy, France, p. 361-373.
- Mathews, W.H., 1986. Physiographic map of the Canadian Cordillera. Geological Survey of Canada, Map 1701A, scale 1:5 000 000.
- Murton, J.B. and French, H.M., 1994. Cryostructures in permafrost, Tuktoyaktuk coastlands, western arctic Canada. *Canadian Journal of Earth Sciences*, vol. 31, no. 4, p. 737-747.
- Natural Resources Canada, 2010. Simplified seismic hazard map for Canada. <http://www.earthquakescanada.nrcan.gc.ca/hazard-alea/simp haz-eng.php>.
- Northern Climate ExChange (NCE), 2011. Mayo Landscape Hazards: Geological Mapping for Climate Change Adaptation Planning. Yukon Research Centre, Yukon College, Whitehorse, YT, 64 p.
- Nebojša, N., Davidson, O., Davis, G., Grübler, A., Kram, T., La Rovere, E.L., Metz, B., Morita, T., Pepper, W., Pitcher, H., Sankovski, A., Shukla, P., Swart, R., Watson, R. and Dadi, Z., 2000. Emissions Scenarios: A Special Report of Working Group III of Intergovernmental Panel on Climate Change. Intergovernmental Panel on Climate Change, Geneva, Switzerland, 27 p.

- Nelson, F.E., Anisimov, O.A. and Shiklomanov, N.I., 2002. Climate change and hazard zonation in the circum-Arctic permafrost regions. *Natural Hazards*, vol. 26, p. 203-225.
- Noson, L., 2002. Hazard Mapping and Risk Assessment. In: *Regional Workshop on Best Practices in Disaster Mitigation*, Bali, Indonesia, September 24-26, 2002; Asian Disaster Preparedness Center (ADPAC), p. 69-94. <http://www.adpc.net/audmp/rlw/PDF/hazard%20mapping.pdf>
- O'Donnell, J.A., Jorgenson, M.T., Harden, J.W., McGuire, A.D., Kanevskiy, M.Z. and Wickland, K.P., 2012. The effects of permafrost thaw on soil hydrologic, thermal and carbon dynamics in an Alaskan peatland. *Ecosystems*, vol. 15, p. 213-229.
- Page, A., 2009. A topographic and photogrammetric study of rock glaciers in the southern Yukon Territory. Unpublished M.Sc. thesis, Department of Geography, University of Ottawa, 160 p.
- Plouffe, A., 1989. Drift prospecting and till geochemistry in Tintina Trench, southeastern Yukon. MSc thesis, Department of Earth Sciences, Carleton University, Ottawa, ON, 81 p.
- Roddick, J.A., 1967. Tintina Trench. *Journal of Geology*, vol. 75, p. 23-32.
- Ross River Dena Council, 2014. About Us. <http://www.rrdc.ca/category/about-us>
- Selwyn Resources Ltd., 2009. Ross River: Socio-Economic & Community Profile. <http://www.yukonwaterboard.ca/registers/quartz/qz10-042/1.2.10.pdf>
- Shur, Y.L. and Jorgenson, M.T., 2007. Patterns of permafrost formation and degradation in relation to climate and ecosystems. *Permafrost Periglacial Processes*, vol. 18, doi:10.1002!ppp. 582.
- Smith, M.W. and Riseborough, D.W., 2002. Climate and the limits of permafrost: a zonal analysis. *Permafrost and Periglacial Processes*, vol. 13, p. 1-15.
- Smith, C.A.S., Meikle, J.C. and Roots, C.F. (editors), 2004. *Ecoregions of the Yukon Territory: Biophysical Properties of Yukon Landscapes*. Agriculture and Agri-Food Canada, PARC Technical Bulletin 04-01, Summerland, British Columbia, 313 p.
- Scenarios Network for Alaska and Arctic Planning (SNAP), 2013. <http://www.snap.uaf.edu/about.php>
- Stanley Associates Ltd., 1986. Groundwater supply investigation, Ross River, Yukon. Report to Department of Community and Transportation Services, Yukon Territorial Government, Whitehorse, YT, 9 p.
- Stephani, E., Fortier, D. and Shur, Y., 2010. Applications of cryofacies approach to frozen ground engineering – Case study of a road test site along the Alaska Highway (Beaver Creek, Yukon, Canada). *GEO2010: 63rd Canadian Geotechnical Conference and 6th Canadian Permafrost Conference*, Calgary, Canada.
- Stephani, E., Fortier, D., Shur, Y., Fortier, R., Doré, G. and Walsh, R., 2014. A geosystems approach to permafrost investigations for engineering applications, an example from a road stabilization experiment, Beaver Creek, Yukon, Canada. *Cold Region Science and Technology*, vol. 100, p. 20-35.
- Tempelman-Kluit, D.J., 1977. Quiet Lake (105F) and Finlayson Lake (105G) map areas. *Geological Survey of Canada*, Open File 486, 1:250 000 scale.
- Tempelman-Kluit, D., 1980. Evolution of physiography and drainage in southern Yukon. *Canadian Journal of Earth Sciences*, vol. 17, no. 9, p. 1189-1203.

- Tempelman-Kluit, D.J., 2012. Geology of Quiet Lake and Finlayson Lake map areas, south-central Yukon – An early interpretation of bedrock stratigraphy and structure. Geological Survey of Canada, Open File 5487, 103 pages and 13 sheets, doi:10.4095/29 1931.
- Turner, D.G., 2014. Surficial geology, Ross River region, Yukon, parts of NTS 105K/1 & 2 and 105F/15 & 16. Yukon Geological Survey, Energy, Mines and Resources, Government of Yukon, Open File 2014-13, 1:25 000 scale.
- Wahl, H.E., Fraser, D.B., Harvey, R.C. and Maxwell, J.B., 1987. Climate of Yukon. Climatological Studies Number 40, Ottawa, Ontario: Atmospheric Environment Service, Environment Canada, 233 p.
- Ward, B.C., 1989. Quaternary stratigraphy along Pelly River in Glenlyon and Carmacks map areas, Yukon Territory. In: Current Research, Part E. Geological Survey of Canada, Paper 89-1E, p. 257-264.
- Ward, B.C. and Jackson, L.E., Jr., 2000. Surficial geology of the Glenlyon map area, Yukon Territory. Geological Survey of Canada, Bulletin 559, 60 p.
- Warren, F.J. and Lemmen, D.S. (eds.), 2014. Canada in a Changing Climate: Sector Perspectives on Impacts and Adaptation. Government of Canada, Ottawa, ON, 286 p.
- Water Survey of Canada, 2015. National Water Quantity Survey Program. Environment Canada, <https://wateroffice.ec.gc.ca>.
- Weinstein, M.S., 1992. Just Like People Get Lost: A Retrospective Assessment of the Impacts of the Faro Mining Development on the Land Use of the Ross River Indian People. Report prepared for the Ross River Dena Council, Ross River, YT, 193 p.
- Yukon Bureau of Statistics (YBS), 2010. Government of Yukon Socio-Economic and Web Portal – Ross River: Housing Tenure, Condition, Period of Construction and Structural Type Census 2006. http://www.sewp.gov.yk.ca/data?regionId=YK.RR&subjectId=POPCOM&groupId=POPCOM.DWELL&dataId=CENSUS_2006_DWELLINGS&tab=region
- Yoshikawa, K., Bolton, W.R., Romanovsky, V.E., Fukuda, M. and Hinzman, L.D., 2003. Impacts of wildfire on the permafrost in the boreal forests of Interior Alaska. *Journal of Geophysics*, vol. 108, doi:10.1029.2001JD000438.
- Zanasi, L. and Taggart, M., 2006. Building on Strength: An Economic Development Strategy for Ross River. Report prepared for the Ross River Dena Council, Ross River, Yukon, 86 p.

APPENDIX A - APPROACH AND METHODS

SURFICIAL GEOLOGY

Surficial geology is the study of unconsolidated material (i.e., the surficial material that overlies bedrock) on the Earth's surface, including all sediments and soils. These sediments may be deposited through a variety of different processes including glacial (deposited directly out of glacial ice); glaciofluvial (formed by glacial rivers and streams); colluvial (deposited on or at the base of hillslopes by gravity); fluvial (river and stream deposits); lacustrine (lake deposits); and eolian (wind deposits). Additionally, organic deposits can accumulate over bedrock or unconsolidated material, particularly in depressions.

Surficial geology mapping involves a combination of aerial photograph interpretation and field work. The maps provide information on the physical properties and characteristics (e.g., texture or grain size) of the surface sediments, the morphology (shape) of the landforms produced, the genesis or origin of the landforms (the past environment in which the landform was produced), and identifies any geomorphological processes that may have significantly modified those materials (e.g., landslides, gullying, or permafrost). In the process of mapping the surficial geology, the distribution of permafrost is also captured, making these maps an essential part of the hazards assessment process.

Previous mapping of surficial geology within the study area was completed by Jackson (1993a,b) at a scale of 1:100 000. The focus of new 1:25 000-scale mapping conducted for this project was to provide more detailed units and descriptions of the surficial geology in and around the developed parts of the study area. An open file map displaying the results of this new work was released by Yukon Geological Survey in 2014 (Turner) and accompanies this report.

Map units were interpreted in the summer of 2013 using remote predictive mapping following the Yukon Terrain Classification System, a variation of the British Columbia Terrain Classification System (Howes and Kenk, 1997). Remote predictive mapping was completed by viewing 1:40 000-scale digital monochrome aerial photographs from 2003 and 2007 with PurVIEW v2.0 3D stereo viewing software in ArcGIS 10.1.

Surficial geological mapping fieldwork and ground truthing was completed in September 2013. Mapped polygons were field checked at 49 locations by truck, helicopter and foot traverses. Several of these sites corresponded to areas targeted for subsequent permafrost investigation. Field checking of units was completed by documenting road and stream-cut exposures of surficial materials, and by digging soil pits (up to ~1 m depth) in a broad range of materials and landforms. Stratigraphic relationships were also examined at five sites in areas that had not previously been described by Jackson (1993a,b).

Other geotechnical data acquired for this project were also incorporated into the 2014 surficial geological map, including shallow borehole logs and geophysical surveys (Ground Penetrating Radar (GPR) and Electrical Resistivity Tomography (ERT)). Historical borehole, test pit, and water well data were also made available from EBA Engineering Consultants Ltd. (R. Trimble, Tetra Tech EBA, pers. comm., 2010).

PERMAFROST

GROUND-PENETRATING RADAR

Ground-penetrating radar (GPR) is a non-invasive method used to identify subsurface features such as stratigraphic boundaries, permafrost, and other anomalies using electromagnetic fields. For this project, GPR was used to gain a two dimensional image below the ground surface. Two GPR systems were used for field investigations. A TerraSIRch Subsurface Interface Radar (SIR) System 3000® with a shielded 200-MHz antenna (Geophysical Survey Systems, Inc. (GSSI)) was employed for shallow profiles (i.e., maximum penetration depth of 3 m). The collection parameters for the SIR-3000 control unit were set to record at 64 scans per second, with a dielectric constant set at 13, which corresponds to a penetration speed of 0.0914 m/ns to 0.1 m/ns, depending on the surface materials. The GPR antenna was hand-towed along the survey line. For deeper profiles (i.e., maximum penetration depth of 8 m) and for sites located in rough terrain, a Pulse Ekko Pro system with 50 MHz antennas was used. The antennas were moved manually with a separation of 2 m and a step size of 0.5 m. The penetration speed used for this system was between 0.1 and 0.11 m/ns, depending on the surface materials.

Where possible, the GPR transects were situated adjacent to sections of the electrical resistivity tomographic profiles and boreholes, and site conditions were described in detail. This enabled a comparison of the results from the three techniques and to verify the findings.

Post collection data processing was conducted using RADAN™ (Version 7, GSSI) and Ekko_Project 2 software and applied to all of the profiles. Processing of the GPR data included the following: the correction of the initial pulse to time-zero to ensure that the first reflection is from the ground surface and the subsequent reflections are from deeper below the ground surface; correction of the penetration depth with a common midpoint method or with borehole information; topographic correction where required; the application of a FIR boxcar filter to remove background horizontal noise where required; and the use of range gain adjustments to recover lower-amplitude waves from reflections deeper in the ground (Conyers, 2004). Overall, the processing procedures were employed to reduce signal attenuation with depth, as well as improve the continuity of stratigraphic reflections and the signal-to-noise ratio.

ELECTRICAL RESISTIVITY

Electrical Resistivity Tomography (ERT) profiling is a geophysical technique that measures variations in the ability of the ground to conduct electricity along a transect, producing a two-dimensional image of changes in electrical conductance. In permafrost areas, variations in conductance relates mainly to the changes in frozen versus thawed ground, because water and ice serve as good and poor conductors of electricity, respectively.

ERT profiling has been used extensively to investigate mountain permafrost in Europe (e.g., Kneisel et al., 2000, 2008; Hauck et al., 2004; Hilbich et al., 2008, 2009) and is growing in importance in North America as a technique for permafrost investigations in both mountains and lowlands (e.g., Lewkowicz et al., 2011; Miceli, 2012). ERT is regarded as one of the best methods to examine changes in frozen ground conditions over short distances, such as in areas underlain by discontinuous permafrost.

Many ERT profiles show very clear distinctions associated with frozen ground conditions which can be correlated to surface changes in drainage, vegetation cover, or land use (Lewkowicz et al., 2011). However, like all geophysical techniques, confidence in the interpretation increases where complementary information is available; this may include data from borehole logs, observations

of natural exposures, ground temperature measurements, probing of the active layer, or other geophysical techniques such as ground penetrating radar.

There is a major difference in the resistivity of water and ice, but there is not always a sharp line between the phase of water in soil pores (frozen or unfrozen) at temperatures above and below 0°C. Instead, percentages of unfrozen moisture gradually increase in the pores of frozen sediments (especially in fine-grained deposits of silt and clay) as their temperatures approach 0°C. Consequently, the difference in the electrical resistivity of frozen and unfrozen sediments can be gradational rather than sharp (Lewkowicz et al., 2011). In addition, because there can be differences in the porewater salinity and in the conductance of the soil minerals, it is not possible to identify a single universal threshold resistivity value below which soils are definitely unfrozen and above which soils are definitely frozen. However, given the scale of the case study sites examined in this project, a threshold value unique to each case study site was determined based on site characteristics and other ground-truthing approaches (e.g., permafrost drilling).

The ERT profiling included in this report was undertaken in September 2013 and 2014, when the active layer (i.e., depth from ground surface to the top of permafrost) was at its thickest. The equipment used was an ABEM Terrameter LS profiling system with the electrode array (stainless steel pins) inserted into the ground in a Wenner configuration. The electricity entering the ground builds up an image of its resistivity along a profile whose depth depends on the spread of the array of electrodes (25 m for an array 160 m in length, and 8 m for a 40-m array). The penetration depth remains at 25 m, even if surveys longer than 160 m are created using a roll-along technique. Seven ERT profiles were completed.

Each ERT site was described in terms of vegetation and other salient features. UTM co-ordinates (relative to the WGS 84 datum) were taken using a hand-held Garmin Etrex Vista GPS. Relative variations in elevation along the individual profiles were measured in the field using an abney level and are expected to have accuracies of ± 1 m.

Resistivity profiles were topographically corrected using the abney level surveys. The actual elevations shown on the surveys are approximate. Measured resistivity data were processed with RES2DINV software (Loke and Barker, 1996) using a robust inversion that can respond to the rapid transitions and high contrasts in resistivity (Loke et al., 2003) that occur between frozen and unfrozen ground. A reversed colour scheme was used to portray the profiles so that blue represents high resistivities (generally indicative of frozen soils) and red represents low resistivities (ice-poor or unfrozen soils). All the resistivity profiles use the same scale to allow for inter-site comparison.

There is no single model that fits the observed resistivities. Instead the modelled results converge by iteration with the measured values. The choice of when to stop iteration in the RES2DINV software is made by the operator. Too few iterations leads to large Root Mean Square (RMS) errors (i.e., the model does not fit the measurements). Too many iterations can result in model 'over-fit' in which the broad patterns are lost. Analyses for this study were stopped after the 4th iteration as RMS errors were all very low (less than 5%) by that point. The profiles are presented with a linear depth scale and no vertical exaggeration. ERT profiles were interpreted in conjunction with the results of frost probing along the profiles, field descriptions of vegetation cover at the site, GPR surveys, borehole and laboratory analyses undertaken by the research team, and surficial mapping.

DRILLING AND SAMPLE COLLECTION

The drill program was carried out in September 2013 and August 2014. The objective was to core and collect permafrost samples from predetermined study sites. These sites were selected in advance through a desktop interpretation based on available maps, aerial photographs, satellite

images and consultation with community members. The drilling and coring operations required the use of four different drills to account for changes in subsurface conditions: two core-drills (a modified GÖLZ™ portable core-drill system and a modified Winkie core-drill system), one auger drill, and one hand auger.

The GÖLZ™ portable core-drill system (Figure A1) is a light, hand-held, core-drill system with a high-rotation speed (600 rpm) that can be controlled by two people, and is therefore used with minimal impact on the environment. Stainless steel rods measuring 1 m in length and 4.5 cm in diameter, and a core barrel 40 cm long and 10 cm in diameter were used, making it possible to drill up to 5 m into unconsolidated, fine to medium-grained sediments (i.e., sand to clay). A core catcher was used to extract the frozen core out of the borehole, which allows for continuous undisturbed permafrost sampling.



Figure A1. Photograph of the GÖLZ™ portable Earth-drill system used for permafrost coring.



Figure A2. Photograph of the Winkie drill, used for permafrost coring.

The Winkie drill is a gas-powered, core-drill with a two-speed transmission made for bedrock drilling; this drill has been modified for permafrost drilling in unconsolidated material using a gearbox that lowers the speed to approximately 1200 rpm. Although it is not as mobile as the GÖLZ™ portable core-drill system, it is one of the lightest shift drills on the market (see Figure A2, above) and has the potential to go down to 30 m in ice-rich, fine-grained sediment. The Winkie core-drill was used with aluminum rods (0.9 and 1.5 m long; Figure A3) and core barrels 10.8 cm in diameter.

The auger drill is equipped with a Honda GVX160 (144 rpm) motor and flight auger extensions with diameters of 5-46 cm (Figure A4). This drill is destructive and is used to pass through unfrozen sediments of the active layer allowing for bulk 'grab' samples. This type of auger is also useful in retrieving deposits of gravel containing clasts that are cobble to boulder sized at the bottom of a borehole.



Figure A3. Photograph of aluminum rods used for the Winkie drill for permafrost coring.



Figure A4. Photograph of the Honda drill, used for permafrost coring.

The hand auger is used to sample the thawed active layer; it has a 10.2 cm-diameter sampling core barrel, and three 1 m-long extension rods (Figure A5). It is ideal for sampling near-surface, fine-grained, unfrozen sediments (e.g., clay, silt, sand and fine gravel containing pebbles with a maximum diameter of 25 mm).



Figure A5. Photograph of the hand auger, used for permafrost coring.

Using a combination of these drills, boreholes were drilled along ERT and GPR profiles in representative areas (e.g., forested areas, open fields) or in an area belonging to a particular surficial geology unit. For each borehole, the same sampling and drilling procedures were followed. The site was first described (e.g., hydrology, vegetation type and density, and topography), photos were taken, and locations were recorded using a handheld GPS. The boreholes were initiated using a hand auger if the ground was soft or an auger drill if the ground was gravelly or compacted. As soon as the permafrost table was reached, the GÖLZ™ portable core-drill system was used. For specific locations where maximum depth was desired, the Winkie core-drill was used.

A sample of every unfrozen layer was collected from each borehole. Each sample was photographed and described in situ (e.g., soil type, soil moisture, presence or absence of organic matter, any particularities). The sample was identified with the borehole name and depth and put in doubled hermetic Ziploc bags for laboratory analyses. Frozen samples were also collected and described on site (Figure A6). Each core was cleaned to remove the drilling mud and photographed.



Figure A6. Photograph of the setup used for in-field core descriptions.

GEOTECHNICAL ANALYSIS OF PERMAFROST

Laboratory analyses were carried out to measure geotechnical properties of active layer and permafrost samples, and additional tests were conducted to evaluate the mechanical behavior of the permafrost upon thawing. Both sediment grain size and ice characteristics were evaluated. To evaluate sediment characteristics, a grain-size analysis was performed on every sample. Additionally, plasticity index, remolded bulk density, porosity, specific gravity and thaw settlement potential were calculated for representative samples. To evaluate ice characteristics in permafrost samples, the cryostructure, volumetric ice content, gravimetric ice content and settlement potential were quantified. These methods are described below.

GRAIN-SIZE ANALYSIS

Sieve and hydrometer analysis of grain size were performed following a specifically modified American Standard and Testing Method protocol (ASTM D422-63, 2000). The sieves typically used were 4, 2, 1, 0.5, 0.25, 0.125 and 0.063 mm. A hydrometer test was performed on samples with enough fine-grained material, or on specific samples. A 40-g subsample was passed through 0.25 mm openings, and after sedimentation started, readings were taken after 0.25, 0.50, 0.75, 1, 1.5, 2, 5, 15, 30, 60, 120, 180, 300 and 1440 minutes. A total of 17 analyses were completed.

SPECIFIC GRAVITY

Specific gravity (the ratio of a solid's grain density to the density of water) was systematically measured for every sample collected, and followed the American Standard and Testing Method (ASTM D854-10, 2000). The results were used to compute the porosity of the sediment for 3 deposit types (see below).

CRYOSTRUCTURE

Cryostructure (i.e., the geometry of ice in permafrost) depends on water availability, as well as the sediment's ice-segregation potential and the time of freezing, resulting in the development of ice structures in the soil matrix. Information such as soil genesis, climate conditions at the time of freezing, permafrost development history, and ground vulnerability when permafrost degrades can be interpreted from cryostructure, cryofacies analysis, and general cryostratigraphy.

Because field descriptions are based only on a visual interpretation of the core, the samples were re-examined in the laboratory using a standard terminology that would provide a more detailed description (Stephani et al., 2010; Murton and French, 1994). Frozen core samples were warmed to near 0°C and any refrozen mud was scrapped off prior to the description.

CONSOLIDATION TESTING

Compaction and consolidation testing were carried out at Laval University. They were measured by thawing a soil sample and measuring the associated total settlement. A load was applied vertically (i.e., stress) on a confined and drained sample to simulate the influence of an embankment or a building weight on consolidation. The total settlement was the sum of two distinct processes: 1) the compaction associated with the water phase change, resulting in a significant decrease in volume, especially when excess ice is present; and 2) the consolidation of the sediment under the applied stress following the expulsion of water out of the pore structure and the rearrangement of soil particles. In general, compaction is more prevalent for samples with excess ice (e.g., segregated ice lenses), whereas consolidation is common in samples with interstitial ice (e.g., unsaturated to saturated soils).

During testing, an initial vertical stress of 25 kPa (corresponding to the approximate weight of a thawed active layer) was applied to frozen samples. Using two thermal baths to control the upper and lower temperatures, the permafrost samples were thawed from above by applying heat with a temperature of 2°C ± 1°C. Ultimately, the temperature of both thermal baths was increased to ensure complete thawing of the sample. After complete thawing, when there was no more vertical deformation, the stress was increased to 150 kPa for a minimum period of 24 hours in order to simulate the weight of an embankment or a medium-sized building. By proceeding in near oedometric conditions, it was possible to estimate the index of final voids (e_f) when thawing and consolidation of the grains were completed (at a given applied force). By also determining the index of initial voids in the frozen state (e_f ; calculated using the frozen density and water content), it was possible to obtain a total settlement value under different forces for the same sample.

To assess the total settlement (s), the sum of the thaw settlement (s_t) and the subsequent consolidation of the soil (s_c) were calculated by using:

$$S = S_t + S_c \quad [1]$$

When the thickness of the original frozen soil layer (H_f) is subject to effective stress (σ'), the components of the total settlement are expressed using:

$$s_t = A_0 H_f \quad [2]$$

$$s_c = m_v \sigma' H_f \quad [3]$$

The thawing compaction parameter (A_0) is expressed as a percentage and represents the relationship between void ratio in frozen (e_f) and thawed (e_t) states which is summarized by using:

$$A_0 = \frac{e_f - e_t}{1 + e_f} \quad [4]$$

The volume change coefficient (m_v) is defined as a volume changing unit added by an effective stress unit. When the effective stress increases from σ' to σ'_0 and the void ratio decreases from e_t to e , this coefficient is expressed using:

$$m_v = \frac{1}{1 + e_t} \cdot \left(\frac{e_t - e}{\sigma' - \sigma'_0} \right) \quad [5]$$

In order to determine the total settlement following the thawing of permafrost under loads imposed by buildings or transportation infrastructure, A_0 and m_v values must be determined from consolidation tests on representative soil samples. Once these values are determined, the total compaction of partially or completely thawed frozen soil layers is determined by using:

$$s = \sum_{i=1}^n A_{0,i} H_i + \sum_{i=1}^n m_{v,i} H_i \sigma'_i \quad [6]$$

BULK DENSITY

Bulk density and voids in aggregate (ρ_b ; the ratio of a dried soil's mass, including its porosity, to its volume (g/cm^3)) were calculated following American Standard and Testing Method protocol (ASTM C29 – 09, 2000). Values were generated by weighing a 45- cm^3 beaker filled with compacted sediment and subtracting the empty beaker weight. The sediment weight was then divided by the beaker's volume using:

$$\rho_s = \frac{(M_{S+B} - M_B)}{V_B} \quad [7]$$

where M_{S+B} is the weight of the beaker full of compacted sediment, M_B is the weight of the empty beaker, and V_B is the beaker's internal volume.

GRAVIMETRIC ICE CONTENT

Ice content was calculated using:

$$u_I = \frac{(M_I)}{(M_S)} \quad [8]$$

where M_I is the ice weight (measured as weight loss after drying (g)) and M_S is dry soil weight (g). Results are expressed as percentages (dimensionless).

VOLUMETRIC ICE CONTENT

An ice volume measurement was taken using a water displacement method. The frozen sample was weighed and lowered into a four-inch diameter PVC tube pre-filled with 1.5 L of water. Water was then extracted from the tube until the initial water level (1.5 L) was achieved. The amount of water displaced was measured using a 250 mL graduated cylinder with a precision of ± 2 ml. The sample was then removed from the tube, placed in a clean tin tray, and dried completely in a

drying oven at 60°C. The dry sample was then weighed, crushed using a mortar and pestle, vacuum sealed in a clear plastic bag, and labelled according to the borehole and sample increment. The volumes of the vacuum-sealed dry samples were measured using the same methods as the frozen cores, and the volume of the vacuum bags volume was subtracted from the measurement to obtain a dry sample volume. Assuming the density of ice to be 1.09 cm³/g, volumetric ice content was calculated using:

$$IVC_{(\%)} = \left(\frac{W_c \times 1.09}{V_{tot}} \right) \times 100 \quad [9]$$

where W_c is the water mass content and V_{tot} is the total (frozen) core volume. Results are expressed as percentages.

VOLUMETRIC EXCESS ICE CONTENT

The volume of excess ice content was calculated using:

$$V_{tot} - V_{sed} = V_{ice} \quad [10]$$

where V_{tot} is the total frozen core volume and V_{sed} is the dry soil volume. The volumetric excess ice content (V_{ice}) is then divided by the total frozen core volume (V_{tot}) and expressed as a percentage (fundamentally meaning cm³/cm³). This method is valid for mineral soils only.

PLASTICITY INDEX

The plasticity index (PI ; the range of water content where the soil has a plastic behaviour) was measured according to the American Standard and Testing method (ASTM D4318-00, 2000) using: where LL is the liquid limit and PL is the plastic limit.

$$PI = LL - PL \quad [11]$$

The LL was calculated using the multipoint liquid limit method (ASTM D4318-00, 2000) which requires one of the trials to be between 25 to 35 blows, one closure between 20 and 30 blows, and one trial with a closure requiring 15 to 25 blows. The PL was calculated using the *Hand Method* which consists of rolling the mass between the palm or fingers and the ground-glass plate with sufficient pressure to roll the mass into a thread of uniform diameter throughout its length. The thread is further deformed on each stroke so that its diameter reaches 3.2 mm (1/8 in).

BOREHOLE LOGS

A log for each permafrost borehole was created using the Rockware Log Plot software. Borehole logs include GPS coordinates; a description of the surrounding environment; the stratigraphy of the sediment; the depth to: the water table, to the frozen table in the active layer, and to the permafrost table; the ice structure (cryostructure); the grain size ratio; the specific gravity; the bulk density; the porosity; the volumetric ice content; and the thaw-settlement potential (see Appendix B for all borehole log descriptions and data).

REFERENCES

- ASTM Standard C29 – 09, 2000. Standard Test Method Bulk Density (“Unit Weight”) and Voids in Aggregate. West Conshohocken, PA, ASTM International.
- ASTM Standard D422 – 63, 2000. Standard Test Method for Particle-Size Analysis of Soils. West Conshohocken, PA, ASTM International.
- ASTM Standard D854 – 10, 2000. Standard Test Methods for Specific Gravity of Soil Solids by Water Pycnometer. West Conshohocken, PA, ASTM International.
- ASTM Standard D4318 – 00, 2000. Standard Test Methods for Liquid Limit, Plastic Limit, and Plasticity Index of Soils. West Conshohocken, PA, ASTM International.
- Hauck, C., Isaksen, K., Vonder Mühll, D. and Sollid, J.L., 2004. Geophysical surveys designed to delineate the altitudinal limit of mountain permafrost: An example from Jotunheimen, Norway. *Permafrost and Periglacial Processes*, vol. 15, p. 191-205, doi:10.1002/ppp.493.
- Hilbich, C., Hauck, C., Hoelzle, M., Scherler, M., Schudel, L., Voelksch, I., Vonder Muehll, D. and Mausbacher, R., 2008. Monitoring mountain permafrost evolution using electrical resistivity tomography: A 7-year study of seasonal, annual, and long-term variations at Schilthorn, Swiss Alps. *Journal of Geophysical Research-Earth Surface*, vol. 113, doi:10.1029/2007JF000799.
- Hilbich, C., Marescot, L., Hauck, C., Loke, M.H. and Mausbacher, R., 2009. Applicability of electrical resistivity tomography monitoring to coarse blocky and ice-rich permafrost landforms. *Permafrost and Periglacial Processes*, vol. 20, p. 269-284, doi:10.1002/ppp.652.
- Howes, D.E. and Kenk, E., 1997. *Terrain Classification System for British Columbia (Version 2)*. Province of British Columbia, Resource Inventory Branch, Ministry of Environment, Lands and Parks; Recreational Fisheries Branch, Ministry of Environment; and Surveys and Resources Mapping Branch, Ministry of Crown Lands, 102 p.
- Jackson, L.E., Jr., 1993a. Surficial geology, Bruce Lake, Yukon Territory. Geological Survey of Canada, Map 1791A, scale 1:100 000.
- Jackson, L.E., Jr., 1993b. Surficial geology, Olgie Lake, Yukon Territory. Geological Survey of Canada, Map 1822A, scale 1:100 000.
- Kneisel, C., Hauck, C. and Vonder Mühll, D., 2000. Permafrost below the timberline confirmed and characterized by geoelectrical resistivity measurements, Bever Valley, eastern Swiss Alps. *Permafrost and Periglacial Processes*, vol. 11, p. 295-304, doi:10.1002/1099-1530(200012)11:4<295::AID-PPP353>3.0.CO;2-L.
- Kneisel, C., Hauck, C., Fortier, R. and Moorman, B., 2008. Advances in geophysical methods for permafrost investigations. *Permafrost and Periglacial Processes*, vol. 19, p. 157-178.
- Lewkowicz, A.G., Etzelmüller, B.E. and Smith, S.L., 2011. Characteristics of discontinuous permafrost from ground temperature measurements and electrical resistivity tomography, southern Yukon, Canada. *Permafrost and Periglacial Processes*, vol. 22, p. 320-342.
- Loke, M.H. and Barker, R.D., 1996. Rapid leastsquares inversion of apparent resistivity pseudosections using a quasi-Newton method. *Geophysical Prospecting*, vol. 44, p. 131-152, doi:10.1111/j.1365-2478.1996.tb00142.x
- Loke, M.H., Acworth, I. and Dahlin, T., 2003. A comparison of smooth and blocky inversion methods in 2D electrical imaging surveys. *Exploration Geophysics*, vol. 34, p. 182-187.

- Miceli, C., 2012. Seasonal cycling in electrical resistivities at ten thin permafrost sites, southern Yukon and northern British Columbia. Unpublished M.Sc. thesis, Department of Geography, University of Ottawa, ON, 201 p.
- Murton, J.B. and French, H.M., 1994. Cryostructures in permafrost, Tuktoyaktuk coastlands, western arctic Canada. *Canadian Journal of Earth Sciences*, vol. 31, no. 4, p. 737-747.
- Stephani, E., Fortier, D. and Shur, Y., 2010. Applications of cryofacies approach to frozen ground engineering – Case study of a road test site along the Alaska Highway (Beaver Creek, Yukon, Canada). GEO2010: 63rd Canadian Geotechnical Conference and 6th Canadian Permafrost Conference, Calgary, Canada.
- Turner, D.G., 2014. Surficial geology, Ross River region, Yukon, parts of N TS 105K /1 & 2 and 105F /15 & 16 (1:25 000 scale). Yukon Geological Survey, Energy, Mines and Resources, Government of Yukon, Open File 2014-13.

APPENDIX B - BOREHOLE LOGS

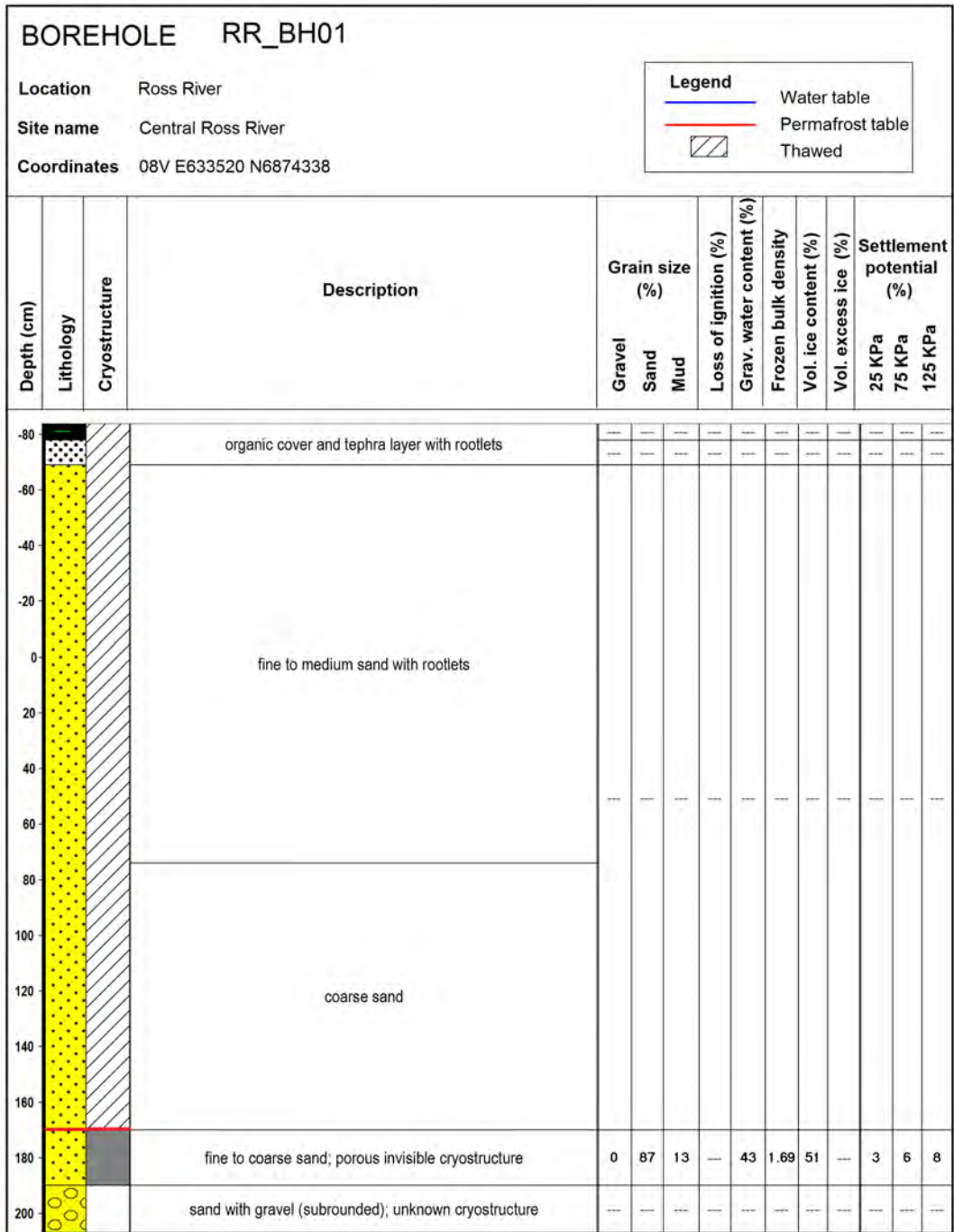


Figure B1. Borehole log for RR_BH01, at the Central Ross River case study site. For location, see Figures 26 and 29 in the main body of this report.

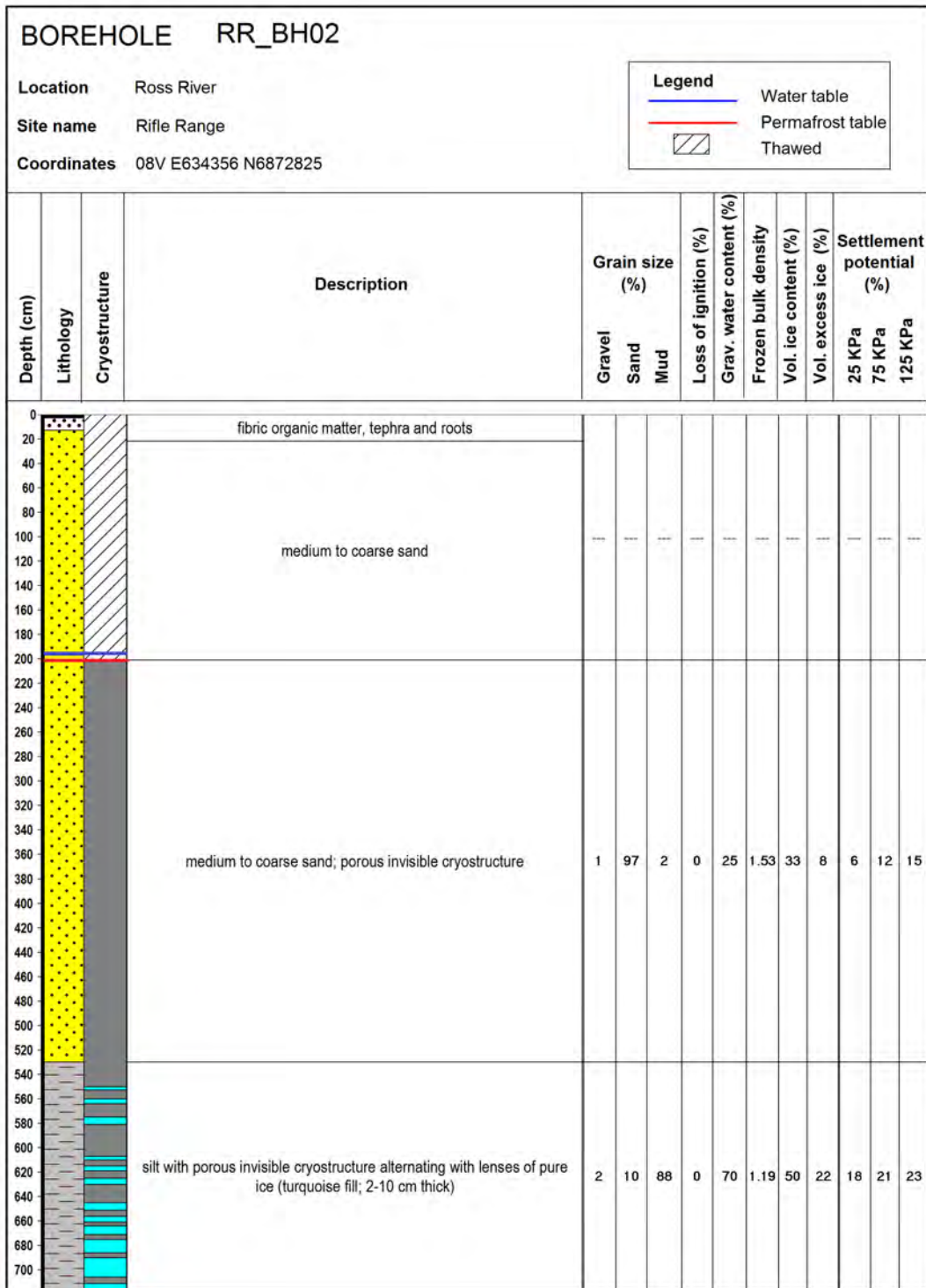


Figure B2. Borehole log for RR_BH02, at the Rifle Range case study site. For location, see Figures 26 and 35 in the main body of this report.

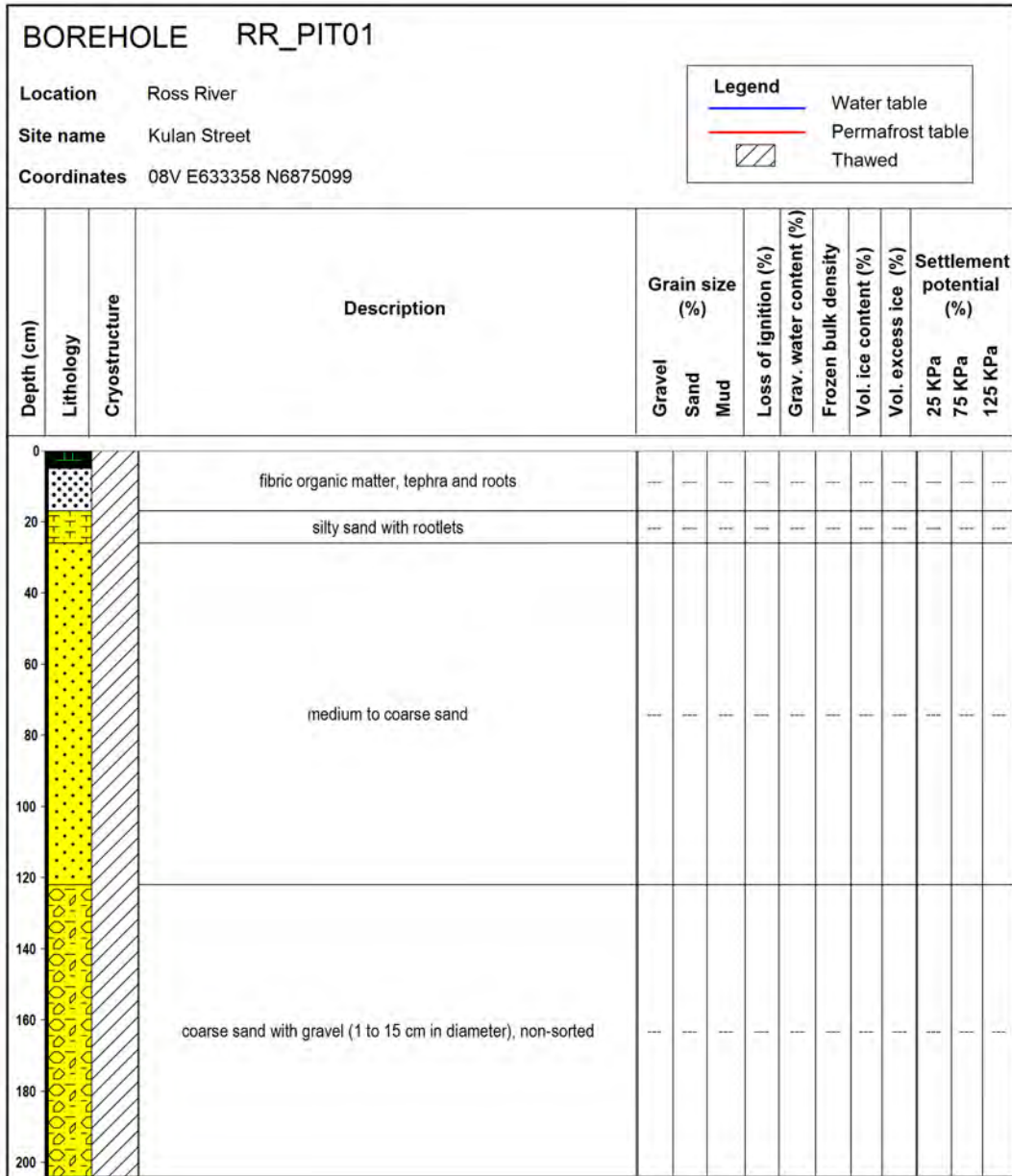


Figure B3. Log for RR_PIT01, at the Kulan Street case study site. For location, see Figures 26 and 40 in the main body of this report.

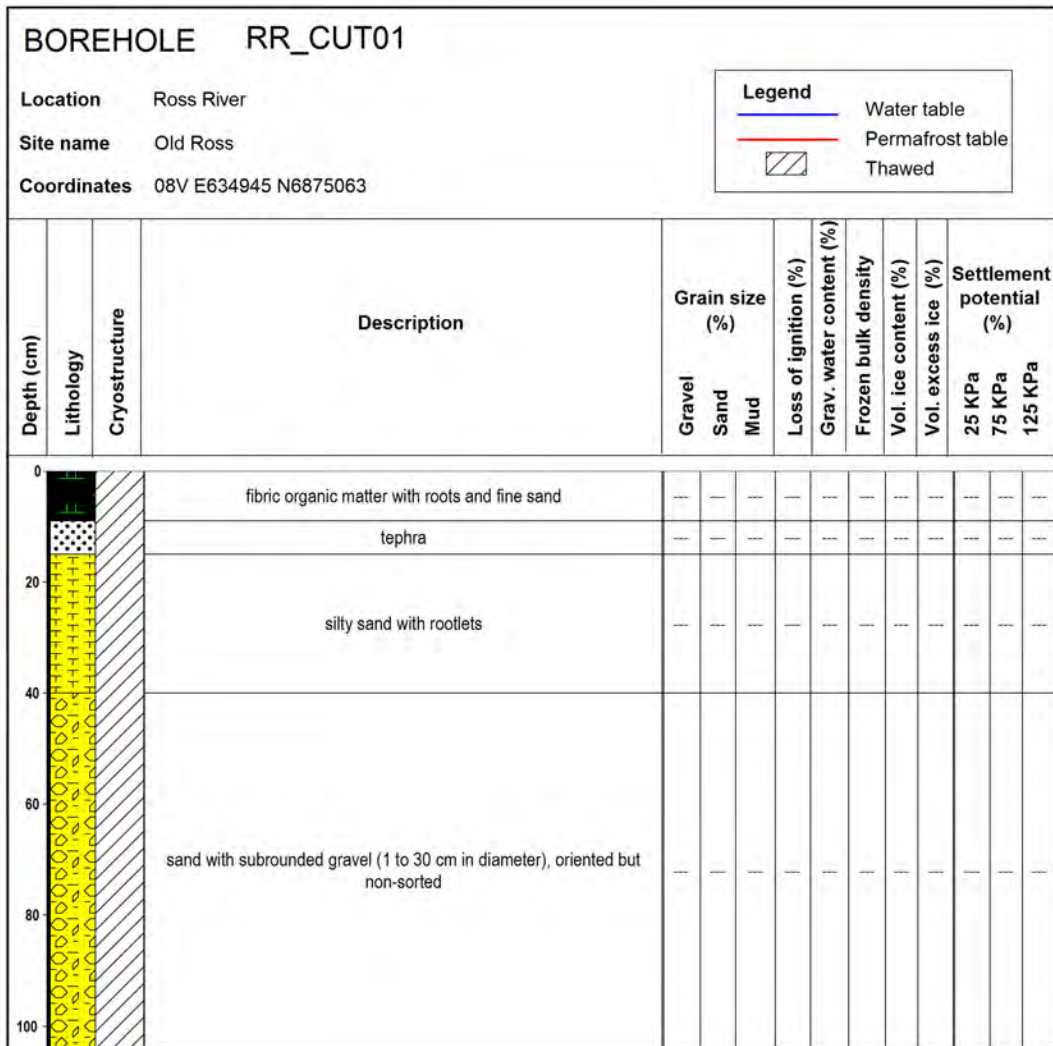


Figure B4. Log for RR_CUT01, at the Old Ross case study site. For location, see Figures 26 and 43 in the main body of this report.

APPENDIX C - GRAIN SIZE ANALYSIS

Table C1. Grain size analysis results for samples collected from boreholes drilled at case study sites in the Ross River area. See Figures 26, 29, 35, 40 and 43 in the main body of this report for location of case study sites and boreholes, and Appendix A for methodology.

Sample Name	RR_BH02_216	RR_BH02_274	RR_BH02_305
Analyst and Date	LPR, 1/13/2015	LPR, 1/14/2015	LPR, 1/15/2015
Sieving Error	0.0%	0.0%	0.0%
Sample Type	unimodal, moderately well sorted	unimodal, moderately sorted	unimodal, moderately sorted
Textural Group	slightly gravelly sand	slightly gravelly sand	slightly gravelly sand
Sediment Name	slightly very fine gravelly medium sand	slightly fine gravelly medium sand	slightly very fine gravelly medium sand
% Gravel	0.1%	1.3%	0.6%
% Sand	99.2%	97.1%	97.9%
% Silt & Clay	0.7%	1.6%	1.4%
% Very Coarse Gravel	0.0%	0.0%	0.0%
% Coarse Gravel	0.0%	0.0%	0.0%
% Medium Gravel	0.0%	0.0%	0.0%
% Fine Gravel	0.0%	0.9%	0.1%
% Very Fine Gravel	0.1%	0.4%	0.6%
% Very Coarse Sand	0.0%	0.0%	0.0%
% Coarse Sand	16.1%	17.0%	27.1%
% Medium Sand	69.8%	54.4%	51.8%
% Fine Sand	12.4%	24.0%	17.7%
% Very Fine Sand	0.8%	1.6%	1.4%
% Very Coarse Silt	0.7%	1.6%	1.4%
% Coarse Silt	0.0%	0.0%	0.0%
% Medium Silt	0.0%	0.0%	0.0%
% Fine Silt	0.0%	0.0%	0.0%
% Very Fine Silt	0.0%	0.0%	0.0%
% Clay	0.0%	0.0%	0.0%

Table C2. Grain size analysis results for samples collected from boreholes drilled at case study sites in the Ross River area. See Figures 26, 29, 35, 40 and 43 in the main body of this report for location of case study sites and boreholes, and Appendix A for methodology.

Sample Name	RR_BH02_343	RR_BH02_392	RR_BH02_434
Analyst and Date	LPR, 1/16/2015	LPR, 1/17/2015	LPR, 1/18/2015
Sieving Error	0.0%	0.0%	0.0%
Sample Type	unimodal, moderately sorted	unimodal, moderately sorted	unimodal, moderately sorted
Textural Group	slightly gravelly sand	slightly gravelly sand	slightly gravelly sand
Sediment Name	slightly very fine gravelly medium sand	slightly very fine gravelly fine sand	slightly fine gravelly medium sand
% Gravel	3.0%	0.0%	0.7%
% Sand	96.1%	95.0%	97.3%
% Silt & Clay	0.9%	5.0%	2.0%
% Very Coarse Gravel	0.0%	0.0%	0.0%
% Coarse Gravel	0.0%	0.0%	0.0%
% Medium Gravel	0.0%	0.0%	0.0%
% Fine Gravel	0.8%	0.0%	0.5%
% Very Fine Gravel	2.1%	0.0%	0.2%
% Very Coarse Sand	0.0%	0.0%	0.0%
% Coarse Sand	42.4%	0.5%	15.1%
% Medium Sand	42.9%	25.0%	49.9%
% Fine Sand	10.5%	67.3%	31.0%
% Very Fine Sand	0.4%	2.2%	1.3%
% Very Coarse Silt	0.1%	0.2%	0.5%
% Coarse Silt	0.2%	0.0%	0.3%
% Medium Silt	0.1%	0.0%	0.1%
% Fine Silt	0.1%	0.2%	0.1%
% Very Fine Silt	0.1%	0.3%	0.1%
% Clay	0.5%	4.3%	1.0%

Table C3. Grain size analysis results for samples collected from boreholes drilled at case study sites in the Ross River area. See Figures 26, 29, 35, 40 and 43 in the main body of this report for location of case study sites and boreholes, and Appendix A for methodology.

Sample Name	RR_BH02_464	RR_BH02_515	RR_BH02_543
Analyst and Date	LPR, 1/19/2015	LPR, 1/20/2015	LPR, 1/21/2015
Sieving Error	0.0%	0.0%	0.0%
Sample Type	bimodal, moderately sorted	bimodal, moderately well sorted	polymodal, very poorly sorted
Textural Group	slightly gravelly sand	slightly gravelly sand	slightly gravelly sandy mud
Sediment Name	slightly fine gravelly medium sand	slightly fine gravelly medium sand	slightly very fine gravelly fine sandy medium silt
% Gravel	1.5%	0.3%	4.3%
% Sand	97.4%	99.1%	35.4%
% Silt & Clay	1.1%	0.7%	60.3%
% Very Coarse Gravel	0.0%	0.0%	0.0%
% Coarse Gravel	0.0%	0.0%	0.0%
% Medium Gravel	0.0%	0.0%	0.0%
% Fine Gravel	1.4%	0.2%	0.4%
% Very Fine Gravel	0.1%	0.1%	3.9%
% Very Coarse Sand	0.0%	0.0%	0.0%
% Coarse Sand	22.6%	2.4%	0.3%
% Medium Sand	51.5%	70.1%	3.8%
% Fine Sand	19.9%	23.2%	26.9%
% Very Fine Sand	3.4%	3.4%	4.4%
% Very Coarse Silt	1.1%	0.7%	4.1%
% Coarse Silt	0.0%	0.0%	10.6%
% Medium Silt	0.0%	0.0%	15.1%
% Fine Silt	0.0%	0.0%	9.6%
% Very Fine Silt	0.0%	0.0%	9.3%
% Clay	0.0%	0.0%	11.7%

Table C4. Grain size analysis results for samples collected from boreholes drilled at case study sites in the Ross River area. See Figures 26, 29, 35, 40 and 43 in the main body of this report for location of case study sites and boreholes, and Appendix A for methodology.

Sample Name	RR_BH02_564	RR_BH02_595	RR_BH02_619
Analyst and Date	LPR, 1/22/2015	LPR, 1/23/2015	LPR, 1/24/2015
Sieving Error	0.0%	0.0%	0.0%
Sample Type	unimodal, very well sorted	bimodal, moderately sorted	unimodal, very well sorted
Textural Group	slightly gravelly mud	gravelly mud	slightly gravelly mud
Sediment Name	slightly very fine gravelly very coarse silt	very fine gravelly very coarse silt	slightly very fine gravelly very coarse silt
% Gravel	0.1%	5.0%	0.1%
% Sand	7.1%	9.0%	7.1%
% Silt & Clay	92.8%	86.0%	92.9%
% Very Coarse Gravel	0.0%	0.0%	0.0%
% Coarse Gravel	0.0%	0.0%	0.0%
% Medium Gravel	0.0%	0.0%	0.0%
% Fine Gravel	0.0%	0.4%	0.0%
% Very Fine Gravel	0.0%	4.6%	0.1%
% Very Coarse Sand	0.0%	0.0%	0.0%
% Coarse Sand	0.0%	0.0%	0.0%
% Medium Sand	1.2%	0.0%	0.0%
% Fine Sand	2.0%	0.0%	0.0%
% Very Fine Sand	3.9%	9.0%	7.1%
% Very Coarse Silt	92.8%	86.0%	92.9%
% Coarse Silt	0.0%	0.0%	0.0%
% Medium Silt	0.0%	0.0%	0.0%
% Fine Silt	0.0%	0.0%	0.0%
% Very Fine Silt	0.0%	0.0%	0.0%
% Clay	0.0%	0.0%	0.0%

Table C5. Grain size analysis results for samples collected from boreholes drilled at case study sites in the Ross River area. See Figures 26, 29, 35, 40 and 43 in the main body of this report for location of case study sites and boreholes, and Appendix A for methodology.

Sample Name	RR_BH02_651	RR_BH02_678	RR_BH02_701
Analyst and Date	LPR, 1/25/2015	LPR, 1/26/2015	LPR, 1/27/2015
Sieving Error	0.0%	0.0%	0.0%
Sample Type	bimodal, very well sorted	bimodal, very well sorted	bimodal, very well sorted
Textural Group	slightly gravelly sandy mud	slightly gravelly sandy mud	slightly gravelly sandy mud
Sediment Name	slightly very fine gravelly very fine sandy very coarse silt	slightly very fine gravelly very fine sandy very coarse silt	slightly very fine gravelly very fine sandy very coarse silt
% Gravel	3.0%	1.0%	0.9%
% Sand	14.8%	10.9%	17.7%
% Silt & Clay	82.2%	88.2%	81.5%
% Very Coarse Gravel	0.0%	0.0%	0.0%
% Coarse Gravel	0.0%	0.0%	0.0%
% Medium Gravel	0.0%	0.0%	0.0%
% Fine Gravel	0.1%	0.1%	0.0%
% Very Fine Gravel	2.8%	0.8%	0.9%
% Very Coarse Sand	0.0%	0.0%	0.0%
% Coarse Sand	0.0%	0.0%	0.0%
% Medium Sand	0.0%	0.0%	0.0%
% Fine Sand	0.0%	2.3%	0.0%
% Very Fine Sand	14.8%	8.6%	17.7%
% Very Coarse Silt	82.2%	88.2%	81.5%
% Coarse Silt	0.0%	0.0%	0.0%
% Medium Silt	0.0%	0.0%	0.0%
% Fine Silt	0.0%	0.0%	0.0%
% Very Fine Silt	0.0%	0.0%	0.0%
% Clay	0.0%	0.0%	0.0%

Table C6. Grain size analysis results for samples collected from boreholes drilled at case study sites in the Ross River area. See Figures 26, 29, 35, 40 and 43 in the main body of this report for location of case study sites and boreholes, and Appendix A for methodology.

Sample Name	RR_BH02_717	RR_BH01_191
Analyst and Date	LPR, 1/28/2015	BL, 1/13/2015
Sieving Error	0.0%	0.0%
Sample Type	Unimodal, Very Well Sorted	Bimodal, Moderately Sorted
Textural Group	Slightly Gravelly Mud	Slightly Gravelly Muddy Sand
Sediment Name	Slightly Very Fine Gravelly Very Coarse Silt	Slightly Very Fine Gravelly Very Coarse Silty Fine Sand
% Gravel	0.1%	0.0%
% Sand	8.6%	87.2%
% Silt & Clay	91.3%	12.8%
% Very Coarse Gravel	0.0%	0.0%
% Coarse Gravel	0.0%	0.0%
% Medium Gravel	0.0%	0.0%
% Fine Gravel	0.0%	0.0%
% Very Fine Gravel	0.1%	0.0%
% Very Coarse Sand	0.0%	0.0%
% Coarse Sand	0.0%	3.7%
% Medium Sand	0.0%	35.2%
% Fine Sand	1.2%	48.3%
% Very Fine Sand	7.4%	0.0%
% Very Coarse Silt	91.3%	12.8%
% Coarse Silt	0.0%	0.0%
% Medium Silt	0.0%	0.0%
% Fine Silt	0.0%	0.0%
% Very Fine Silt	0.0%	0.0%
% Clay	0.0%	0.0%

APPENDIX D - CLIMATE PROJECTIONS

Projections of changes in mean annual air temperature (MAAT) were prepared for this report based on annual air temperature modelling, and were enhanced to reflect heterogeneity in the local landscape (specifically, mountainous terrain). This represents a significant increase in the understanding of MAAT. This approach incorporated specific topographical features in the study region (e.g., mountains) and knowledge about related area-specific surface lapse rates (SLRs) at fine resolution (30 x 30 m). To develop these enhanced air temperature models and predictions, current MAAT modeling was conducted. Work drew on data from clusters of previously established air temperature monitoring stations in Yukon. Each monitoring station consisted of a radiation shield mounted at 1.5-1.6 m on a metal pole. An Onset Hobo Pro data-logger (accuracy $\pm 0.2^{\circ}\text{C}$), equipped with an external thermistor, was used to monitor air temperature inside the screen. In order to predict MAAT across the region, a 3rd order polynomial trend surface of annual SLR values below treeline was generated (Lewkowicz and Bonnaventure, 2011). This surface was then combined with a 4th order polynomial trend surface of treeline elevations, which was separately developed from sampling topographic maps and Google Earth images to limit the application of the SLR values to terrain below treeline. Above this level, it was assumed that standard environmental lapse rates of $-6.5^{\circ}\text{C}/\text{km}$ prevail. In addition, a 3rd order polynomial trend surface of projected sea level temperature was generated from the long-term records of 18 climate stations in the region (Environment Canada, 2013), which had been reduced to sea level (e.g., Etzelmuller et al., 2007) by applying the projected SLR value for each station based on its continentality (Lewkowicz and Bonnaventure, 2011). The projected sea level temperature surface was then readjusted using a digital elevation model at 30 x 30 m resolution, the SLR grid for elevations up to treeline, and the standard environmental lapse rate from treeline upwards. The result was a gridded model of MAAT for the region based on elevation with the measured variability in SLR taken into account but not including aspect or localized topographic effects on cold-air pooling.

The basis for developing projections of MAAT incorporating the SLRs (also called perturbed MAAT models) involved using statistically downscaled GCM data obtained from the Scenarios Network for Arctic and Alaska Planning at the University of Alaska Fairbanks (SNAP, 2012; www.snap.uaf.edu). The SNAP dataset contains multiple GCM scenarios for mean annual air temperatures, as well as modelled average temperature surfaces for past climate normals (e.g., 1980-2009). The data used to obtain the perturbed MAAT models included the 2 km-resolution projection surfaces provided by SNAP for the IPCC scenarios of A1B, A2 and B1 (IPCC, 2015). These particular scenarios were chosen for this application because they represent the most commonly used scenarios in GCM modelling and represent a broad range of potential climate conditions. To develop each scenario, SNAP drew on data from five separate models, thereby ensuring the greatest range of predictions within each scenario. Perturbed MAAT models were developed by examining the difference (and thus change) between what the SNAP model predicted for the current climate (i.e., the 1980-2009 climate normal) and each of the three scenarios for the years 2020, 2050 and 2080. In addition, a backcasted model was also produced which examined the difference between current climate (1980-2009) and the climate normal from 1950-1979. Hence, modelling efforts examined the predicted difference between each time slice for each scenario and adjusted the previously created MAAT model accordingly. In order to incorporate the data from the 2 x 2 km grid cells for each SNAP model, the cell size was resampled to 30 x 30 m. This effectively provided a broad geographic basis for sample change at a territorial scale (macroclimate), which could then be topographically corrected to site specific SLRs in the Ross River study area. The differences between the predicted SNAP models were then added (forecasting) or subtracted (backcasting) to the current MAAT model using raster calculator in ArcGIS© 10.1 (ESRI, USA). The results of

these models provide significantly more information about the variable nature of spatial climate in geographically mountainous areas than the raw GCM data itself, which typically displays high levels of inaccuracies in the mountainous regions of Yukon.

Results are presented in Figures D1-D10, below. Current (i.e., 1980-2009) MAAT results in the area of Ross River fall within the range of -2.6 to -3.1°C, and temperatures were found to be colder in the backcasted (1950-1979) model for the area by about 1°C. A summary of temperature results for each model for the study region are presented Table D1.

Note that additional climate projections, based on data provided by SNAP (2012), are available by contacting the Northern Climate ExChange (Yukon Research Centre, Yukon College). Projections are available for mean annual and seasonal temperature and precipitation, as well as freeze and thaw dates and growing degree days, for the A1B and B1 scenarios, for the 2020s and 2050s, as well as the 1960-1990 time period.

Table D1. Statistics generated for the B1, A1B and A2 climate scenarios, showing mean, minimum and maximum air temperature in the 2020s, 2050s and 2080s.

Projection	Air Temperature (°C)		
	Mean	Minimum	Maximum
Current MAAT	-2.7	-3.1	-2.6
1950 - 1979	-3.8	-4.2	-3.7
B1 2020s	-2.5	-2.9	-2.4
B1 2050s	-1.9	-2.4	-1.8
B1 2080s	-0.9	-1.4	-0.8
A1B 2020s	-2.6	-3.0	-2.4
A1B 2050s	-1.3	-1.7	-1.2
A1B 2080s	0.1	-0.4	0.2
A2 2020s	-2.6	-3.1	-2.5
A2 2050s	-1.6	-2.0	-1.5
A2 2080s	0.3	-0.1	0.4

REFERENCES

- Environment Canada, 2013. Canadian Climate Normals 1971-2000. Ottawa, Ontario: Environment Canada. [http://www.climate.weatheroffice.gc.ca/climate_normals/index_e.html]. Accessed January 2013.
- Etzel Müller, B., Farbrot, H., Guomundsson, A. and Humlum, O., 2007. The regional distribution of mountain permafrost in Iceland. *Permafrost and Periglacial Processes*, vol. 18, p. 185-199.
- Intergovernmental Panel on Climate Change (IPCC), 2015. Fifth Assessment Report. IPCC, Geneva, Switzerland. [<https://www.ipcc.ch/index.htm>]. Accessed January, 2015.
- Lewkowicz, A.G. and Bonnaventure, P.P., 2011. Equivalent elevation: A new method to incorporate variable lapse rates into mountain permafrost modelling. *Permafrost and Periglacial Processes*, vol. 22, p. 153-162.
- SNAP (Scenarios Network for Alaska and Arctic Planning), 2012. www.snap.uaf.edu.

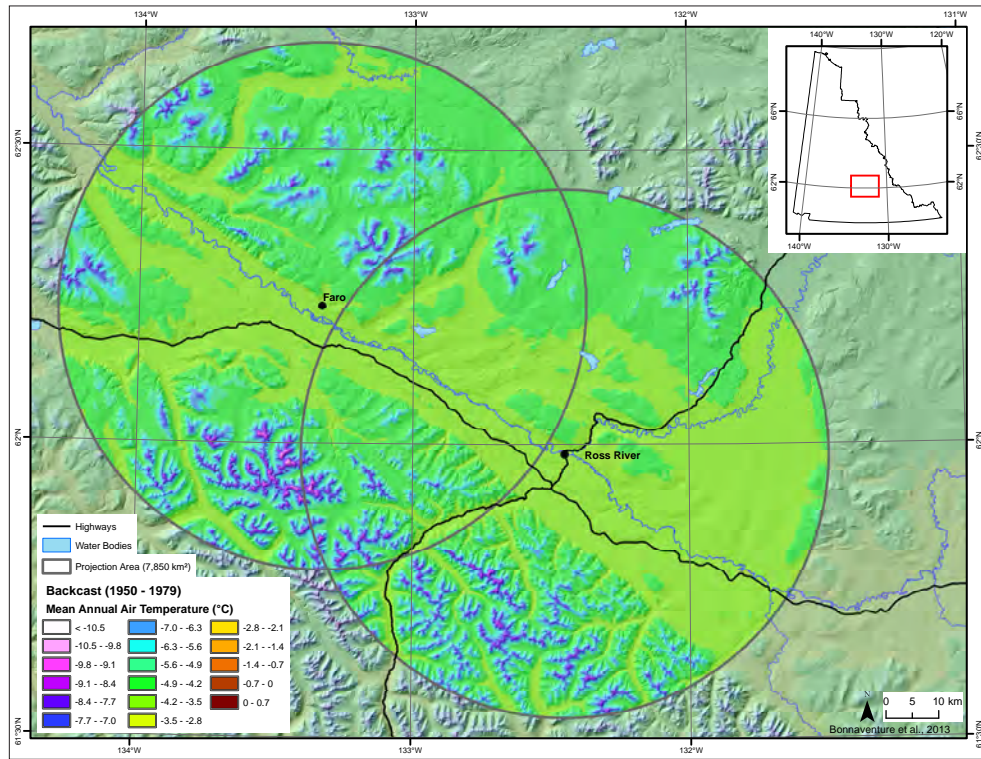


Figure D1. Mean annual air temperature for the Ross River area, backcasted for the 1950-1979 period.

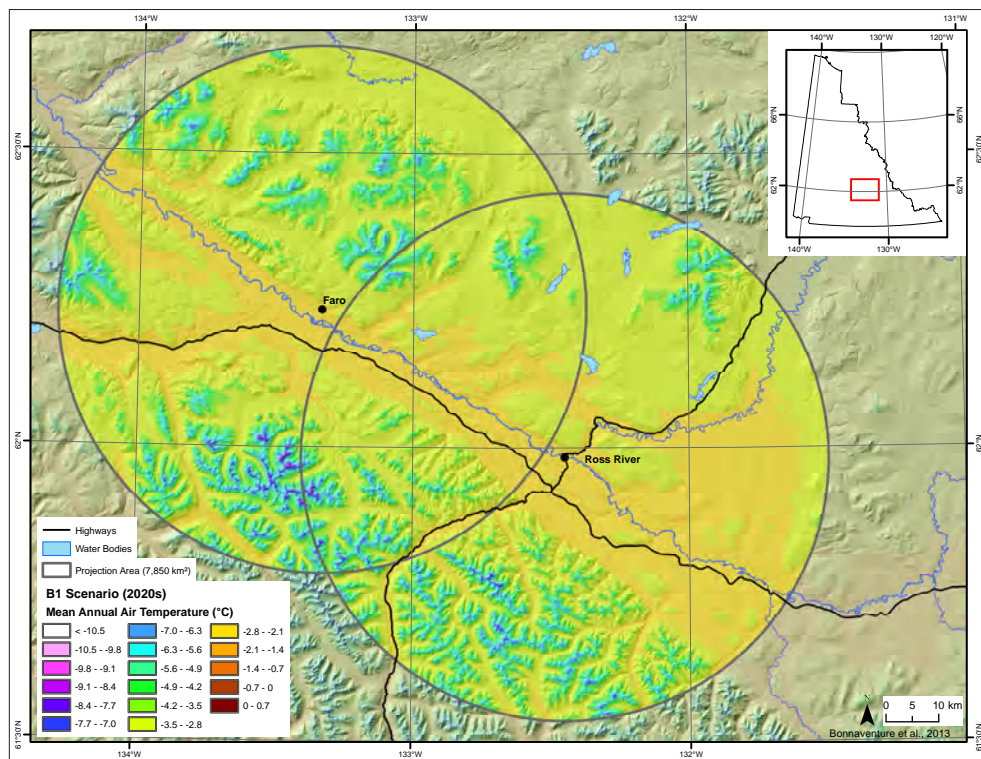


Figure D2. Mean annual air temperature for the Ross River area for 2020, projected using the B1 scenario.

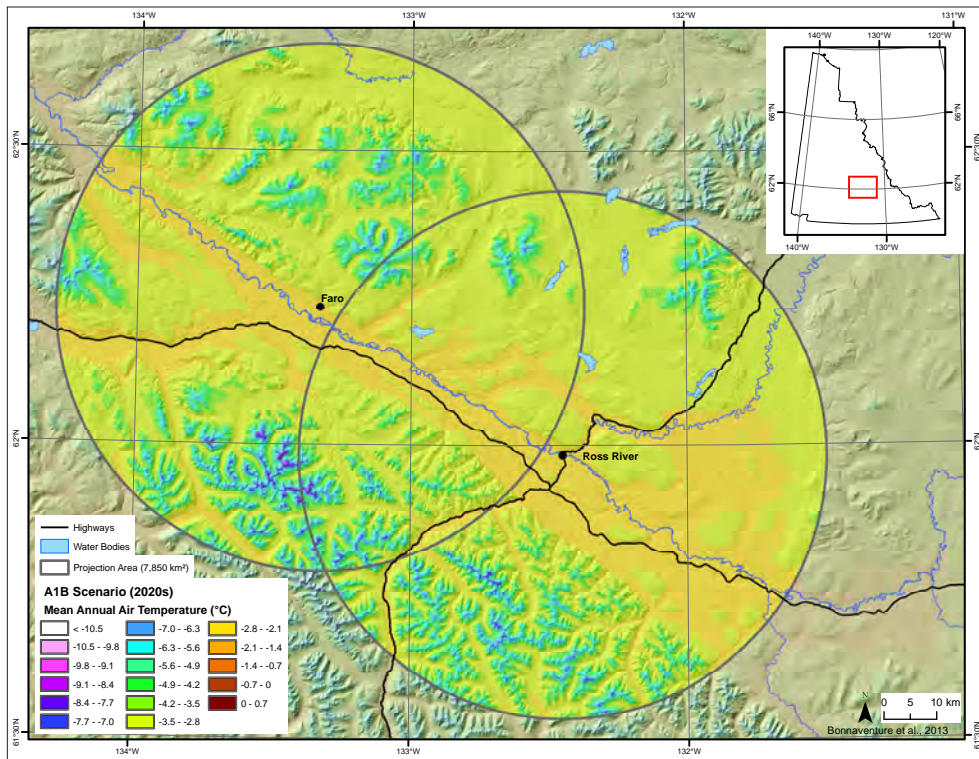


Figure D3. Mean annual air temperature for the Ross River area for 2020, projected using the A1B scenario.

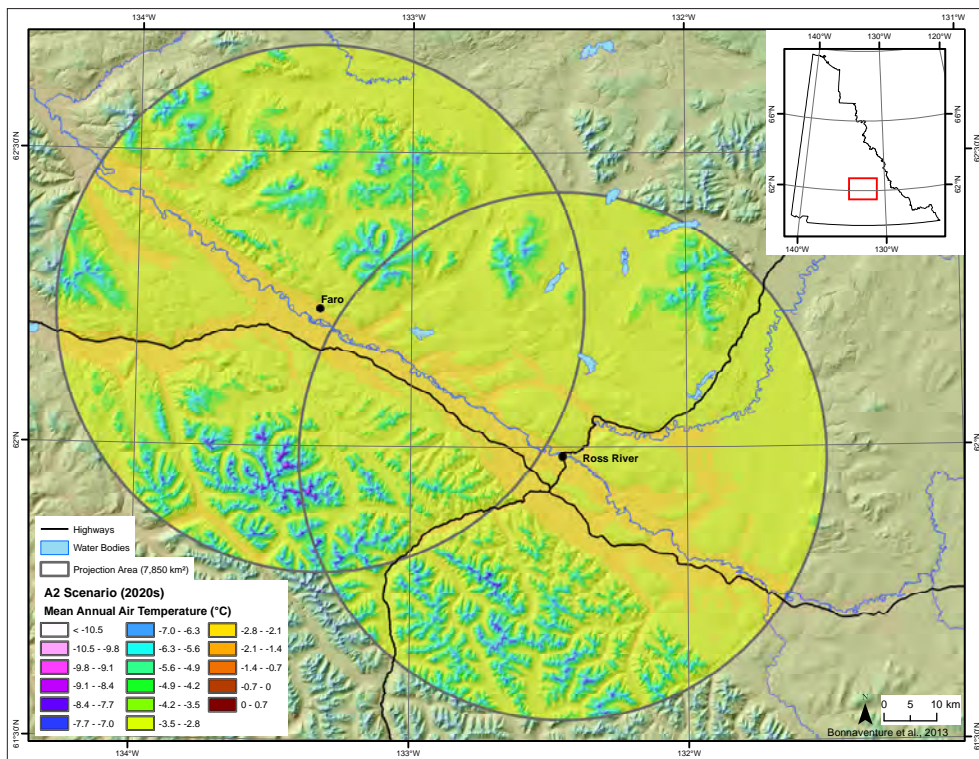


Figure D4. Mean annual air temperature for the Ross River area for 2020, projected using the A2 scenario.

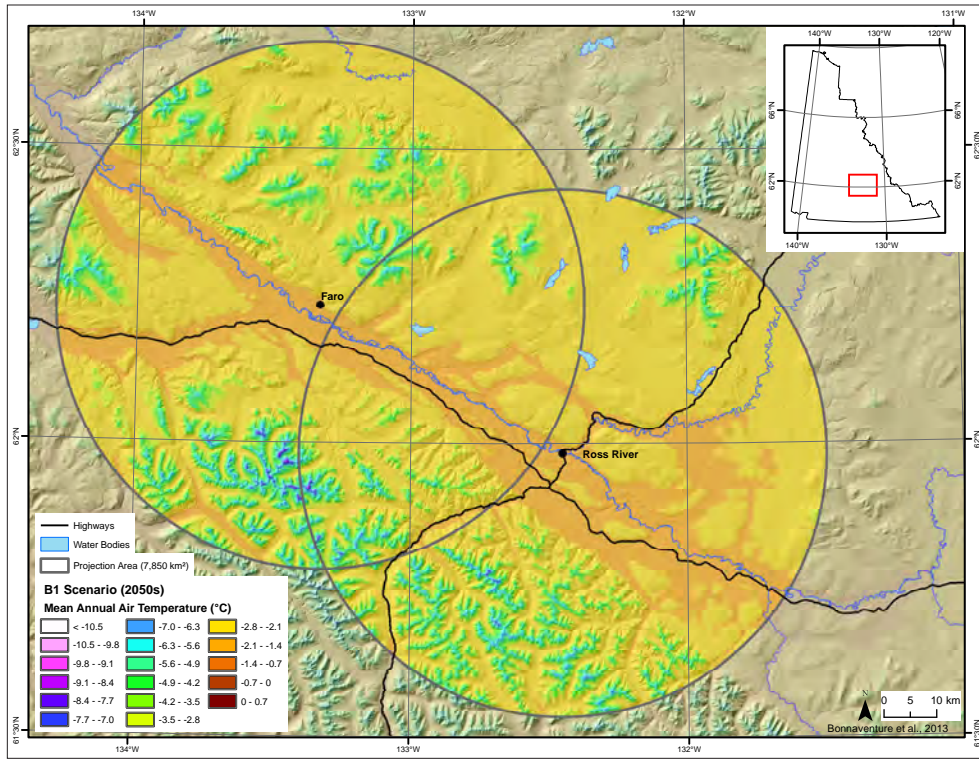


Figure D5. Mean annual air temperature for the Ross River area for 2050, projected using the B1 scenario.

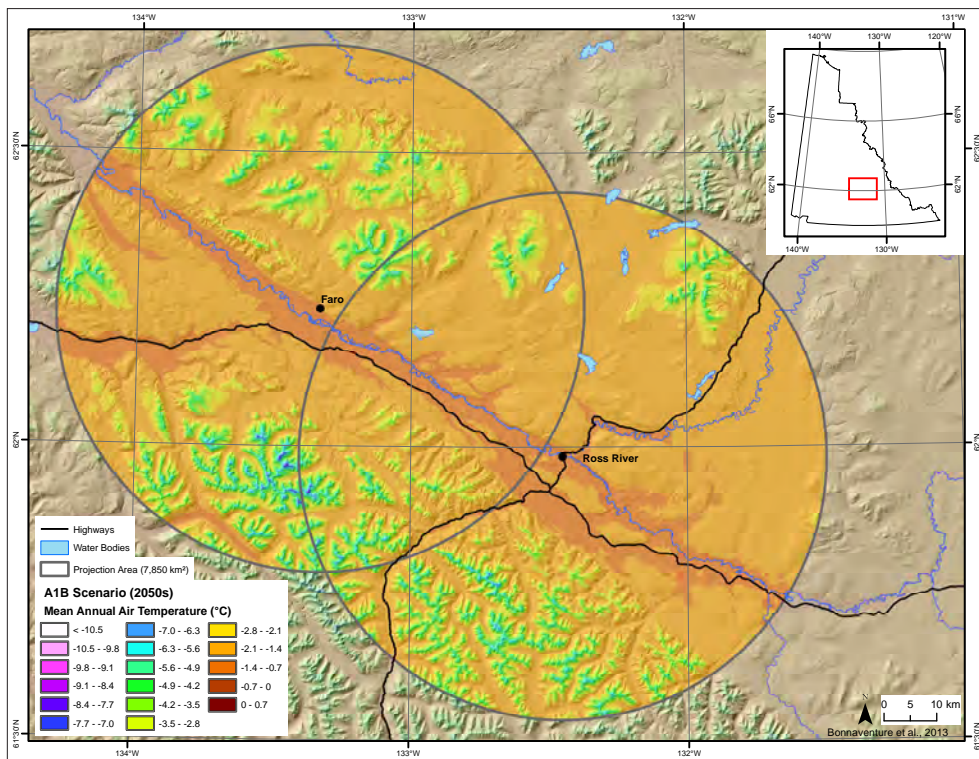


Figure D6. Mean annual air temperature for the Ross River area for 2050, projected using the A1B scenario.

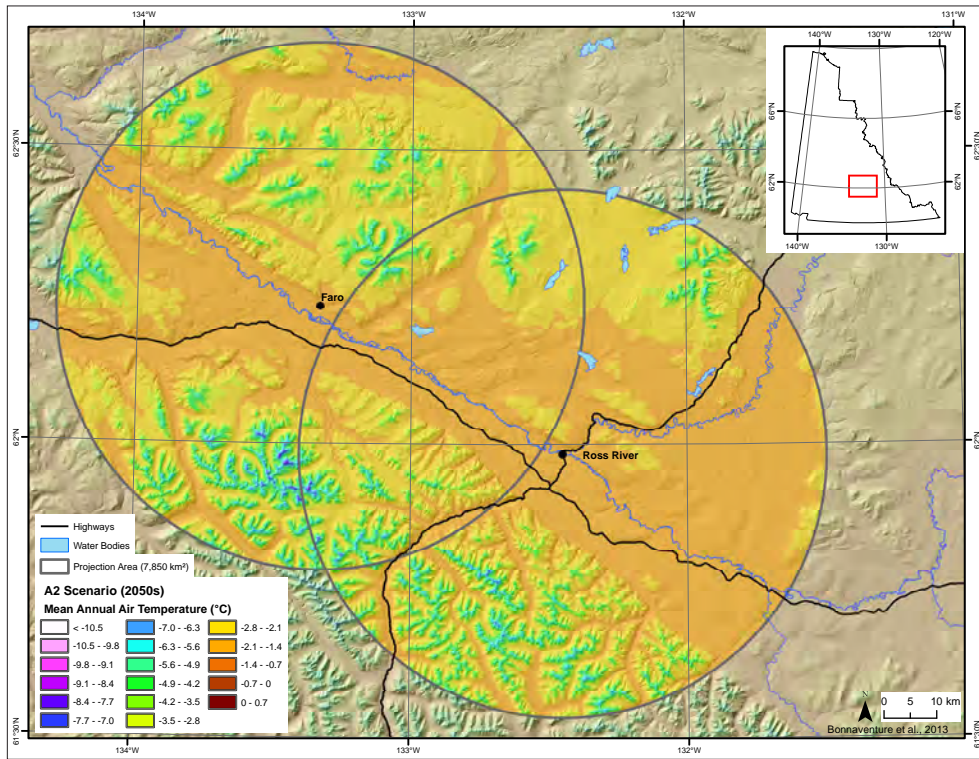


Figure D7. Mean annual air temperature for the Ross River area for 2050, projected using the A2 scenario.

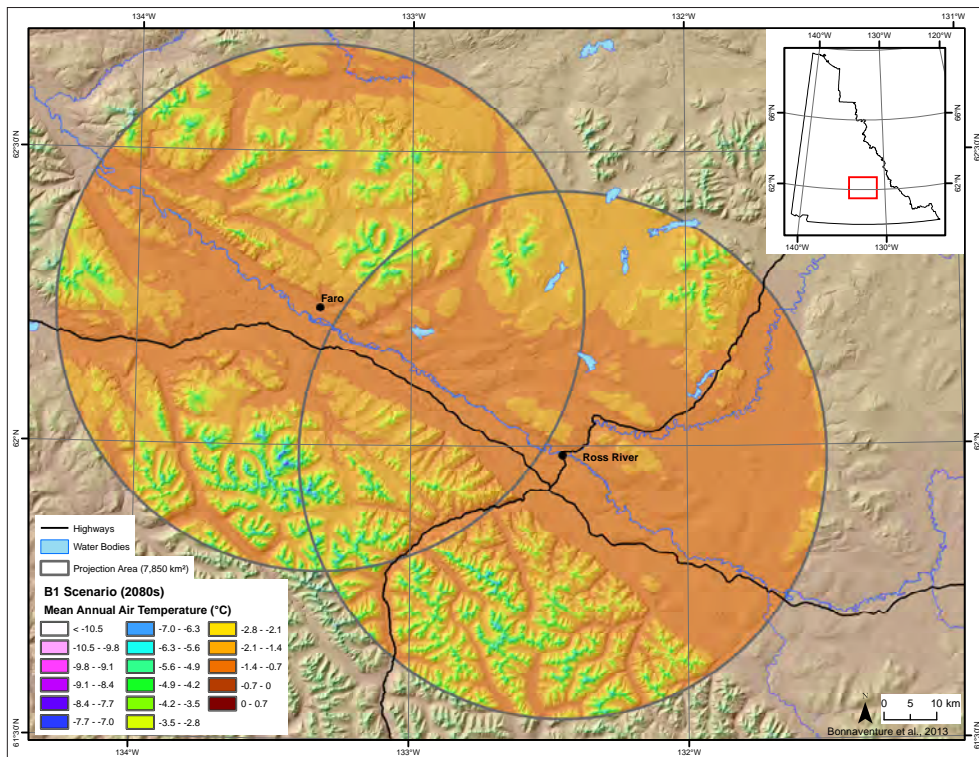


Figure D8. Mean annual air temperature for the Ross River area for 2080, projected using the B1 scenario.

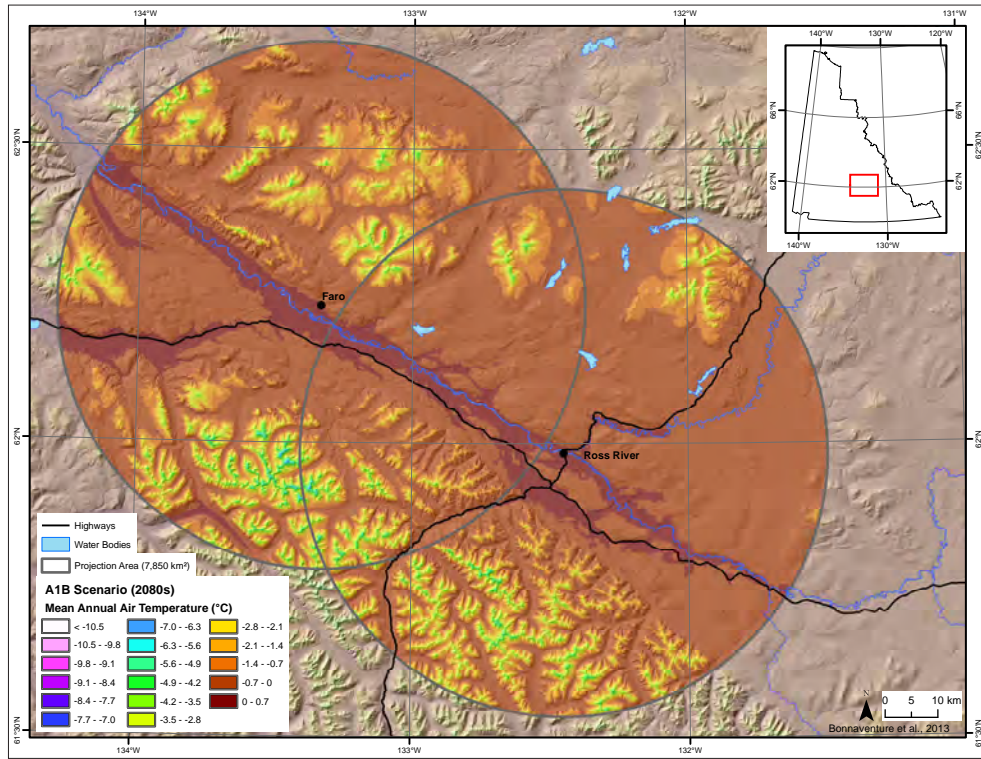


Figure D9. Mean annual air temperature for the Ross River area for 2080, projected using the A1B scenario.

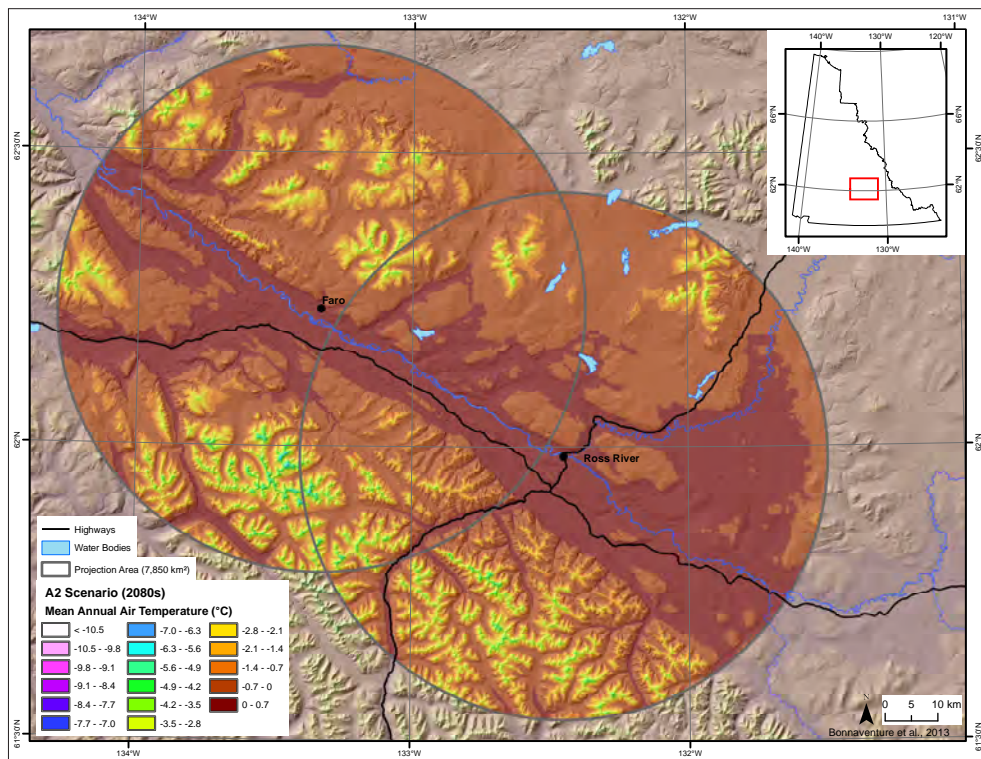


Figure D10. Mean annual air temperature for the Ross River area for 2080, projected using the A2 scenario.

APPENDIX E - HAZARD RANKINGS

Table E1. Hazard classification results for polygons labeled on Figure 52 in the main body of this report (see larger print version of the map in back pocket).

Polygon Number	Surficial Geology	Hazard Ranking	Hazard Description
1	Morainal (till) (M)	3	gullyng
2	Morainal (till) (M)	1	
3	Morainal (till) (M)	1	
4	Morainal (till) (M)	1	
5	Morainal (till) (M)	1	
6	Morainal (till) (M)	1	
7	Fluvial (F)	2	inactive floodplain
8	Morainal (till) (M)	3	gullyng
9	Morainal (till) (M)	1	
10	Glaciolacustrine (LG)	3	gullyng
11	Colluvium (C)	3	debris flows
12	Morainal (till) (M)	1	
13	Morainal (till) (M)	1	
14	Morainal (till) (M)	3	gullyng
15	Fluvial (F)	2	inactive floodplain
16	Fluvial (F)	2	ice-rich permafrost
17	Fluvial Active (FA)	3	flooding; shifting channels
18	Morainal (till) (M)	1	
19	Fluvial (F)	3	flooding; thermokarst
20	Colluvium (C)	2	active slopes
21	Morainal (till) (M)	3	gullyng
22	Fluvial (F)	3	flooding
23	Morainal (till) (M)	1	
24	Organic (O)	3	flooding; ice-rich permafrost
25	Bedrock (R)	1	
26	Morainal (till) (M)	1	
27	Glaciolacustrine (LG)	2	ice-rich permafrost
28	Morainal (till) (M)	1	
29	Morainal (till) (M)	3	gullyng
30	Morainal (till) (M)	1	
31	Morainal (till) (M)	3	gullyng
32	Morainal (till) (M)	1	
33	Fluvial (F)	2	inactive floodplain
34	Colluvium (C)	3	debris flows
35	Glaciofluvial (FG)	3	gullyng
36	Morainal (till) (M)	1	
37	Morainal (till) (M)	3	flooding; thermokarst

Table E1, *continued*. Hazard classification results for polygons labeled on Figure 52 in the main body of this report (see larger print version of the map in back pocket).

Polygon Number	Surficial Geology	Hazard Ranking	Hazard Description
38	Morainal (till) (M)	1	
39	Morainal (till) (M)	1	
40	Morainal (till) (M)	1	
41	Fluvial (F)	2	inactive floodplain
42	Fluvial (F)	2	inactive floodplain
43	Colluvium (C)	3	debris flows
44	Glaciofluvial (FG)	1	
45	Morainal (till) (M)	3	gullying
46	Morainal (till) (M)	1	
47	Morainal (till) (M)	1	
48	Colluvium (C)	2	active slopes
49	Morainal (till) (M)	1	
50	Morainal (till) (M)	2	moderate-steep slopes
51	Organic (O)	3	flooding; thermokarst
52	Morainal (till) (M)	3	gullying
53	Organic (O)	3	flooding; ice-rich permafrost
54	Fluvial (F)	2	inactive floodplain
55	Anthropogenic (A)	2	mine pit walls
56	Morainal (till) (M)	1	
57	Morainal (till) (M)	1	
58	Morainal (till) (M)	1	
59	Colluvium (C)	2	active slopes
60	Morainal (till) (M)	3	gullying
61	Morainal (till) (M)	3	gullying
62	Organic (O)	3	flooding; thermokarst
63	Morainal (till) (M)	3	gullying

APPENDIX F - SAFE HOME CONSTRUCTION ON PERMAFROST

Prepared by

Julie Malenfant-Lepage (M.A., Eng.) and Benoit Loranger (Jr. Eng.)

Northern Climate ExChange, Yukon Research Centre, Yukon College

TABLE OF CONTENTS

INTRODUCTION	102
CONSTRUCTION ON PERMAFROST	102
Problems Related to House Construction on Permafrost.....	103
Types of Surface Materials and the Thawing Processes.....	104
SITE INVESTIGATION	105
Preliminary Observations.....	106
Frost Probing.....	106
Drilling.....	106
Geophysics.....	106
FOUNDATIONS IN PERMAFROST	107
Construction Data Requirements.....	107
Foundation Types.....	108
<i>Surface gravel pads</i>	108
<i>Insulation</i>	109
<i>Screw-jack foundations</i>	110
<i>Timber-block foundations</i>	111
<i>Space-frame foundations</i>	111
<i>Pile foundations</i>	111
<i>Foundations with heat exchangers</i>	113
BASIC PRINCIPLES TO MAINTAIN PERMAFROST	114
Drainage.....	114
Ventilation.....	115
Shading.....	115
Heat Extraction.....	115
Monitoring.....	115
CONCLUSIONS AND RECOMMENDATIONS	115
REFERENCES	116

INTRODUCTION

Construction in permafrost environments requires a good understanding of the nature of permafrost as well as the surficial geology. There are several principles and techniques for building on permafrost that have been proven efficient in various parts of northern Canada and Alaska. This report aims to briefly present the different approaches applied in construction of new buildings. In some ways, it can be considered as an introductory guide for basic principles, design and construction on permafrost. It is important to note, however, that this report is not prepared as an engineering design text and should not be used as such.

This report on safe home construction in permafrost environments will provide an overview of building construction on permafrost including issues related to house construction on permafrost, types of surface materials and thawing processes, preliminary investigation procedures, construction data requirements, types of foundations built in northern regions, basic principles to maintain permafrost under existent structures, and finally, recommendations that should be followed throughout the construction process.

CONSTRUCTION ON PERMAFROST

The best advice that could be given to an individual or to a contractor is to avoid building on permafrost terrain. If possible, it is always better to find a new site than to face the extra expense and maintenance involved in construction on permafrost. However, in many regions where permafrost is extensive (e.g., in northern Canada, including the Yukon) or where other factors preclude construction on non-permafrost terrain, this advice is sometimes impossible to follow. Building directly on bedrock is a good practice and should be done whenever possible (Figure F1).



Figure F1. Houses in Ilulissat, western Greenland, built directly on bedrock.

In areas underlain by continuous permafrost, permafrost is one of the major controlling factors in design parameters. As a result, it is important to design and build in a way that will preserve the underlying permafrost. Stability and lifetime of the infrastructure depend directly on the success of this endeavour.

Areas that are underlain by discontinuous permafrost offer the greatest engineering challenge since it is very difficult to determine exactly where there is underlying permafrost as it may change on a very local scale. Despite the high costs associated with the analysis of a potential construction site by drilling, these analyses will never confidently ensure the presence or absence of permafrost. If the site is located in a thaw-stable area, more conventional and less expensive construction techniques can be used without risk of destabilizing the ground. However, if the site is located in an area of ice-rich soil, which is considered thaw-unstable, standard structural foundations may thaw the underlying permafrost and potentially lead to an eventual failure of the structure. It is sometimes possible to remove or thaw permafrost on a site before starting construction, but this is a process that is rarely performed. The choice of a good structural foundation design and good mitigation techniques will help preserve permafrost, as well as respect a budget, which is the main challenge in regions underlain by discontinuous permafrost (Permafrost Technology Foundation, 2000).

PROBLEMS RELATED TO HOUSE CONSTRUCTION ON PERMAFROST

The most significant impact to permafrost usually occurs immediately beneath the house as heat is conducted downwards into the soil foundation. If a heated building is directly placed on permafrost, it will warm the ground throughout the entire year (Figure F2). However, if the building is not in contact with the ground surface, as is commonly found in northern communities, thawing is still possible due to the following: obstructed water drainage, insulation of ground by snow piling, and wind obstruction beneath the house. Furthermore, impacts from site preparation and infrastructure construction such as vegetation clearance, surface grading, and removal or compression of the organic layer, can increase heat intake by the ground surface. These ground disturbances usually result in an increase of ground temperatures, deepening of the thaw depth, and subsequent thaw settlement. In most cases, it will take several years for permafrost temperatures to reach a new equilibrium following construction.

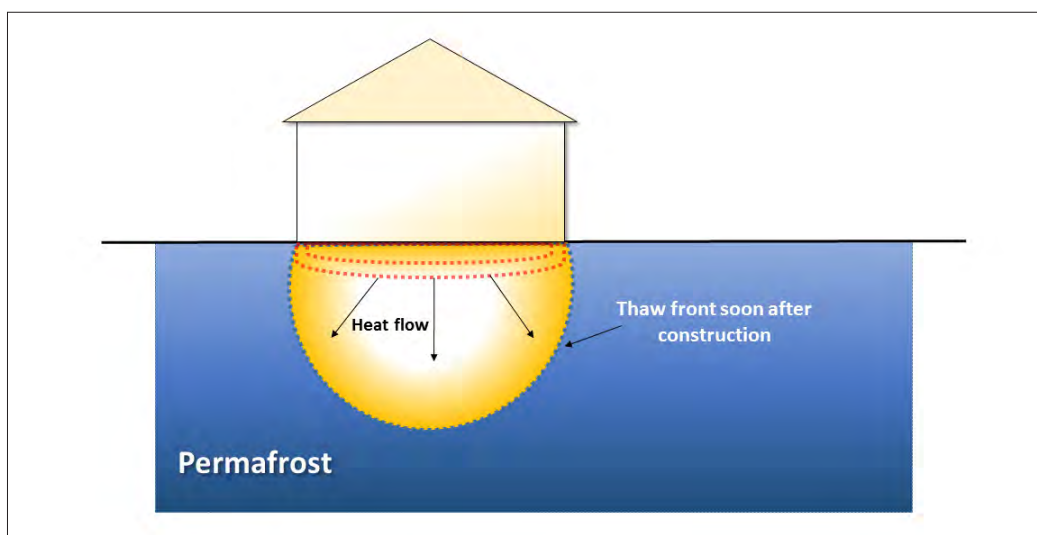


Figure F2. Cross section displaying the evolution of permafrost degradation under house construction. Based on Barriault (2012).

Foundation failure does not normally occur in a short period of time. Sudden collapse is extremely rare in the context of permafrost and is more likely associated with thermal erosion by water. The

time it takes for heat generated by a building to diffuse into the underlying permafrost depends on permafrost type, as well as factors such as the thickness of the active layer (i.e., layer of soil that thaws and freezes annually), the soil type, the temperature of the permafrost, the presence of water in the soil, and the amplitude of temperature change at the surface. However, once the process of warming is initiated, thawing of the soil is irreversible.

If buildings are left unattended, soil degradation can end up affecting the structure and will lead to the formation of cracks and bindings on doors, walls and ceilings (Figure F3). Tilted floors can also be associated with permafrost-related problems. Eventually, a building can become non-functional and even condemned. Damage associated with permafrost degradation should therefore be monitored and repaired as soon as possible to ensure viability of the structure. Monitoring can also be used to collect relevant data that would be useful in assessing permafrost-related damage. It is by far more cost effective to initiate repairs at the first signs of permafrost-related failures.



Figure F3. Examples of unmaintained buildings in Pyramiden, Svalbard, displaying cracks and uneven settlement in response to permafrost thaw.

TYPES OF SURFACE MATERIALS AND THE THAWING PROCESSES

In permafrost regions, coarse, granular surface material (sand and gravel) and rocks without ice inclusions are typically the best material on which to construct a foundation. Upon thawing, these materials are stable and have good bearing capacity. Bearing capacity refers to the load a surface material can safely withstand, without significant compaction or settlement. Foundation design in such materials should follow the current practice of moderate temperature regions.

Conversely, fine-grained surface materials, which are often ice-rich, have low permeability and tend to be oversaturated after thawing. Pore-pressure generated during thawing may result in a significant loss of stiffness (bearing capacity) and volume (Figure F4). For fine-grained deposits, foundation design in permafrost poses several challenges when attempting to control differential settlement of the materials that leads to the deformation of structures. The bearing capacity of fine-grained materials is largely a function of the amount and temperature of ground ice present.

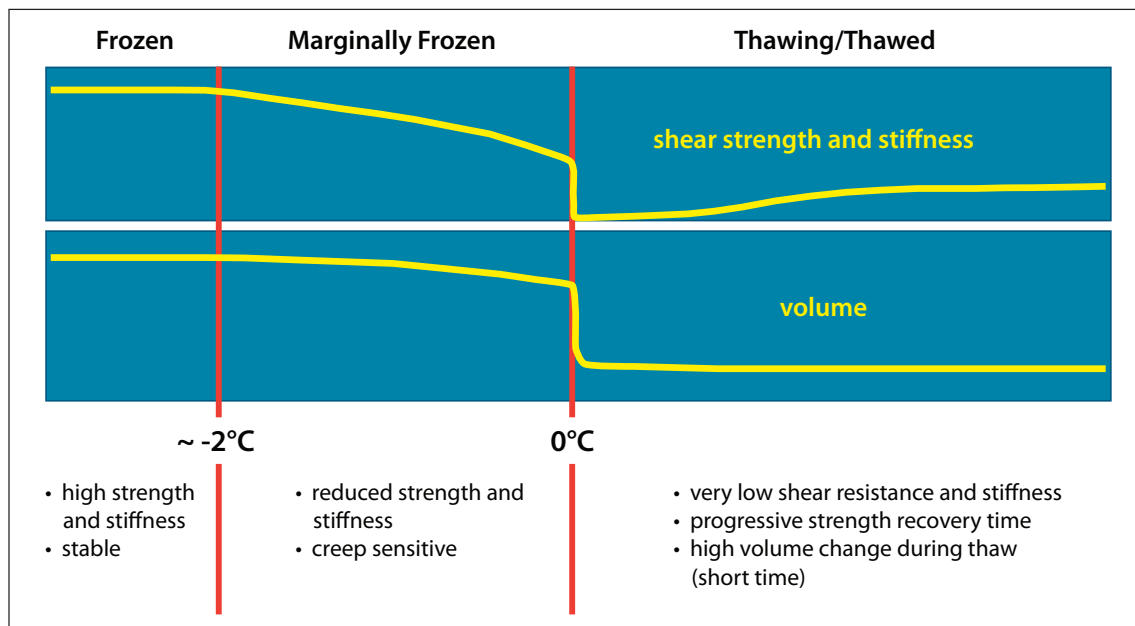


Figure F4. Mechanical properties of frozen ground undergoing thaw (Doré, 2011).

As the amount of ground ice commonly varies across a construction site in zones of discontinuous permafrost, bearing capacity may differ within a foundation, causing different portions of the structure to experience settlement at different rates. Furthermore, since ice-rich deposits consolidate and discharge excess water as they thaw, variably distributed ground ice can result in the settlement of specific areas of the ground, causing distortion in the structure above. Therefore, these types of surface materials do not offer good support for construction of buildings (Canadian Standard Association (CSA), 2010).

It is also important to note that permafrost with a temperature between -2°C and 0°C is marginally frozen (i.e., considered to be 'warm permafrost') and may not appear to be warming rapidly. At this temperature, a significant amount of heat transfer is mainly used to melt ground ice instead of warming the surface materials. Consequently, the strength of permafrost under the structure will be reduced significantly as the ground ice melts even if the temperature of the sediments remains below 0°C (see Figure F4). Moreover, several problems of creeping related to thick gravel pads and heavy structures are commonly associated with warm permafrost. Creep is related to slow ice deformation within the ground under a constant load. Ice then reacts as a malleable material and tends to flow laterally, away from the load source.

In summary, fine deposits of silt and clay are more likely to be problematic because of their frost susceptibility. Well-drained materials such as sand and gravel will be more stable; however, it is important to note that many sandy and gravelly deposits may contain a significant amount of fines that could pose a threat to the integrity of a structure. Frost susceptibility appears when approximately 10% of the mass of the surface deposit is composed of material with a fine grain size, i.e., 80 µm. If in doubt, it is best to seek advice from a geotechnical engineer.

SITE INVESTIGATION

The objectives of the site investigation are to identify terrain units, determine relevant surface material properties, and identify areas of thaw-sensitive or unstable deposits. The type of building

and its lifespan define the quantity and complexity of information necessary. The following section provides the current practices used during the site investigation.

PRELIMINARY OBSERVATIONS

The first step is an attentive observation of all permafrost-related features that could be present at the site. Features such as frost mounds, cracks, depressions and uneven terrain are typical characteristics of a permafrost landscape. Therefore, it is important to pay close attention to terrain morphology and topography since these are indicators of underlying permafrost conditions.

FROST PROBING

When the top of the permafrost is shallow and the active layer is relatively soft, frost probing is an effective method for locating depth to permafrost (Figure F5). This technique uses a steel rod with a handle, which is pushed into the ground manually until the top of the permafrost is reached. With this method, shallow permafrost can easily be detected, and its depth measured. Frost probing is inexpensive, fast and very useful for preliminary site investigations.



Figure F5. Frost-probing to determine depth to permafrost.



Figure F6. Example of ice-rich permafrost core from the Beaver Creek area, Yukon.

DRILLING

The most effective way to determine ground ice conditions at a potential site is to drill boreholes and collect samples of permafrost for geotechnical analysis (Figure F6). This provides specific information about soil characteristics and conditions at the subsurface at a particular location. A good borehole log will provide information at varying depths, including the thickness of the active layer, the soil or rock types, the ice content, the depth and characteristics of permafrost, the presence of massive ice bodies, and in some cases, the depth to bedrock.

The information derived from multiple boreholes in a given area can be extrapolated to obtain a spatial representation of subsurface conditions. It is very important to drill deep enough to obtain the appropriate information for each project. Generally speaking, the larger the building, the deeper the drilling must be. Permafrost drilling requires trained personnel with proper equipment adapted to site conditions.

GEOPHYSICS

If a larger area is being surveyed, complementary geophysical approaches like electrical resistivity tomography (ERT) and ground penetrating radar (GPR) surveys should be considered. Both applications work by sending signals into the ground and measuring the rate or strength of their return, and using those results to map subsurface conditions.

Geophysical surveys can be applied to help extrapolate information between boreholes. It is particularly useful for determining the thickness and extent of permafrost bodies, and zones of unfrozen ground within permafrost (Figure F7 a,b). ERT and GPR are applied for different detection purposes and professional geophysicists will select the most appropriate technique for the site. Geophysical surveys have the advantage of covering a relatively large area in a short period of time. Furthermore, ERT and/or GPR surveys are a cost-effective way to minimize the number of boreholes that need to be completed at any given site. The results obtained by drilling, coupled with geophysical surveys allow for a more comprehensive analysis of the subsurface conditions of the entire site.

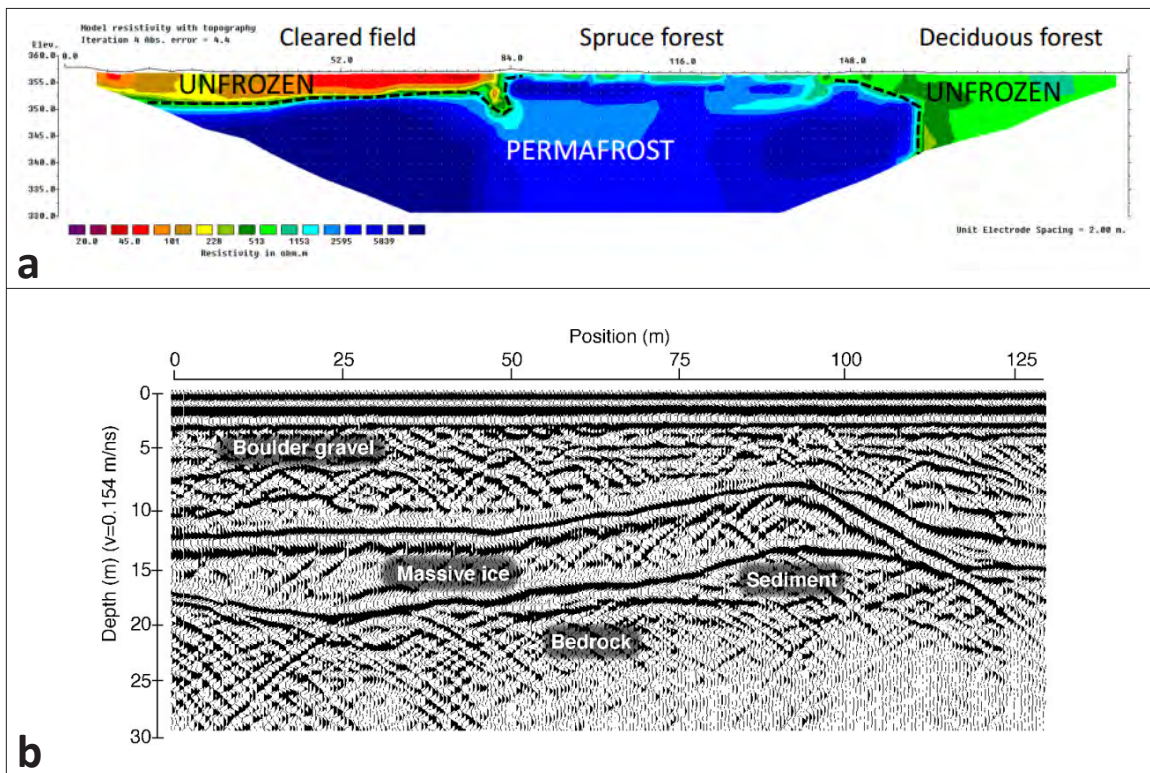


Figure F7. (a) ERT profile from the Klondike Valley, Yukon (Lewkowicz et al., 2014). **(b)** GPR profile along an ice-cored esker near Carat Lake, Northwest Territories (Moorman et al., 2007).

FOUNDATIONS IN PERMAFROST

Robust foundations for infrastructure in permafrost areas are critical for long-term building stability. General data requirements and the most common types of foundations are presented below.

CONSTRUCTION DATA REQUIREMENTS

The following list indicates principal information requirements related to construction and foundation design (Andersland and Ladanyi, 2004). This list is for large-scale projects and only needs to be fully applied in those cases. However, some elements are essential in the selection of the right type of foundation, such as the amount and temperature of ground ice, as well as the active layer thickness. It is good practice to gather as much information as possible about a site prior to construction.

1. Site data:
 - a. location
 - b. climate
 - c. physiography and geology
 - d. subsurface materials and their characteristics
 - e. thermal regime
 - f. hydrology and drainage
 - g. materials and construction
 - h. transportation facilities and access
 - i. construction cost factors
 - j. Availability of :
 - i. labor, skills, and knowledge
 - ii. construction equipment
 - iii. support facilities and equipment
2. Design policies, general criteria, and cost limitations
3. Technology (state of the art)
4. Facility technical data
 - a. size and design life (e.g., permanent versus temporary)
 - b. foundation loading
 - c. thermal conditions
 - d. movement and distortion

FOUNDATION TYPES

Good foundation construction in the North is essential to assure a full service life of a structure. Proper foundation design will be the difference between a safe, stable structure with relatively low maintenance costs, and one with constant stability problems leading to a shorter lifespan. The selection of a foundation type will generally depend on the soil behaviour upon thawing. Foundations built on permafrost can be divided into three main categories: 1) surface pads; 2) deep foundations, and; 3) foundations with heat exchangers.

SURFACE GRAVEL PADS

Construction on a surface pad to preserve the temperature of the underlying permafrost is common in northern Canada. According to Allard et al. (2010), houses built on properly designed, compacted, granular foundations should not undergo significant thaw settlement because the adjustment of the thermal profile to the new geometry leads to a rise of the permafrost into the gravel pad (Figure F8 a,b). The active layer then becomes limited to the non-frost sensitive foundation, which ensures stability over cycles of freezing and thawing. Gravel pads are frequently used with insulant panels and techniques that allow airflow beneath the building.

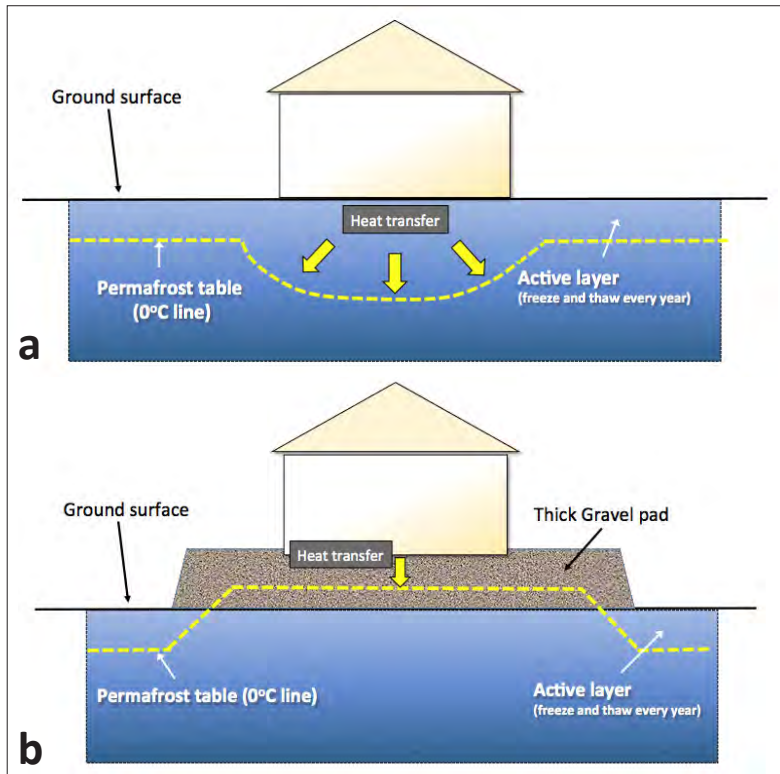


Figure F8. Schematics demonstrating the theoretical position of the permafrost table underneath (a) a building built directly on the ground, and (b) a building built on a gravel pad.

INSULATION

Structures may be built directly on insulating material (Figure F9). Insulation will slow the rate at which heat enters the ground, but it does not eliminate heat exchange. It is possible to add enough layers of insulation to establish a new thermal balance between heat input from the area around the building and winter cooling, but this procedure is almost never performed due to the high cost. Insulation is commonly applied along with a gravel pad.

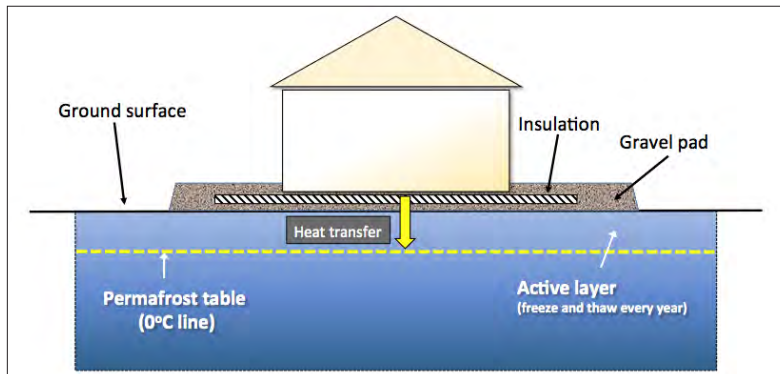


Figure F9. Basic insulation-pad foundation design (modified from CSA, 2010).

Several types of insulation can be considered in the construction of an unheated foundation. An insulated layer that is intended to be in contact with the soil must be able to withstand deterioration of its thermal properties and physical shape in the presence of soil moisture, soil chemicals, physical loading and other outside forces (Permafrost Technology Foundation, 2000).

SCREW-JACK FOUNDATIONS

In the 1980s, the Société d’Habitation du Québec developed a concept for house foundations to preserve permafrost. It involved buildings that are constructed on adjustable metal jacks over a compacted granular foundation (Figure F10). The granular foundation is laid directly on the ground surface without the removal of the vegetation cover. To date, this construction technique has been proven very effective for preserving permafrost (Gravel, 2012). The foundation must raise the building high enough to promote uninhibited air circulation beneath the building. It allows the wind to flow freely under the building, mainly to avoid snow accumulation that could increase the soil temperature (by insulation) under the foundation. Under these conditions, a snow bank will form approximately six metres away from the dwelling’s foundation. It is important that nothing be stored in the space between the floor and the ground surface so as to not interfere with the free air circulation during the winter months. The winter airflow allows for the extraction of heat from the ground beneath the building, and helps preserve permafrost. Sufficient insulation should be placed under the floor of the structure so the energy loss from the bottom of the building is minimized and the floor inside the building is comfortable for residents.

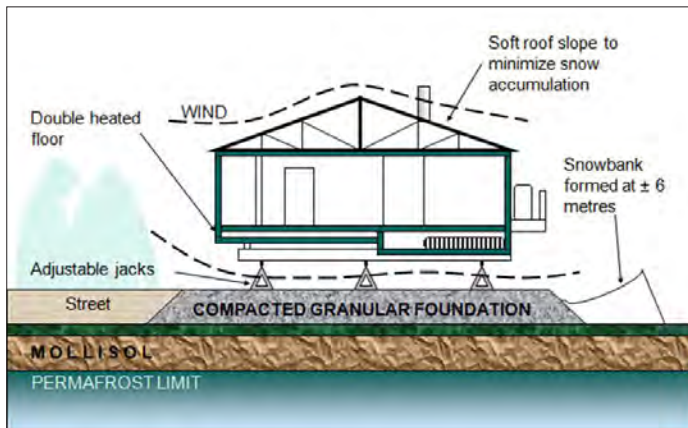


Figure F10. Conceptual design of a screw-jack foundation on a compact granular foundation (Gravel, 2012).

Once or twice a year, maintenance of a building on jacks needs to be performed in order to preserve the building’s stability. During the maintenance process, screws in the middle of the jacks are used to raise or lower the height of the building (Figure F11). For a small, single-family house, it is common to use about nine adjustable jacks which can withstand nearly 35 000 kg each (Gravel, 2012). It is important to ensure that the slope of the terrain around the building allows for adequate drainage of surface water away from the structure.



Figure F11. Examples of adjustable-jack foundations from Gravel (2012) and CSA (2010).

TIMBER-BLOCK FOUNDATIONS

Timber-block foundations (Figure F12) work on the same principle as the screw-jack technique. However, screw jacks are not always easily obtainable and it can be more convenient to use timber blocks. Timber blocks are normally screwed together to ensure lateral stability. Timber blocks are commonly sited directly on natural ground (without a gravel pad).



Maintenance operations are almost the same as for screw-jack foundations, described above; however, the operator must use a hydraulic jack to lift the load of the building before shimming the timber blocks. Maintenance for this style of foundation is therefore more labour intensive than for screw-jack foundations.

Figure F12. Example of a timber-block foundation used in Nunavut (Government of Nunavut, 2013).

SPACE-FRAME FOUNDATIONS

Another surface foundation that has proven successful in permafrost regions is the rigid, three-dimensional, truss-type foundation (Figure F13). This is a commercially available, pre-manufactured foundation that consists of metal tube members flattened on each end and connected by metal node pieces at the top and bottom to form approximately one metre-square cells. It is custom-made to fit the building, and is assembled directly on-site on a compacted, granular foundation.

A screw at each structural node is used to level the building in the event of permafrost thaw underneath the building. These types of foundations are quite expensive, and are used mainly for service buildings and large, public infrastructure.



Figure F13. Examples of space-frame foundations in Nunavut (Barriault, 2012).

PILE FOUNDATIONS

In the far North, the majority of public and private dwellings, as well as commercial buildings, are built on steel piles. Piles are long steel pipes driven into the ground to stabilize buildings into the permafrost or bedrock (Figure F14). This type of foundation requires little to no gravel,

which can be a very expensive resource to procure and transport to northern communities. The use of steel piles also allows for construction on harsher and steeper terrain compared with conventional foundations. The steel piles are also more resilient to climate change compared to other foundation types when they are placed directly on bedrock.



Figure F14. Example a steel-pile foundation in Nunavik (Gravel, 2012).

There are two principal pile types currently in use in the Canadian North: 1) adfreeze piles (driven and slurry), and 2) rock-socketed piles. Their design and applications are fundamentally different. Adfreeze piles are commonly installed where permafrost extends to substantial depths without encountering bedrock. These piles rely on the bond with the surrounding ground for their load-bearing capacity. They can be driven directly into the ground, or a drill hole can be fixed to accommodate the pile. Slurry is then used to fill the empty space between the soil and the pile. For this application, the ground can be ice-rich, but should be below -3°C , or colder if the soil is saline (CSA, 2010).

Rock-socketed piles are used where bedrock occurs within a practical depth below the surface. These piles are designed to transfer the full load of a structure to the underlying bedrock. In Nunavut, rock-socketed piles are commonly used. Adfreeze piles have been either discontinued or are being driven deeper due to a deepening of the active layer (Barriault, 2012).

In response to ground warming, if the active layer deepens, foundation systems that rely on piles may experience increased frost heaving (Figure F15 a,b,c). This frost heaving occurs when a small part of each pile's surface is frozen to the surrounding soil year-round, while a larger part of the pile's surface is exposed to the lifting force exerted through soil expansion when the water in the active layer re-freezes in the autumn and winter (CSA, 2010). If piles are used in a frost-sensitive soil and cannot be placed directly on bedrock, the piles must be equipped with anti-lift shafts to prevent the exertion of a vertical force by seasonal frost, which can distort the building's structure. Various methods can prevent frost heaving when using pile jacking and a competent engineer should be consulted if this method is being considered.



Figure F15. Examples of pile jacking in Nunavut (Barriault, 2012).



Figure F16. Example of thermosyphons, a foundation system that requires a significant amount of expertise to design, install, maintain and monitor (CSA, 2014).

FOUNDATIONS WITH HEAT EXCHANGERS

Foundations enhanced with heat exchangers are now widespread in Canada’s North. They are generally used where heated crawl spaces and warm first floors at finished grade are required. For such structures, systems are built to intercept heat that would otherwise flow into the ground and affect the underlying permafrost. Thermosyphons are the most widely used heat exchangers (Figure F16). Two-phase thermosyphons work passively during the winter to extract heat from the ground and preserve permafrost (Figure F17 a,b,c). When designs using thermosyphons are being considered, detailed geothermal analyses are required. The inclusion of climate warming in the design process requires careful consideration of the conditions of the site chosen for the design, particularly in winter when low temperatures drive heat removal (CSA, 2010). Due to their high cost, thermosyphons are mainly placed in strategic locations next to high-risk service buildings, bridges or pipelines.

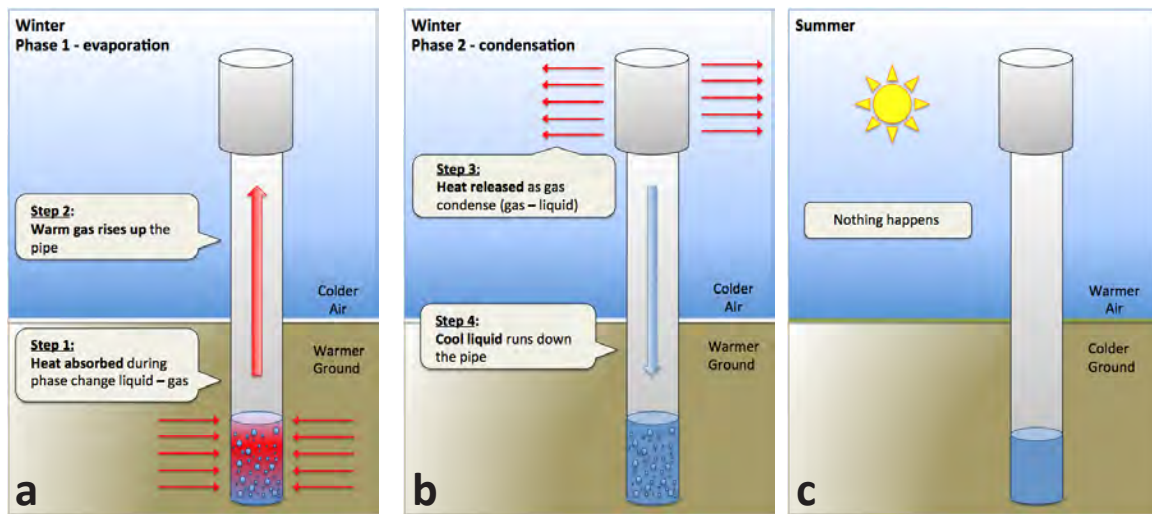


Figure F17. Schematic demonstrating (a) and (b) a winter two-phase thermosyphon cycle, as well as (c) the non-operative state during summer.

BASIC PRINCIPLES TO MAINTAIN PERMAFROST

Once construction of a building is finished, it is essential to maintain the permafrost beneath and around it. Basic elements to consider are outlined below. For more detail, please refer to the Canadian Standards Council (CSA, 2014 and 2013).

DRAINAGE

Because water transfers heat to the ground and can negatively impact permafrost, ditches should not be excavated in permafrost. Proper surface drainage to avoid water ponding beneath or next to the building is very important (Figure F18), especially with regards to spring meltwater (which can result in a high volume of flow during a short period of time). Slopes of approximately 4% are considered sufficient to drain any water at least 4 m (and preferably 6 m) from a building. Any terrain modification that could alter water paths should be carefully considered.



Figure F18. Example of water ponding around a foundation built on permafrost (Government of Nunavut, 2013). Water ponding can have a negative impact on permafrost thermal regimes.

VENTILATION

Winter airflow under buildings extracts considerable heat from the ground and thereby keeps the ground frozen. Air space should be at minimum 0.5-1 m to allow free circulation. Nothing should be stored beneath the building, in order to avoid restricting ventilation. Furthermore, snow should be managed such that it does not reduce ventilation and insulate the ground near the building. Frequent snow clearing may be required.

SHADING

In some cases, vegetation cover or a sun shade may be put in place to shade the ground surface. As mentioned above, it is important to not interfere with airflow or to enhance snow accumulation near the building. Natural vegetation and trees that exist prior to construction should not be disturbed in order to promote shading.

HEAT EXTRACTION

Active heat extraction systems like thermosyphons may be installed if required. These are described in more detail above.

MONITORING

The effectiveness of measures used to preserve permafrost should be monitored to ensure performance is maintained. Ground temperature should also be monitored to detect changes to the ground thermal regime that may affect permafrost – the temperature regime can be a powerful forecasting tool. For example, thermistor cables may be inserted along a pile if drilling is used during the construction phase.

CONCLUSIONS AND RECOMMENDATIONS

Construction in regions underlain by permafrost is a process that requires many steps, including preliminary site investigation, drilling, data analysis, as well as the appropriate choice of foundation design, construction and maintenance. In summary, several recommendations related to building on permafrost can be made:

- Foundations need to be adapted to local permafrost and landscape conditions.
- The organic layer should not be removed before construction.
- The best available geotechnical measures and techniques should be applied for all construction.
- A geotechnical investigation should be completed before construction.
- Compacted granular foundations should be built at least two years in advance of construction to allow the rise of the permafrost table and the stabilization of the soil (Allard et al., 2010).

The permafrost thermal regime should be considered in the design-phase of construction while at the same time integrating the anticipated effects of climate warming in northern Canada.

It may also be appropriate, in some areas, to develop a municipal program with appropriate regulations to ensure yearly maintenance of houses and infrastructure (Allard et al., 2010).

It must be reiterated that this guide does not replace the necessary engineering design needed for building on permafrost. It is important to consult permafrost experts in order to get appropriate advice at the preliminary investigation stages, as well as through the construction and maintenance phases. Additionally, for detailed guidance with respect to roads and permafrost, the *“Guidelines for Development and Management of Transportation Infrastructure in Permafrost Regions”* should be consulted (McGregor et al., 2010).

REFERENCES

- Allard, M., L’Hérault, E., Gybérien, T. and Barrette, C., 2010. Impact des changements climatiques sur la problématique de la fonte du pergélisol au village de Salluit (Nunavik). Rapport final, Centre for Northern Studies, Université Laval, Quebec City, QC, 69 p.
- Andersland, O.B. and Ladanyi, B., 2004. Frozen Ground Engineering, 2nd Edition. Wiley, Hoboken, NJ, 384 p.
- Barriault, A., 2012. Climatic Adaptations to Construction in Nunavut. Nunavut Housing Corporation, Northern Forum, April 18 2012, Quebec City, QC.
- Canadian Standards Association (CSA), 2014. Standards Council of Canada Approves New National Standard to Help Address the Effect of Climate Change on Canada’s North. [<https://www.scc.ca/en/news-events/news/2014/standards-council-canada-approves-new-national-standard-help-address-effects-climate-change-canadas>]. Accessed February, 2015.
- Canadian Standards Association (CSA), 2010. Technical guide: Infrastructure in permafrost: A guideline for climate change adaptation, 1st edition. Canadian Standards Association Publication, 112 p.
- Canadian Standards Association (CSA), 2013. Moderating the Effects of Permafrost Degradation on Building Foundations. Document S501 Draft Standard No. 3, 42 p.
- Doré, G. 2011, Advanced Seminar on Permafrost Engineering Applied to Transportation Infrastructure, lecture notes, Yukon College, Whitehorse.
- Government of Nunavut, 2013. A Homeowner’s Guide to Permafrost in Nunavut: Keep Your House on Solid Ground. Government of Nunavut, 28 p.
- Gravel, J.-F., 2012. Impact of climate change on habitat development in Nunavik (Société d’habitation du Québec). Northern Forum, Quebec City, QC.
- Lewkowicz, A., Miceli, M., Duguay, M., Bevington, A., 2014. Electrical Resistivity Tomography (ERT) as an Essential Tool to Investigate Sites in Discontinuous Permafrost. University of Ottawa. EUCOP, June 18-21 2014.
- Moorman, B.J., Robinson, S.D. and Burgess, M.M., 2007. Imaging Periglacial Conditions with Ground-Penetrating Radar. University of Calgary, Alberta, Canada. 17 p.
- Permafrost Technology Foundation, 2000. Design Manual for New Foundations on Permafrost. Permafrost Technology Foundation publications, 94 p.
- McGregor, R., Hayley, D., Wilkins, D., Hoeve, E., Grozic, E., Roujanski, V., Jansen, A. and Doré, G., 2010. Guidelines for Development and Management of Transportation Infrastructure in Permafrost Regions. Transportation Association of Canada, Ottawa, ON, 177 p.